106p

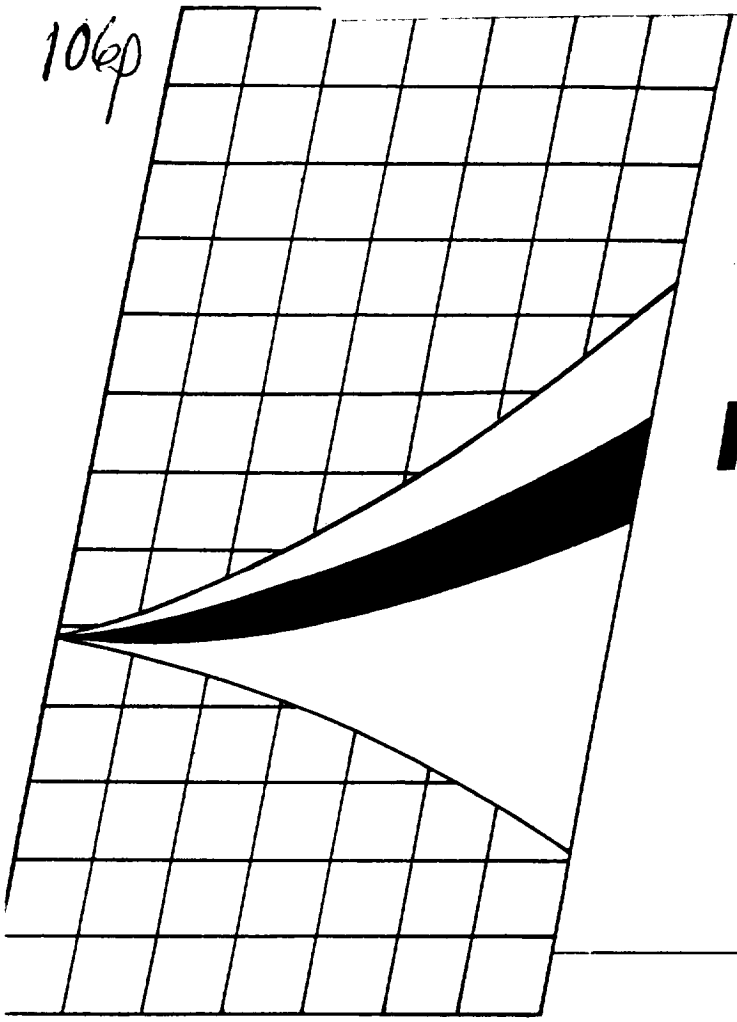

PLUG-NOZZLE PROGRAM (19)

CONTRACT NAS5-445

FINAL REPORT

to

NATIONAL AERONAUTICS AND SPACE ADMINISTRATION

FLIGHT PROPULSION LABORATORY DEPARTMENT
GENERAL ELECTRIC

[redacted]

[redacted]

PLUG NOZZLE PROGRAM (C)

(21) (NASA CONTRACT NAS5-445)

(NASA CR-55977) (DM-61-154)

FINAL REPORT

OCTOBER 1, 1961 106p (cy)

TO

NATIONAL AERONAUTICS AND
SPACE ADMINISTRATION

Submitted By: Edward K. Graham
A. R. Graham, Project Engineer

Approved By: Kurt Berman
K. Berman, Manager, Liquid Rocket Engine Sub-Operation

GROUP 4
Downgraded at 3 year intervals; declassified after 12 years

Assigned to Automatic Regrade Group 4. Authority General Electric Co. letter, dated Nov 8, 1966.

(2) FLIGHT PROPULSION LABORATORY DEPARTMENT Dept.
FLIGHT PROPULSION DIVISION
09 84 062 → GENERAL ELECTRIC COMPANY
CINCINNATI 15, OHIO

[redacted]

TABLE OF CONTENTS

TABLE OF CONTENTS (CONT'D)

LIST OF TABLES

TABLE OF CONTENTS (CONT'D)

LIST OF ILLUSTRATIONS

TABLE OF CONTENTS (CONT'D)

TABLE OF CONTENTS (CONT'D)

SECTION I

INTRODUCTION

During the past five years, the General Electric Company has been investigating the Plug Nozzle Rocket Engine design concept (1). This concept has evolved as the result of studies to establish a rational scaling approach for the development of high thrust rocket engines. The principal advantages claimed for this concept are:

1. A less expensive and more rapid method for the development of high thrust rocket engines. Subdividing the annular combustor into a discrete number of small cells virtually eliminates combustion instability problems. In addition, the majority of developmental type tests can be conducted with these individual cells, and only after satisfactory performance is obtained (from the standpoint of stability, heat transfer, injector and nozzle performance, etc.) is it necessary to conduct full scale engine tests. Hence, developmental testing can be conducted more rapidly and inexpensively.

2. Aerodynamic steering without the need of a gimbal system. Since the annular combustor is divided into a discrete number of cells, thrust vector control can be obtained by modulating the chamber pressures in the various cells, hence creating side forces to steer the vehicle. Consequently, no gimbaling system is required with this type rocket engine.

3. Improved performance at "off-design" pressure ratios. The plug nozzle offers thrust coefficients approaching those of an ideal bell type nozzle at all pressure ratios below the design point. That is, it acts like a variable area nozzle.

The results of investigations conducted to date (2, 3) under the auspices of NASA and the General Electric Company have been quite

gratifying. Approximately 18 different plug type nozzles have been investigated, both in conjunction with a 15,000 pound thrust hydrogen peroxide rocket motor, and in a wind tunnel, in order to demonstrate Items 2 and 3 above. In addition, tests were conducted with a 30,000 pound thrust segment of a million pound thrust class rocket engine under the auspices of NASA (1). These tests were conducted at a chamber pressure of 600 psia using liquid oxygen and RP-1 as the propellants, and demonstrated that this type of combustor could be operated most satisfactorily.

The investigations reported herein (conducted under NASA Contract No. NAS5-445) are a further extension of the aforementioned work, and were aimed primarily at demonstrating Item 1 above; that is, that a complete plug nozzle rocket engine could be developed quite rapidly and inexpensively by this method of approach. More detailed program objectives are outlined in Section II.

SECTION II

PROGRAM OBJECTIVES

As stated in the introduction, the principal purpose of this investigation was to demonstrate the feasibility of the Plug Nozzle Rocket Engine design concept. The specific objectives of the program were as follows:

1. To demonstrate that a single cell for use in an annular-plug-nozzle-type rocket engine could be developed rapidly and inexpensively.

2. To demonstrate that after such a basic cell was developed, that a group of these cells could be easily assembled to form a complete, integrated unit. This would show that the segmented development approach is a more rapid and less expensive means for producing rocket motors.

3. To demonstrate that an actual bipropellant plug-nozzle-type rocket motor could be designed, built, and operated satisfactorily.

4. To demonstrate both performance and thrust vector control for a bipropellant plug-nozzle-type rocket motor.

5. To demonstrate that such a motor could be adequately cooled.

SECTION III
SUMMARY

To accomplish the above five objectives a four-task program was undertaken, consisting of : Injector Development Tests (Task I), Segment Development Tests (Task II), Complete Uncooled Chamber Tests (Task III), and Complete Cooled Chamber Tests (Task IV). The development model consisted of a 50,000-pound-thrust plug nozzle rocket engine operating on Lox and RP-1; the operating chamber pressure and area expansion ratio were 250 psia and 10:1 respectively.

It will be shown that the development test cycle was arranged to provide a building block approach starting with injector development and ending with the test firing of a complete regeneratively cooled engine. A detailed description of the development program is presented below.

TASK I. INJECTOR DEVELOPMENT TESTS

Task I was concerned with injector development tests. The objective of this task was to develop an injector for use throughout the remainder of the program. During the first part of this task (Task IA), uncooled tests were conducted with each of three different types of injectors. These tests were employed to evaluate each of the injectors with respect to : a) stability, b) injector performance, and c) heat transfer (by transient temperature techniques). Since these parameters are independent of the chamber geometry downstream of the throat, the uncooled one-eighth segment test chambers employed in Task IA extended only a short distance downstream of the throat. Each of the injectors was a complete one-eighth segment injector and was curved as in the final design. The completion of Task IA resulted in the selection of the best of the three types of injectors from the standpoint of stability, performance and heat transfer.

Task IB consisted of additional tests employing the injector selected under Task IA. The tests were conducted using a special water-cooled chamber, hereafter termed heat transfer segment, which was capable of measuring four values of local heat transfer rate as a function of chamber length. The information obtained in these tests indicated that the initial heat transfer design of the cooled one-eighth segment was adequate and no injector or cooling passage changes were required.

TASK II. SEGMENT DEVELOPMENT TESTS

Task II of the program was concerned with segment development tests. The objective of this part of the program was to substantiate the design of the final cooled segment to be employed in the complete engine. Since internal manifolding of the final injector differed slightly from the development model tested in Task IB, the first part of this task (Task II-A) consisted of a series of water-cooled tests for checking out the final injector to be employed in Task II-B.

Task II-B consisted of testing complete one-eighth water-cooled and regeneratively cooled segments with the final injector. After minor modifications of the cooled segments during this phase of the program, satisfactory operation was obtained. This series of runs resulted in a total of eleven regeneratively cooled tests conducted over the range of chamber pressures later employed in the thrust vector control tests; the majority of these runs had a duration of 20 seconds.

TASK III. COMPLETE UNCOOLED CHAMBER TESTS

Task III of the program involved the testing of a complete uncooled 50K engine. The objective of Task III-A was to establish starting techniques. The objectives of Task III-B were: a) to acceptance test all of the injectors which were to be subsequently employed in the regeneratively cooled chambers and b) to obtain performance and thrust vector control data. The results indicated that the plug nozzle offered about 5 percent higher performance than the conventional bell type nozzle operating under the same conditions. Vector

control results indicated that approximately 3.5 degrees of effective vector angle was attainable with this engine when operating half of the cells at 15 percent above the design chamber pressure and the other half 15 percent below the design chamber pressure.

TASK IV. COMPLETE COOLED CHAMBER TESTS

This phase of the program was divided into two parts. The first part, Task IV-A, was concerned with substantiating the start techniques defined by Task III. The second half of this phase of the program, Task IV-B, was concerned with performance and thrust vector tests under regeneratively cooled conditions. Two tests were completed, each of which had a full thrust duration of approximately 5 seconds (approximately 11 seconds total duration). Although minor difficulties were encountered with the hardware, these two tests conclusively proved the plug nozzle concept.

As a result of contract expiration, it was not possible to complete the planned series of Task IV testing. However, since previous Task II testing demonstrated the operating capability of cooled segments identical to those employed in the final engine, and Task III results established the perfomance and thrust vector capabilities of the engine, it was felt that the plug nozzle concept had been shown to be technically sound. It was, therefore, deemed inadvisable to renew the contract simply to complete the last few tests of this final series.

SECTION IV
DISCUSSION OF RESULTS

The over-all specifications of the thrust chamber developed under this program were based on a design study which is presented in Appendix A; the more pertinent specifications are given in Table I.

TABLE I
THRUST CHAMBER SPECIFICATIONS

Sea level thrust, lb.	50,000
Propellants	Liquid oxygen and RP-1
Area expansion ratio	10
Chamber pressure, psia (total pressure at nozzle entrance)	250
Chamber characteristic length, in.	30
Number of segments	8
Nozzle configuration	Partial internal expansion

Figure 1 is a schematic drawing which gives the over-all engine configuration, and shows that it consists of an annular type combustor divided into eight individual segments.

The objectives of the program were discussed in Section II, and the method of accomplishment (plus a brief summary of the program) was presented in Section III. A detailed discussion of each of the major tasks within the program follows:

A. TASK I. INJECTOR DEVELOPMENT TESTS

This task was concerned with injector development tests. Its objective was to establish an injector for use throughout the remainder of the program.

1. Task IA. Uncooled Tests

During this task uncooled tests were conducted with each of three different types of injectors. These tests were concerned with evaluating each of the injectors with respect to: a) stability, b) injector performance, and c) heat transfer (by transient temperature techniques). Since these parameters

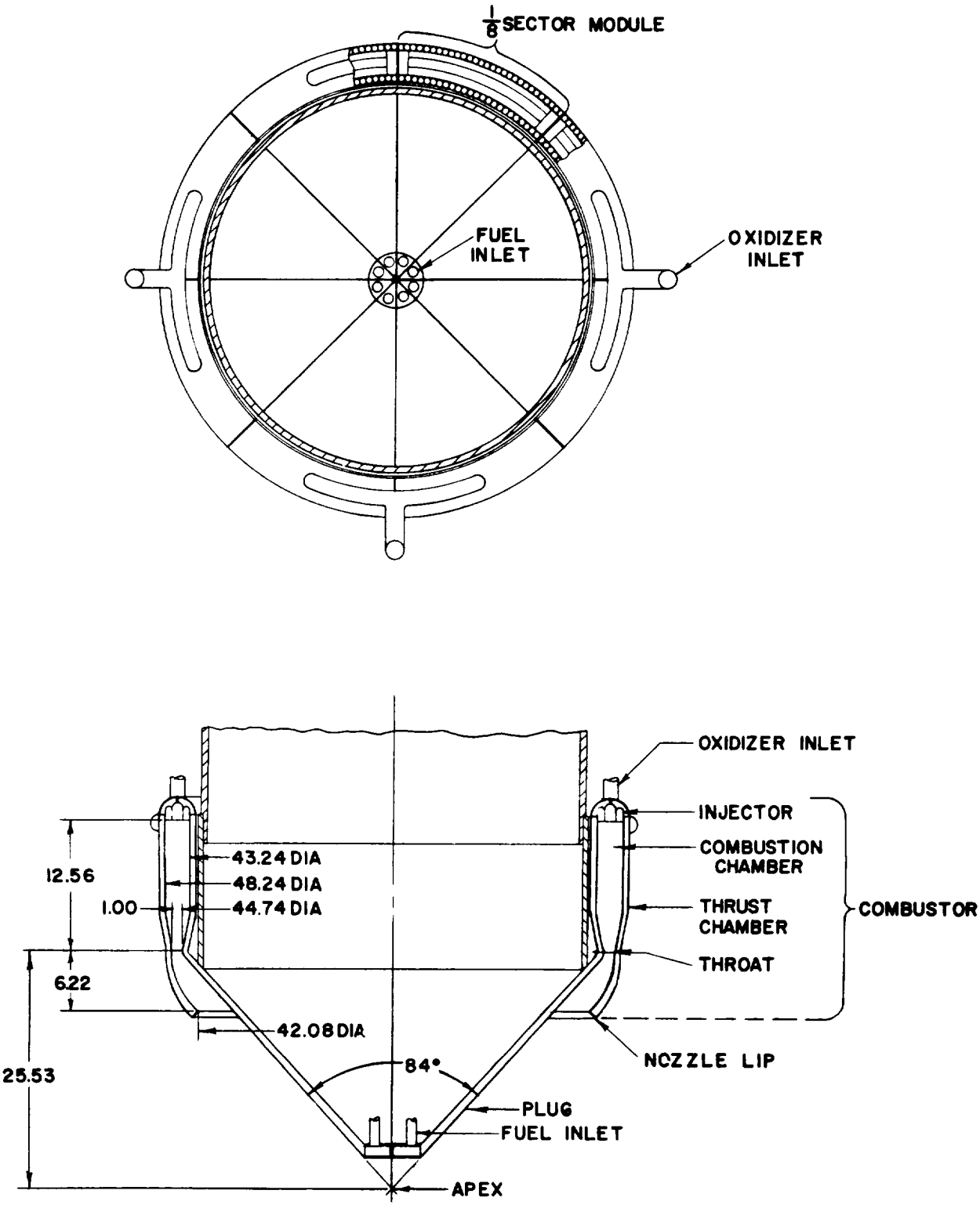

Figure 1 50K Plug Nozzle Engine

are independent of the chamber geometry downstream of the throat, the uncooled one-eighth segment test chambers which were employed extended only a short distance downstream of the throat. Each of the injectors was a complete one-eighth segment injector and was curved as in the final design.

A photograph of one of the one-eighth segment thrust chambers is presented in Figure 2. These chambers were equipped with suitable thermocouples (located on the internal surface) for obtaining heat transfer data, and high frequency pressure transducers for evaluating injector stability. Descriptions of the three injectors employed in the program are presented below.

Figure 3 is a photograph of Injector Model I, which is a complete one-eighth segment injector. The injector comprised five circumferential (lengthwise) rows of spray nozzles which were alternately arranged to inject fuel and oxidizer into the chamber. The two outer rows and the center row supplied fuel, while the two remaining rows supplied oxidizer. The two outermost rows of spray nozzles (fuel) provided a fuel curtain along the circumferential walls of the combustion chamber.

The detailed views of Injector Model I-1* given in Figures 4 and 5 will help clarify its operation. The oxidizer and fuel manifolds were located one above the other, the upper manifold (see Figure 4) being the oxidizer manifold. In operation, oxidizer was supplied to the oxidizer spray nozzles through vertical tubes which passed through the fuel manifold. The fuel, on leaving its manifold, was supplied directly to the fuel spray nozzles. All of the spray nozzles across the short ends of the injector also supplied fuel for purposes of curtain cooling in that area. The detailed view of Injector I-1 in Figure 5 shows the injector face.

---

* The designation Model I-1 refers to Injector Model I, Serial Number 1. This method of identification is used throughout this section.

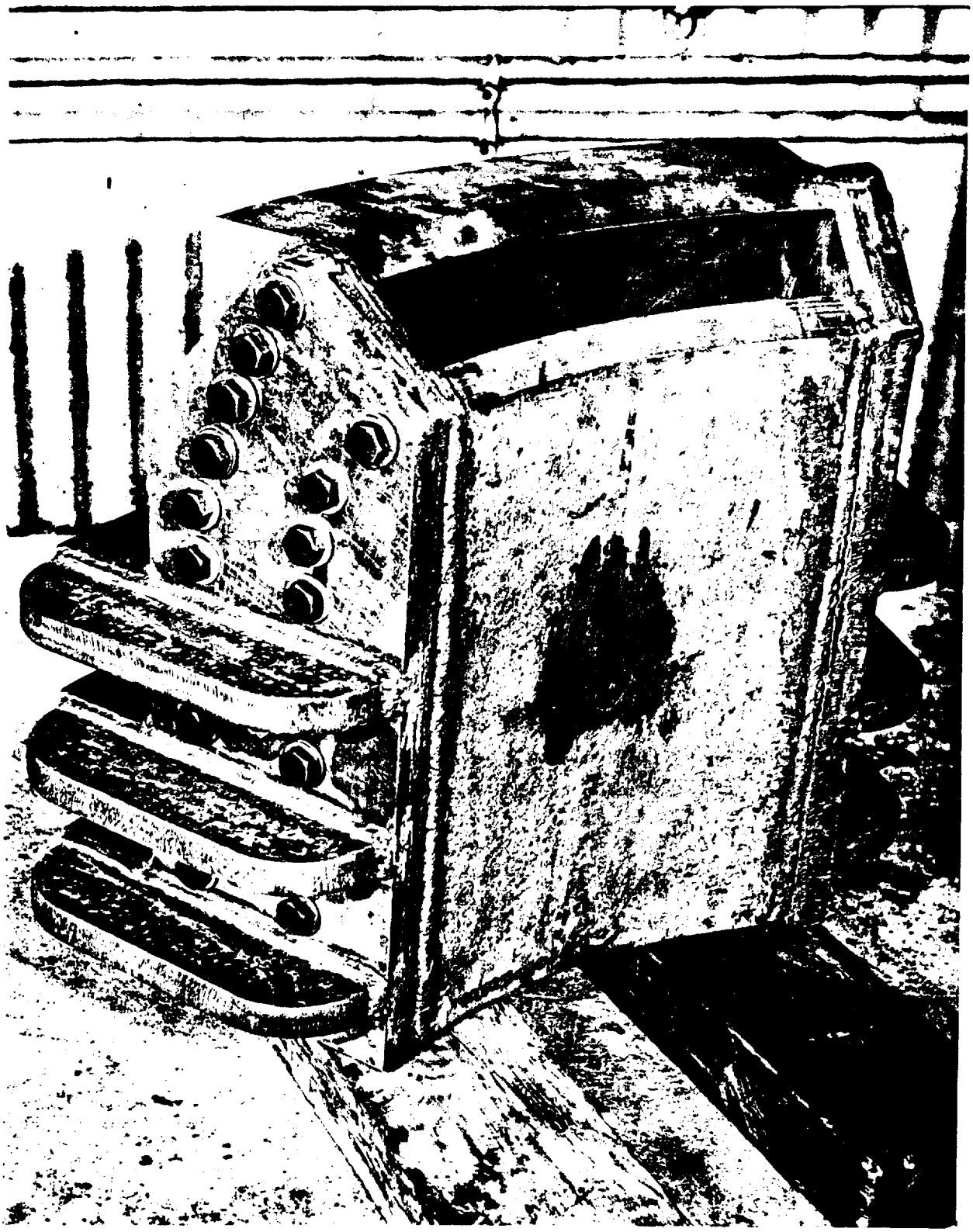

Figure 2 Uncooled Thrust Chamber

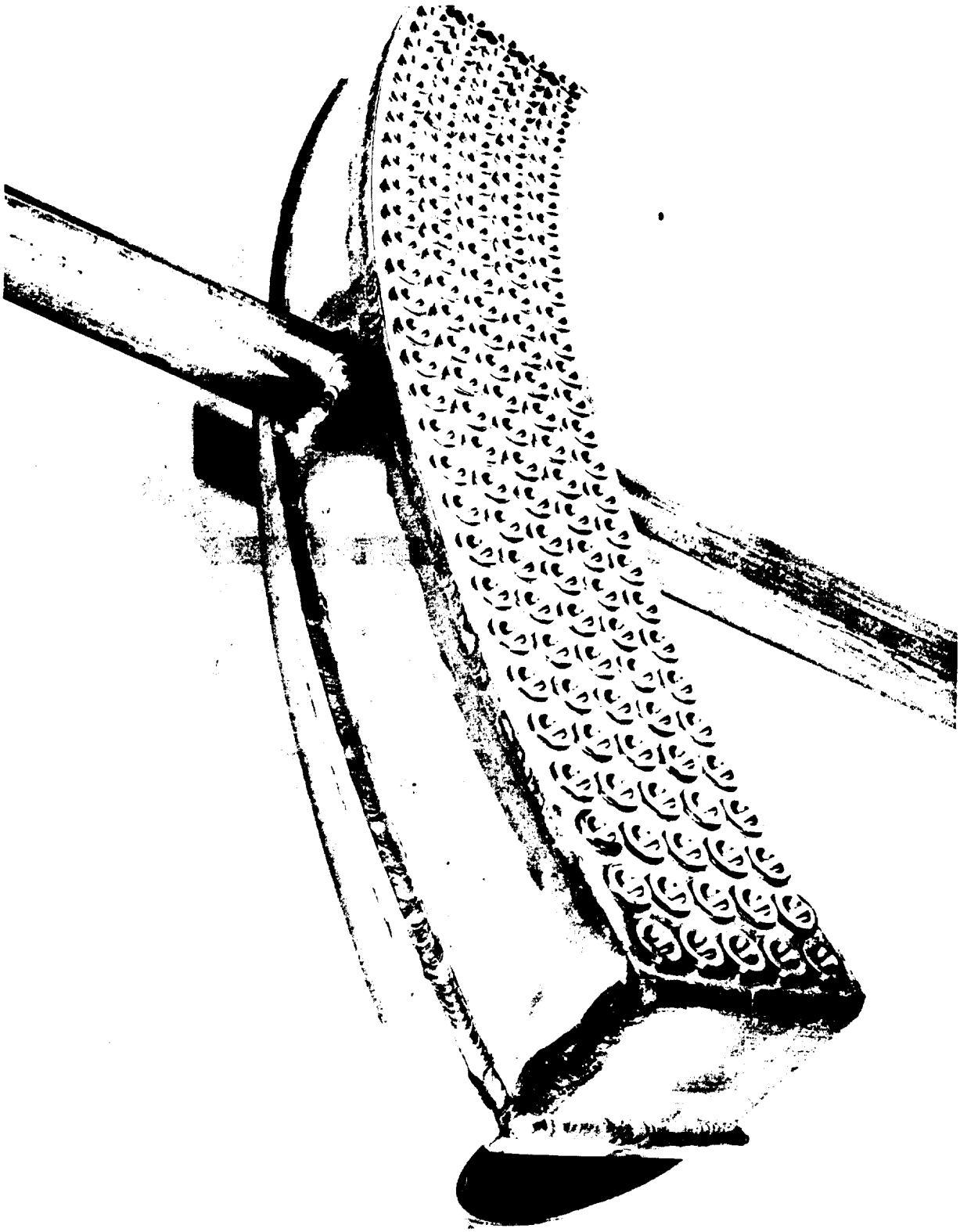

Figure 3 Injector Model I

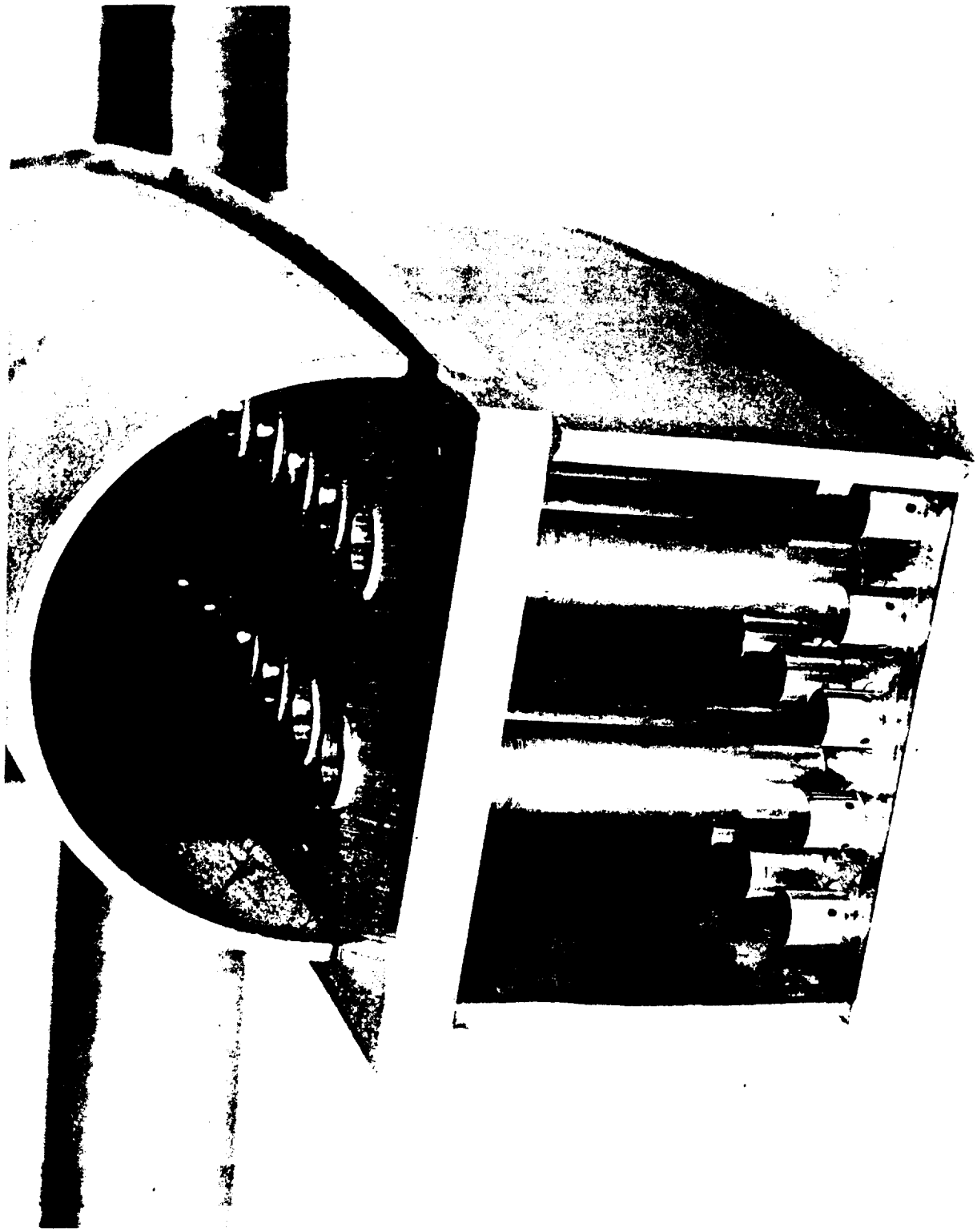

Figure 4 Injector Model I-1

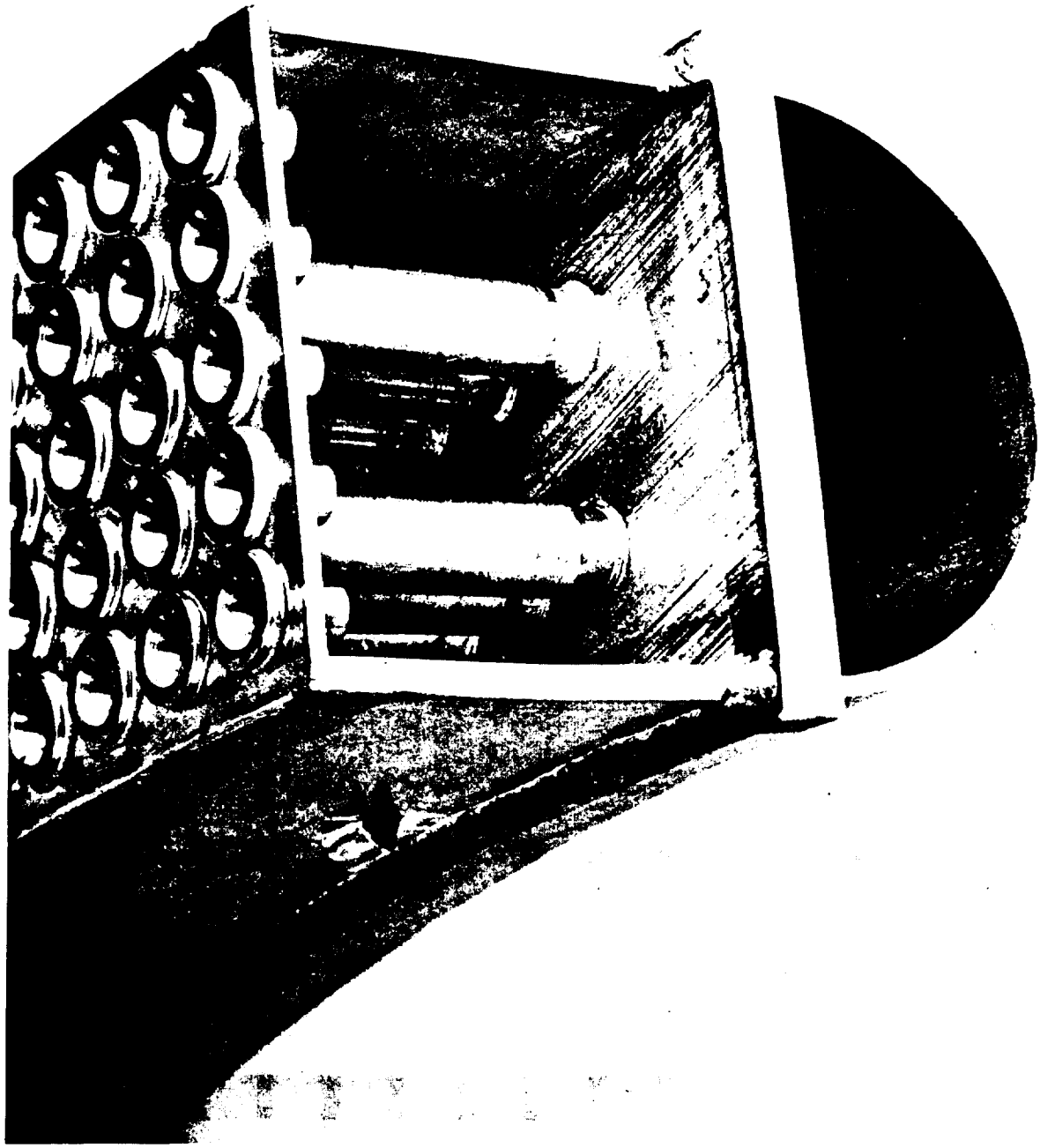

Figure 5 Injector Model I-1

All parts of this injector were fabricated from Type 347 stainless steel. The oxidizer tubes and spray nozzles were copper-brazed into place; all other injector joints were of welded construction.

Figure 6 presents a photograph of Injector Model II, and Figure 7 is a detailed view of a mock-up of the injector. This injector employed three tubes with oblong cross-section as the fuel and oxidizer manifolds (see Figure 7). The two outer manifolds supplied fuel while the center manifold supplied oxidizer. Fuel and oxidizer were injected into the combustion chamber through spray nozzles similar to those employed in the Model I type injector. The nozzles were so arranged that the fuel and oxidizer sprays impinged on one another after being injected into the chamber. This injection arrangement provided fuel-curtain cooling along the circumferential walls of the chamber. To insure an excess of fuel for cooling the end walls of the combustion chamber, no oxidizer spray nozzles were included at either end of the injector (see Figure 7).

All parts of this injector were also fabricated from Type 347 stainless steel. The oxidizer tubes and spray nozzles were copper-brazed into place; all other injector joints were of welded construction.

Figure 8 presents a photograph of Injector Model III, while Figure 9 shows the principle parts which comprise this injector. Injector Model III is similar in design to the lengthwise like-on-like injector employed under the NASw-40 contract (1). A total of nine lengthwise strips were employed (see Figure 8), which alternately supplied fuel and oxidizer to the rocket chamber through like-on-like pairs of holes located in the strips. Both of the outer lengthwise strips supplied fuel for purposes of curtain cooling along the circumferential walls of the chamber. Crosswise strips at either end of the injector provided curtain cooling along the end walls of the chamber.

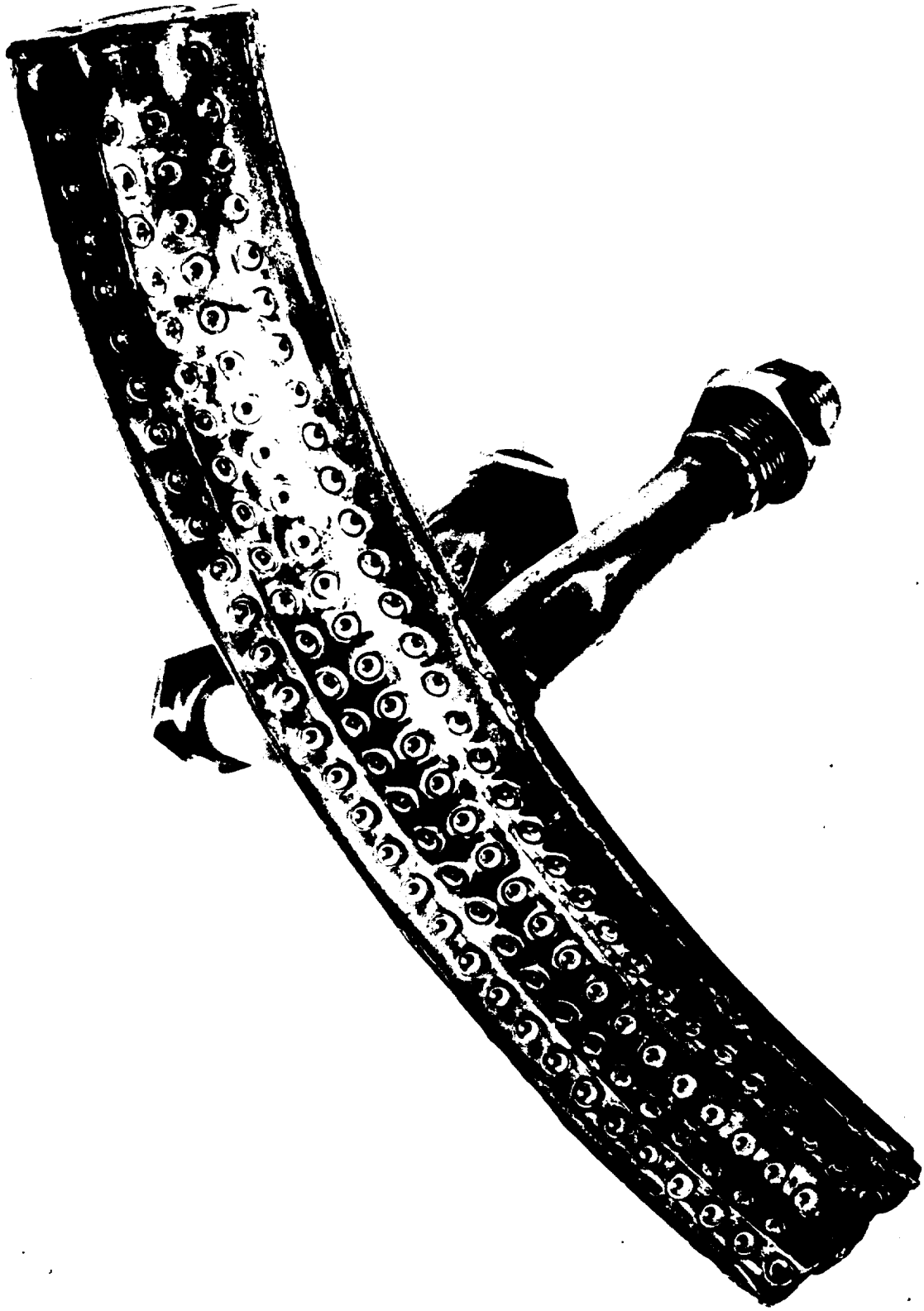

Figure 6 Injector Model II

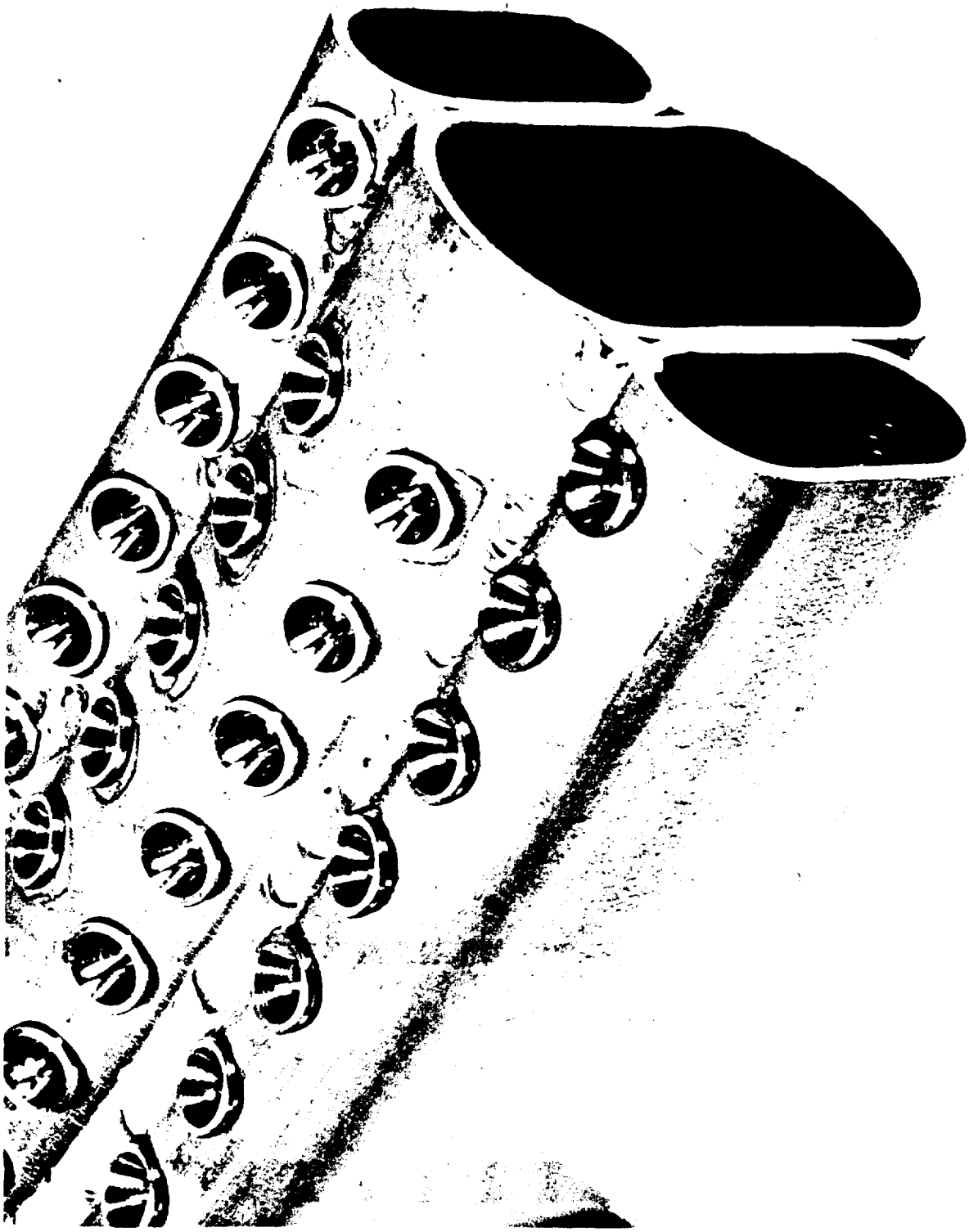

Figure 7 Injector Model II-1

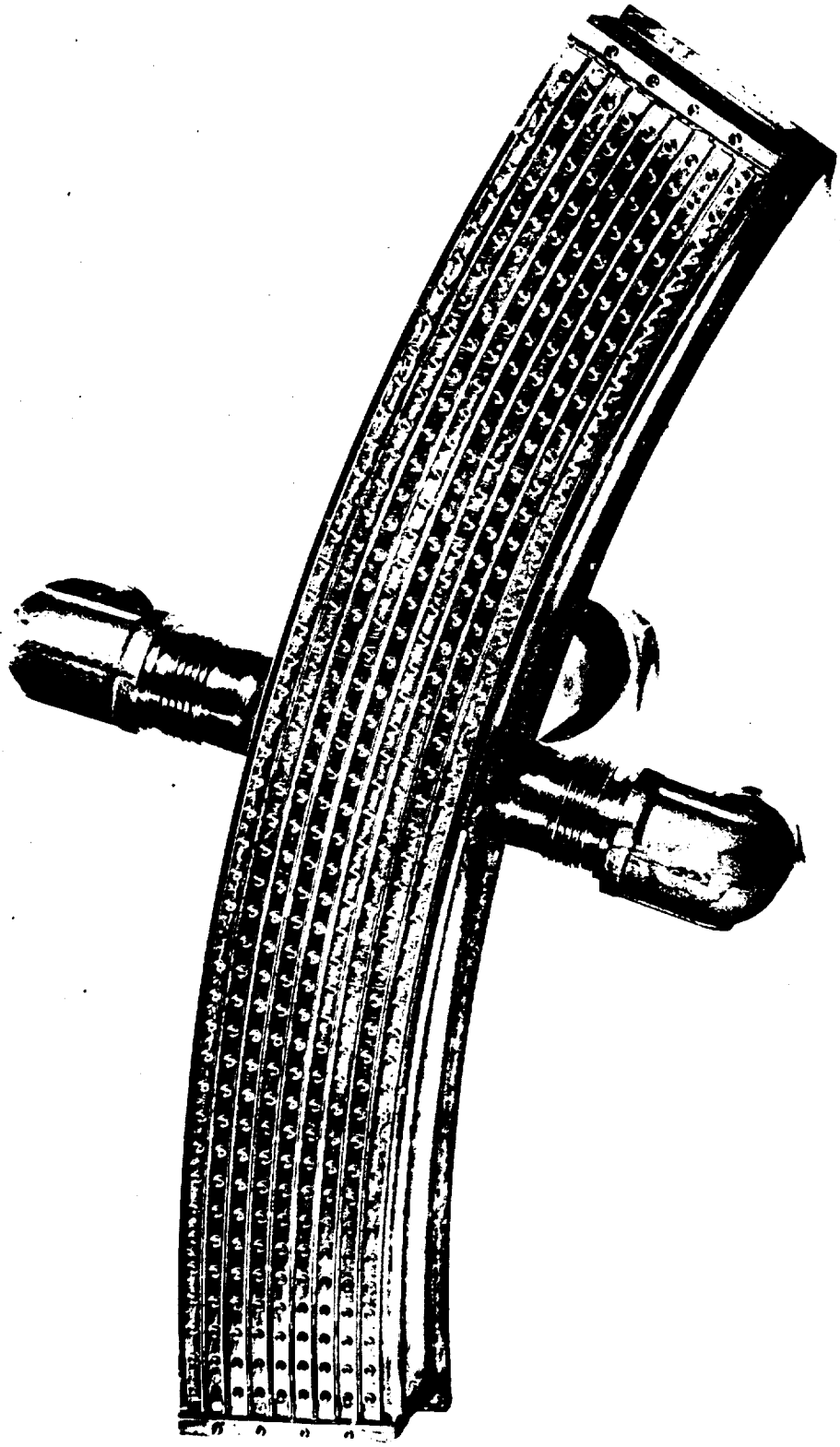

Figure 8 Injector Model III

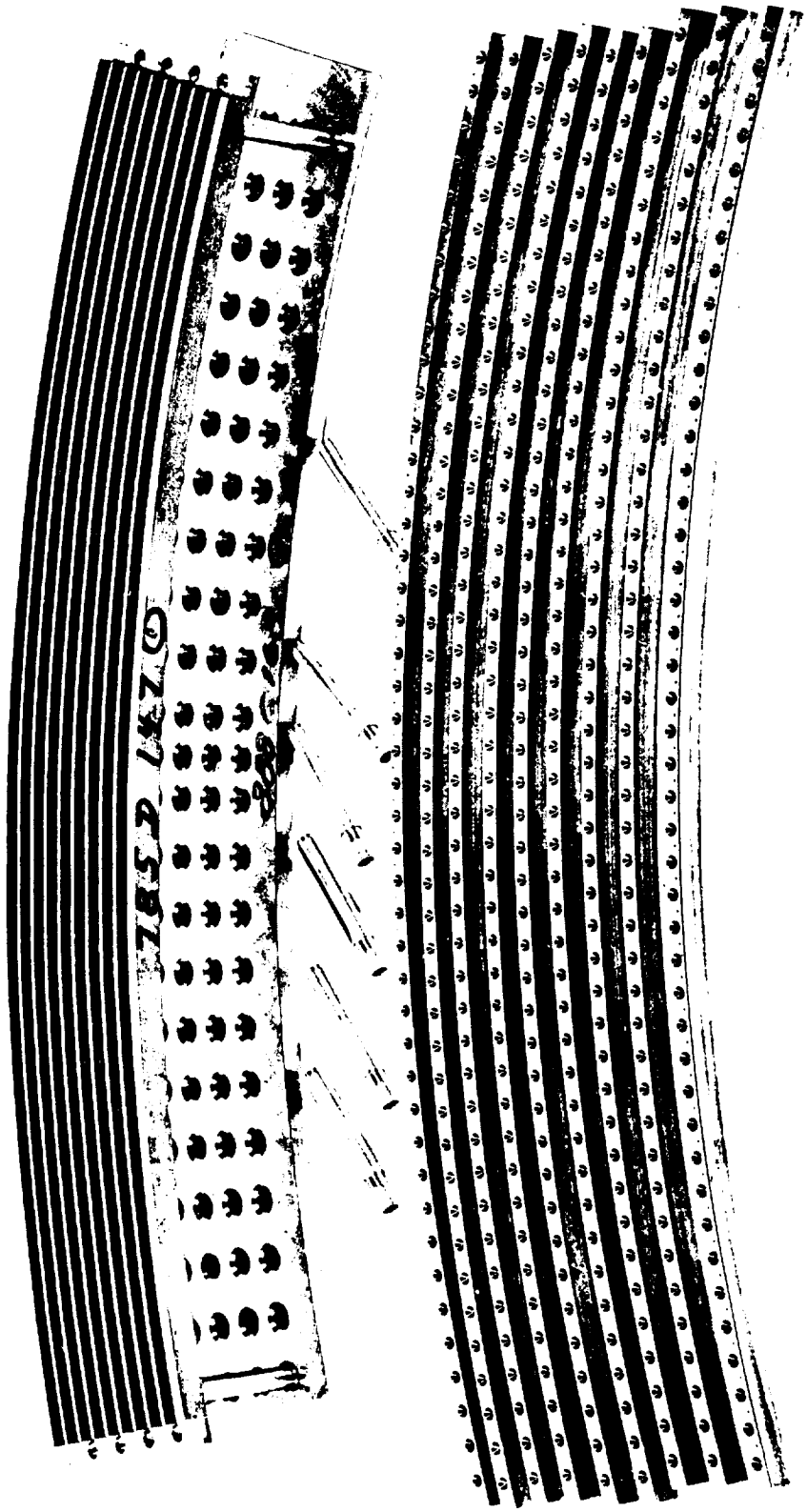

Figure 9 Injector Model III - Parts Grouping

The construction of these injectors, insofar as manifolding is concerned, was very similar to that of the Model I type injector (see Figure 4). The oxidizer was supplied from the oxidizer manifold to each of the oxidizer strips through four rows of vertical tubes which passed through the fuel manifold. As in the case of the Model I injector, fuel was supplied directly from the fuel manifold to the fuel strips.

This injector was also fabricated entirely from Type 347 stainless steel. The oxidizer supply tubes and strips were copper-brazed in place, and all other joints were of welded construction.

In addition to the tests conducted with Injector Models I, II and III, other tests were conducted using flameholders (similar to those employed in Reference 1) inserted directly in front of Injector Models I and II. Injectors I and II with flameholders will hereafter be referred to as Injectors IA and II-A respectively.

The tests conducted with the various injectors resulted in the selection of Injector Model III for use throughout the reaminder of the program. A brief description of the tests conducted with the Model I and II injectors, and a detailed description of the tests conducted with the Model III injector follow.

Four tests (Runs 1 through 4) were conducted with Injector I-1 for the purpose of checking out the test system and its start-up characteristics. Run 5 was conducted with Injector I-1 under nominal operating conditions; the run was unstable and resulted in injector burnout. Five tests (Runs 6 through 10) were conducted with Injector II-1 at nominal operating conditions. These runs all yielded random pulses (several per second) in the chamber pressure, which in some cases resulted in combustion instability. Analysis of the data from these runs indicated that: 1) the flame front was being established a considerable distance downstream from the injector

face, and 2) the chamber pressure pulses resulted from the flame front attempting to establish itself near the injector face (as it should). To check the latter hypothesis a flameholder was installed directly in front of Injector II.

Runs 11 and 12 were conducted with Injector II-A. Both runs were of approximately 10 seconds duration and resulted in a considerable improvement with respect to chamber pressure pulses. However, a single pulse in the chamber pressure was noted near the end of each run. In view of this, and also the fact that all of the tests with both Injectors II and II-A indicated marginal performance (see Table B-1 - Appendix B) no further tests were conducted with this injector.

Run 13 was conducted using Injector IA (Injector I combined with a flameholder) and resulted in combustion oscillations and injector burnout. Consequently no further tests were conducted with this injector.

Following the critical development tests conducted with the Model I, IA, II and II-A injectors, twenty-two successful tests (Runs 14-35) were conducted with Injector III-1. Tabulated results of these tests are presented in Appendix B, Table B-II. These runs covered a range of chamber pressures from approximately 150 to 400 psia, and reactant ratios from 1.8 to 2.4.

Figure 10 presents a stability diagram of chamber pressure versus reactant ratio for this injector. It shows that stable operation occurred between chamber pressures of 220 and 300 psia (total pressure at nozzle entrance of 210 and 290 psia) as was required under conditions of thrust vector control (Tasks III and IV). Figure 11 presents the measured C* (Characteristic exhaust velocity based on total pressure at nozzle entrance) as a function of reactant ratio, and indicates that Injector III-1 yielded very good performance (approximately 93 percent of theoretical). The curve

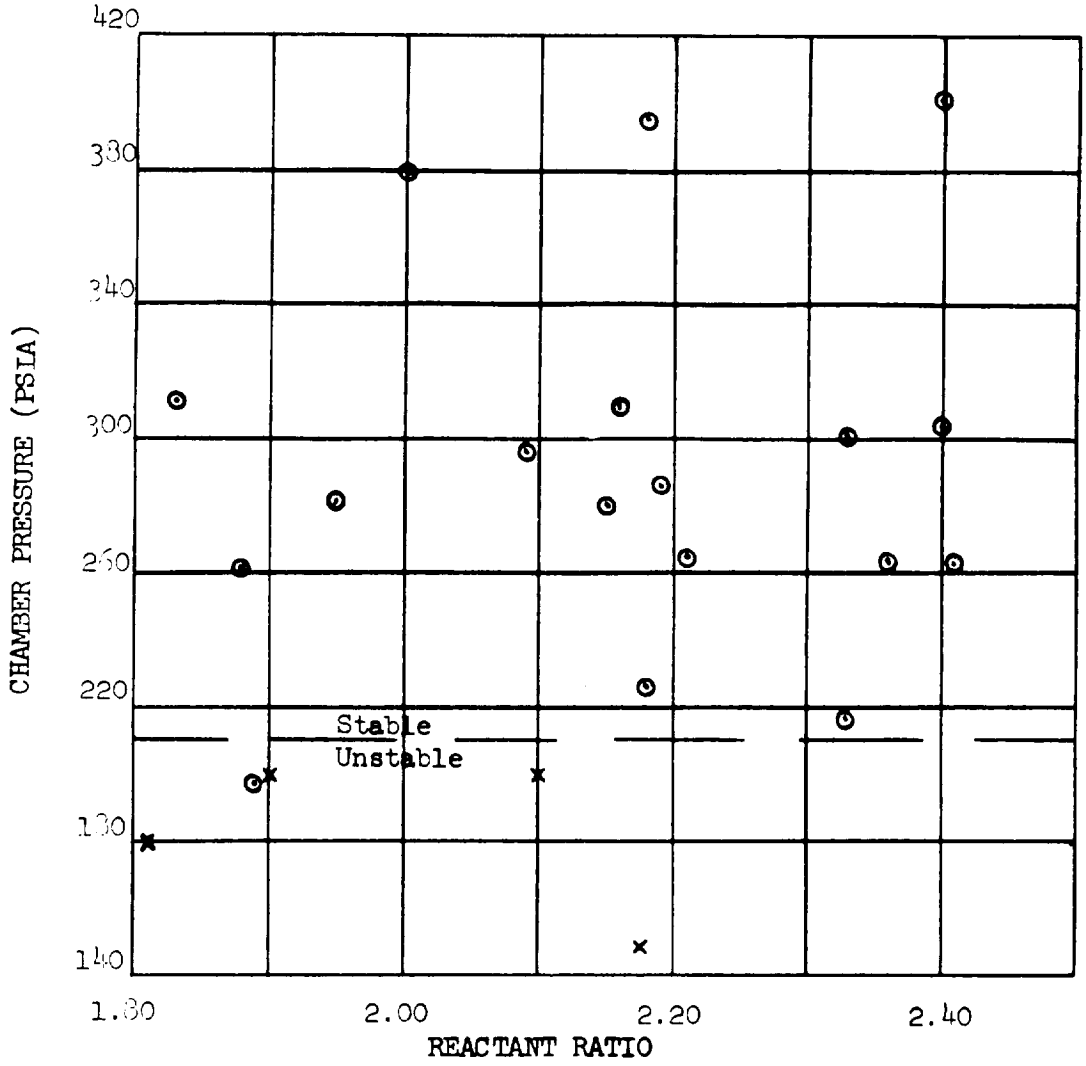

Figure 10 Stability Diagram for Injector III-1 (Uncooled Runs Only)

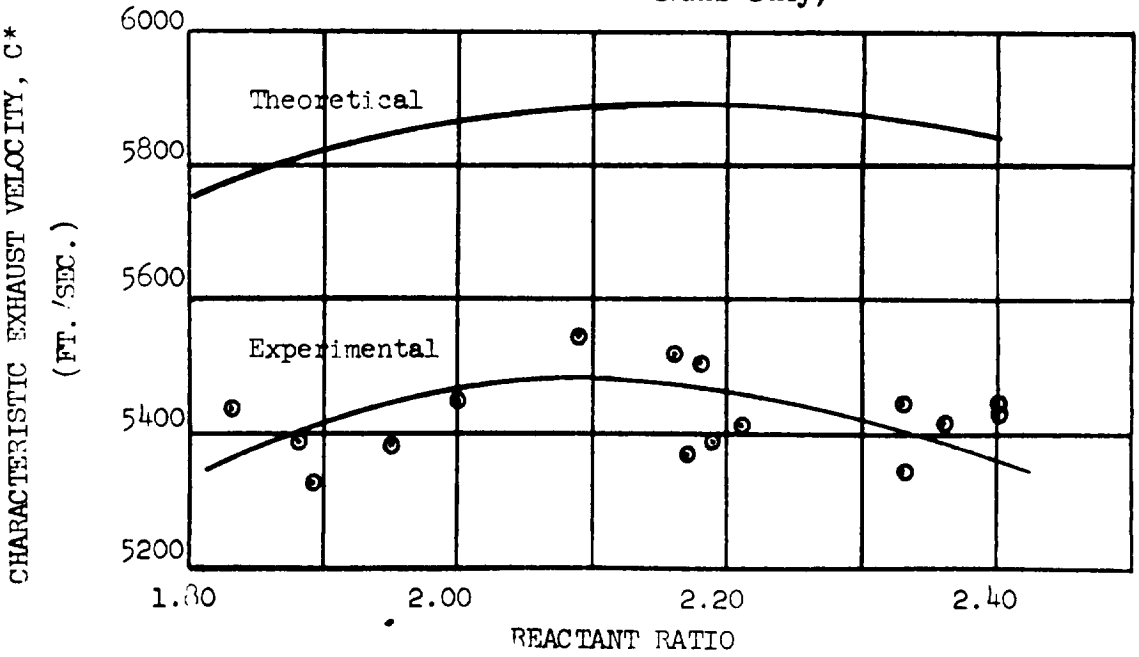

Figure 11 Injector III-1 Performance (Uncooled Runs Only)

indicates that maximum performance occurred at a reactant ratio of approximately 2.1, where the injector yielded C* = 5480 feet per second.[1]

As mentioned earlier, heat transfer data were also obtained in this series of runs by measuring transient state temperatures on the inside surface of the chamber. Although the data were somewhat scattered, they indicated that Injector III-1 yielded fairly reasonable heat transfer rates in the chamber. More exact values of the chamber heat transfer rates with Injector III-1 were later determined under Task IB which will be discussed shortly.

On the basis of the aforementioned tests, Injector Model III was selected for use throughout the remainder of the experimental program. It should be noted that, with a reasonable amount of development effort, Injector II-A could undoubtedly have been operated satisfactorily. If a large number of engines were to be produced, Injector II-A would be desirable because of its low cost; however, for this particular experimental program, where only a small amount of hardware was required, it was actually more economical to accept the more expensive Injector III than to carry out further development effort and tests with Injector II-A.

2. Task IB. Cooled Tests

Task IB consisted of an additional series of tests employing Injector Model III (selected under Task IA). This particular series of tests was conducted using a special water-cooled chamber, hereafter termed the heat transfer segment. Figure 12 is a photograph of the heat transfer segment and shows that it ended at the throat. It comprised four individual sets of coolant passages, so arranged that local heat transfer rates could be determined as a function of longitudinal distance by measuring the water

---

1. The values of performance indicated in Figure 11 (Task IA) were found to be slightly higher than those obtained later under Task IB employing the cooled heat transfer segment. The reason for this difference in the measured performance of Injector III-1 (which is quite negligible) will be discussed later under Task IB.

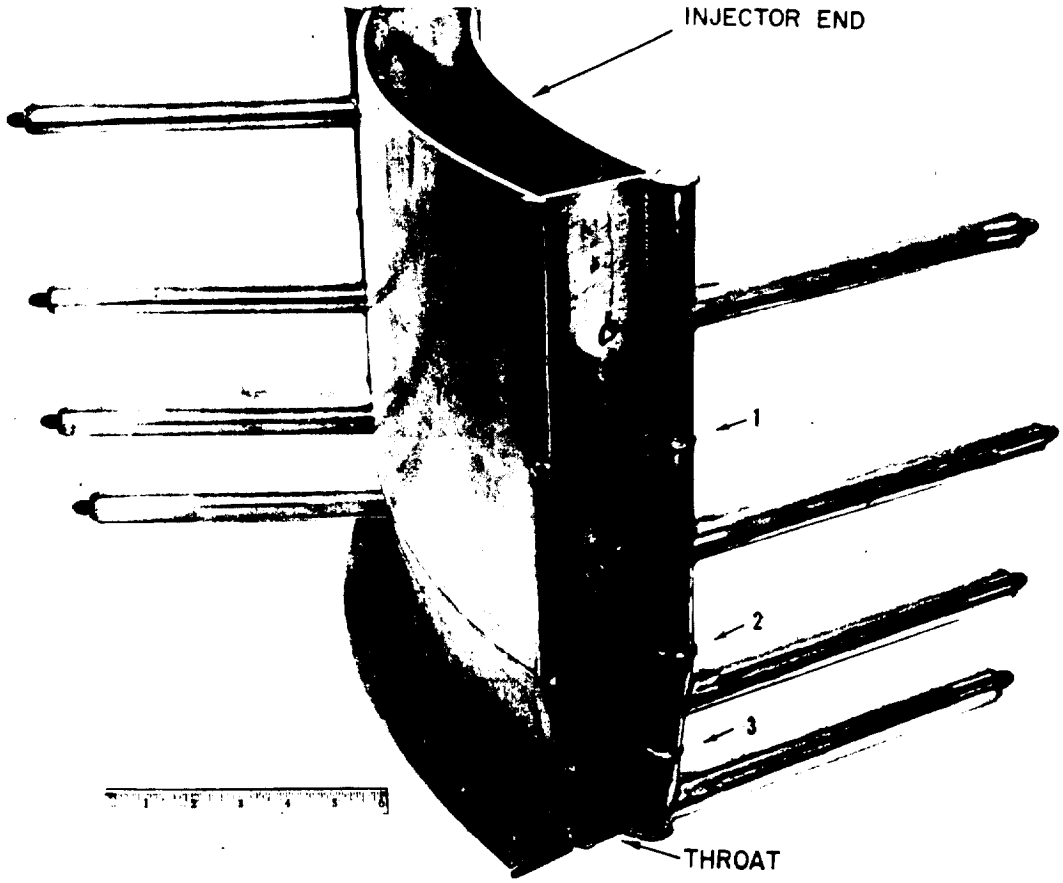

Figure 12 Heat Transfer Segment (Numbered Arrows Show Individual Coolant Passage Boundaries)

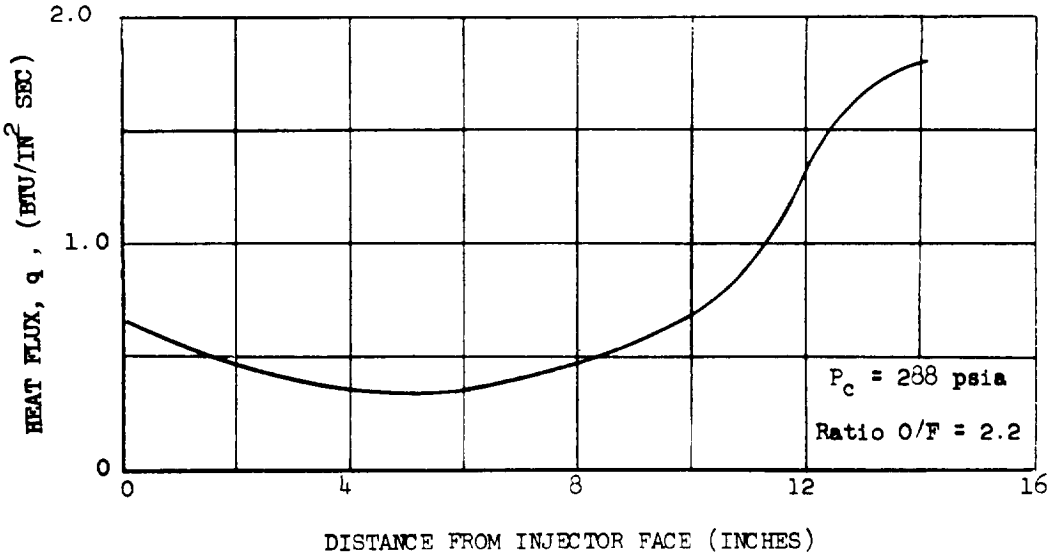

Figure 13 Typical Heat Flux Distribution

coolant flow rate through each set of coolant passages, and the coolant temperature rise. In total, fifteen tests (Runs 36 through 50) were conducted, employing the heat transfer segment in conjunction with Injector Model III (see Table B-II, Appendix B).

Figure 13 presents typical heat transfer results, showing the heat flux, q, as a function of distance from the injector face. It will be noted that the heat flux was fairly constant in the chamber section and increased to a maximum value at the throat (corresponding to 14.1 inches). Figure 13 also indicates that the heat flux decreased slightly with increasing distance from the injector face (in the chamber section). The reason for this is not known; however, the heat flux in the chamber section is so nearly constant that its variation may be attributed to experimental error and is probably not a real effect.

The data of Figure 13 and other similar data can be correlated into a more meaningful form . For the case of heat transfer in the absence of curtain cooling effects, the gas side heat transfer coefficient is generally correlated in the form of:

$$Nu = 0.023\ (Re)^{0.8}\ (Pr)^{1/3} \qquad (1)$$

Where:

Re = Reynolds Number of hot gases based on bulk conditions.

Pr = Prandtl Number of hot gases based on bulk conditions.

Nu = Nusselt Number of hot gases based on bulk conditions.

For the case where curtain cooling is employed, it is reasonable to assume an equation of similar form; that is:

$$Nu = 0.023\ F_c\ (Re)^{0.8}\ (Pr)^{1/3} \qquad (2)$$

where F_c is defined as the curtain cooling factor. By comparing Equation 2 to Equation 1, it can be seen that the curtain cooling factor F_c is a measure of the amount of curtain cooling that is effected by the injector. The meaning of F_c is further clarified in Figure 14, which presents the heat flux, q, as a function of the distance from the injector face. The solid curve in Figure 14 presents the experimental data shown earlier in Figure 13 for P_c = 288 psia and Ratio O/F = 2.2. The dashed curves in the figure are theoretical curves based on the same operating conditions for various values of F_c (curves derived from Equation 2). It will be noted that the actual curtain cooling effectiveness decreased from approximately F_c = 0.2 near the injector to approximately F_c = 0.1 part way down the chamber, and then increased to approximately F_c = 0.3 in the vicinity of the throat. In general, the curtain cooling factor increased with distance from the injector face, indicating that the fuel curtain was becoming less effective as it proceeded along the chamber wall (larger values of F_c indicate less effectiveness - see Equation 2). The decrease in F_c with distance near the injector end of the chamber is probably false, and due to experimental error, as mentioned earlier.

Based upon the above results the curtain cooling factor F_c was correlated as a function of distance for all of the runs by employing the following technique. With the heat transfer rate as a function of distance known in each of the runs, the corresponding heat transfer coefficient were determined; then with the physical properties of the gases and the geometry of the chamber known, the Nusselt Number, Nu, Reynolds Number Re, and the Prandtl Number, Pr, were computed. By substituting those values into Equation 2, the value of F_c as a function of length was determined for each of the runs. The results of these calculations (for all valid runs) are presented in Figure 15, which shows the curtain cooling factor, F_c, as a function of distance from injector face. When plotted in this form, the results are independent of chamber pressure and reactant ratio.

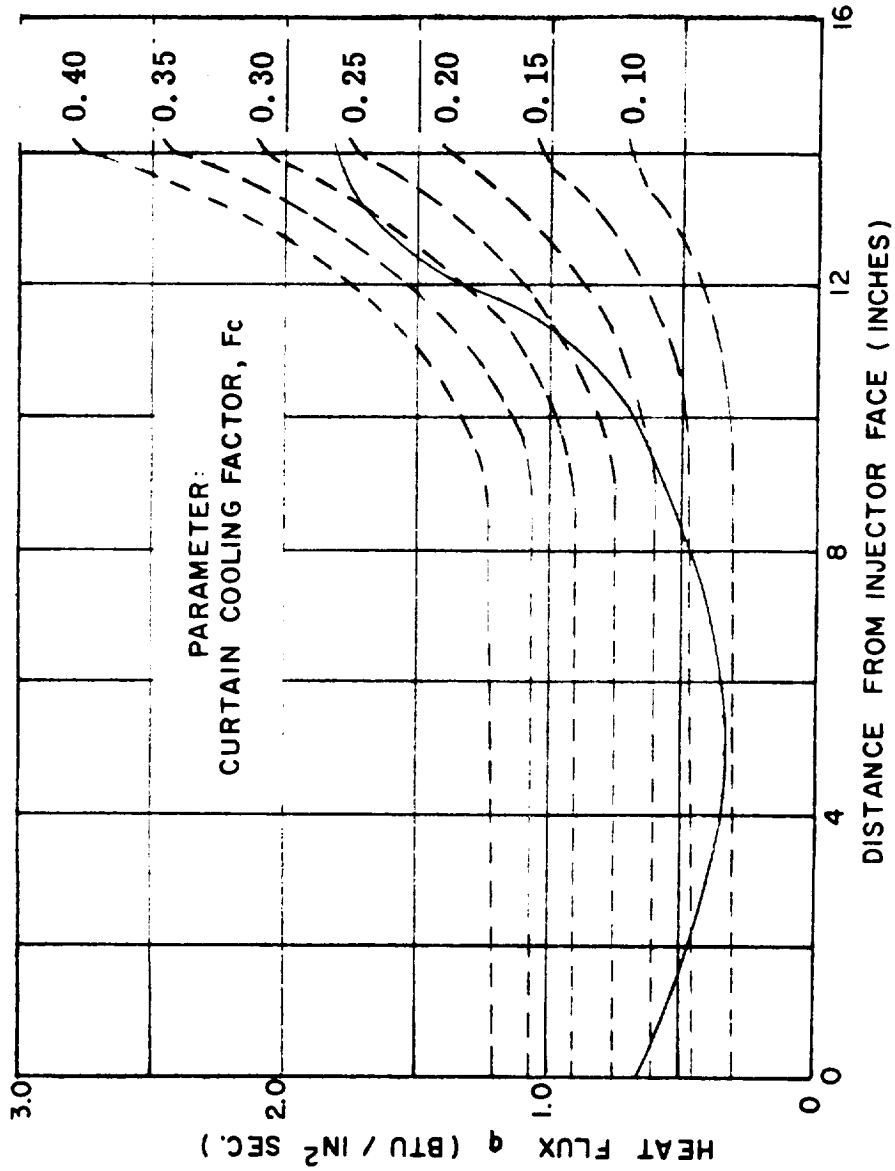

Figure 14 Curtain Cooling Effectiveness

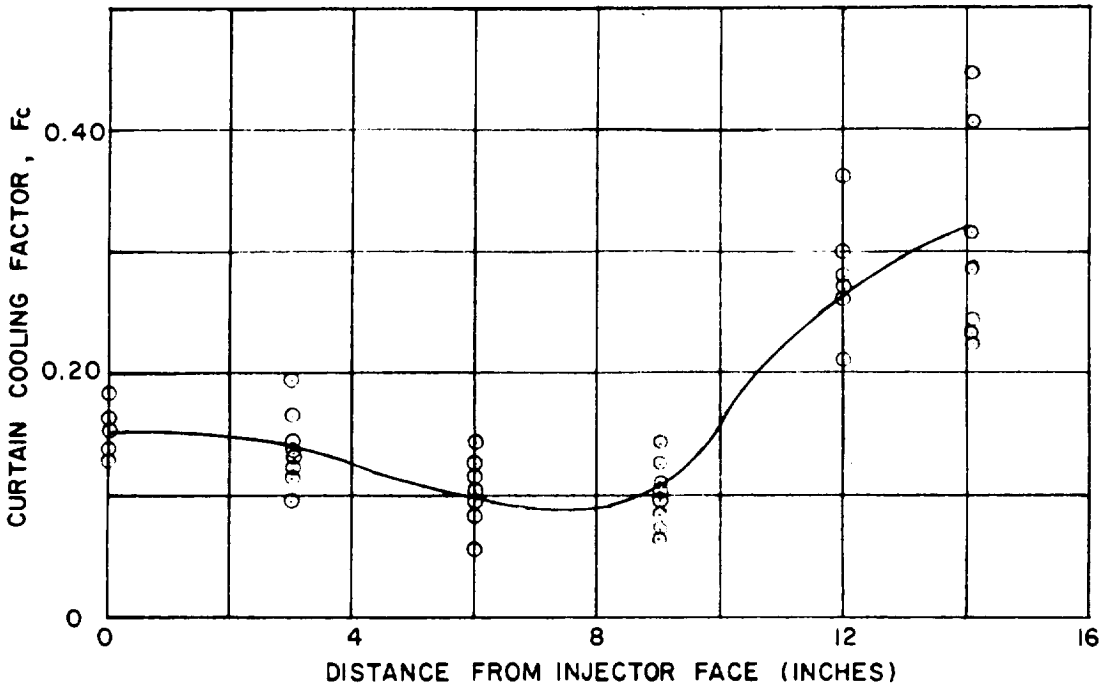

Figure 15 Curtain Cooling Factor Correlation

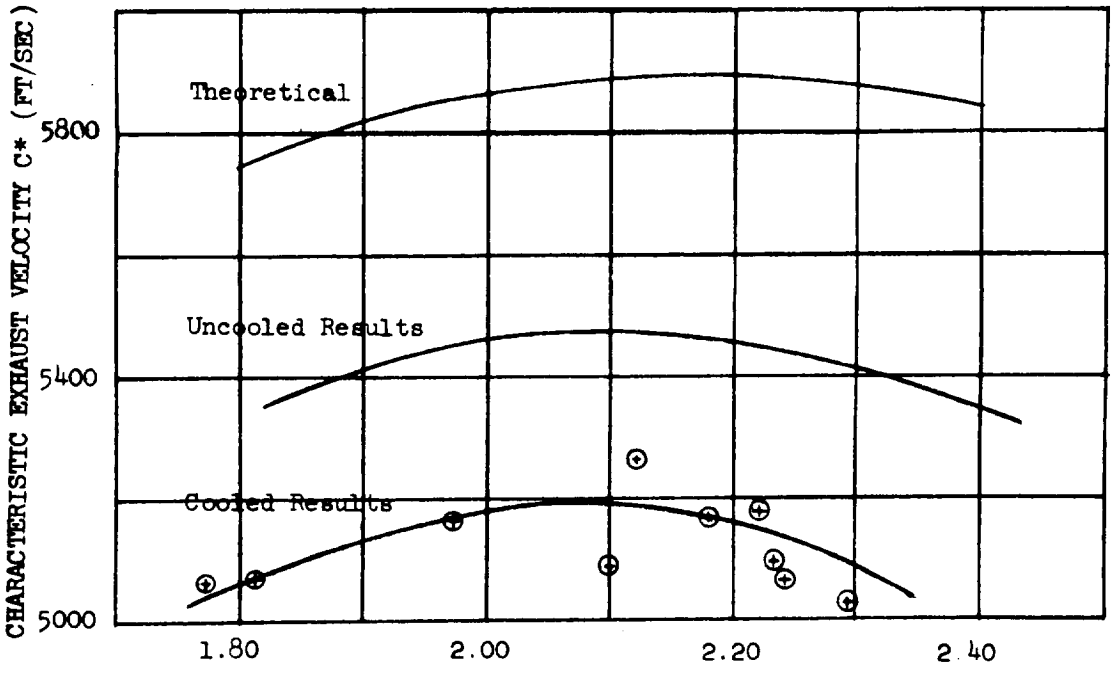

NOTE: Data Points Shown are for cooled runs only

Figure 16 Injector III-1 Performance
(Cooled and Uncooled Runs)

The coolant passage design for the engine was based on a constant curtain cooling factor of $F_c = 0.35$, since most of the measured values of F_c were less than $F_c = 0.35$.

Figure 16 presents the measured performance of Injector Model III as a function of reactant ratio and gives the results obtained with both the uncooled and cooled segments. The curve entitled "Uncooled Results" is the same curve that was presented earlier in Figure 11, with the data points omitted. The data points shown in Figure 16 with the derived curve entitled "Cooled Results" are those that were obtained with the cooled heat transfer segment. It will be noted that the cooled results indicate slightly lower performance than the uncooled results. Because of difficulties encountered in measuring the throat area of the uncooled chamber it is believed that the results obtained in the cooled tests (see Figure 16) are more reliable. These results indicate a characteristic exhaust velocity equal to approximately 91 percent of theoretical.

B. TASK II. SEGMENT DEVELOPMENT TESTS

Task II of the program was concerned with the development of the final regeneratively cooled segment (Figure 17) to be employed throughout the remainder of the program. This task was divided into two parts. Since the internal manifolding of the final injector differed slightly from that of Injector Model III (selected under Task I), the first part of this task (Task II-A) consisted of a series of water-cooled tests with the heat transfer segment, to check out the actual injector to be employed throughout the remainder of the program; hereafter this injector will be designated as the final injector. The final injector differed from Injector III in some minor modifications of the manifolding, dictated by the complete engine design; the injector face pattern remained unaltered. Figure 18 is a photograph of the final injector; Figures 19 and 20 show the injector at various stages of assembly.

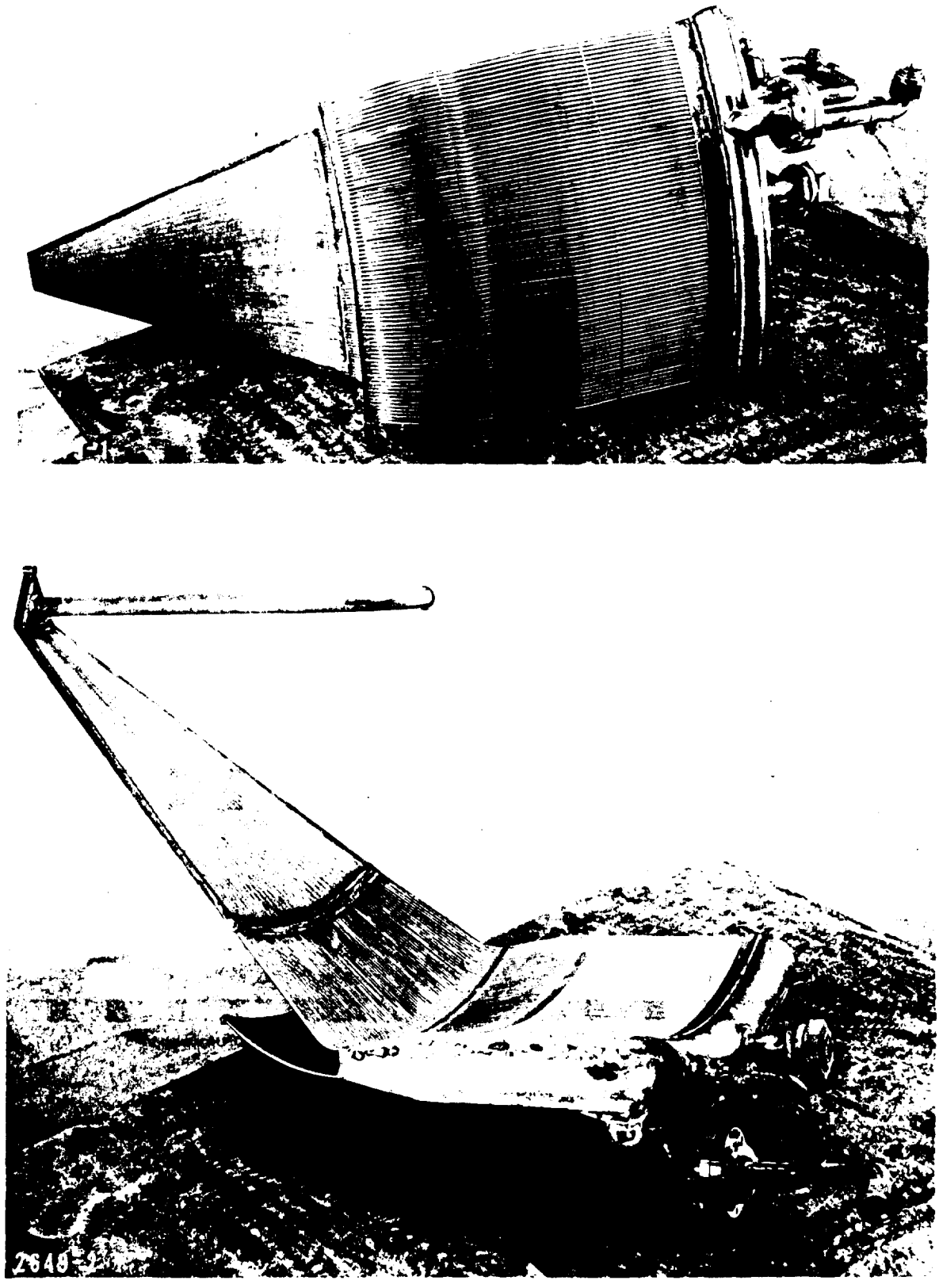

Figure 17 Cooled Segment Assembly

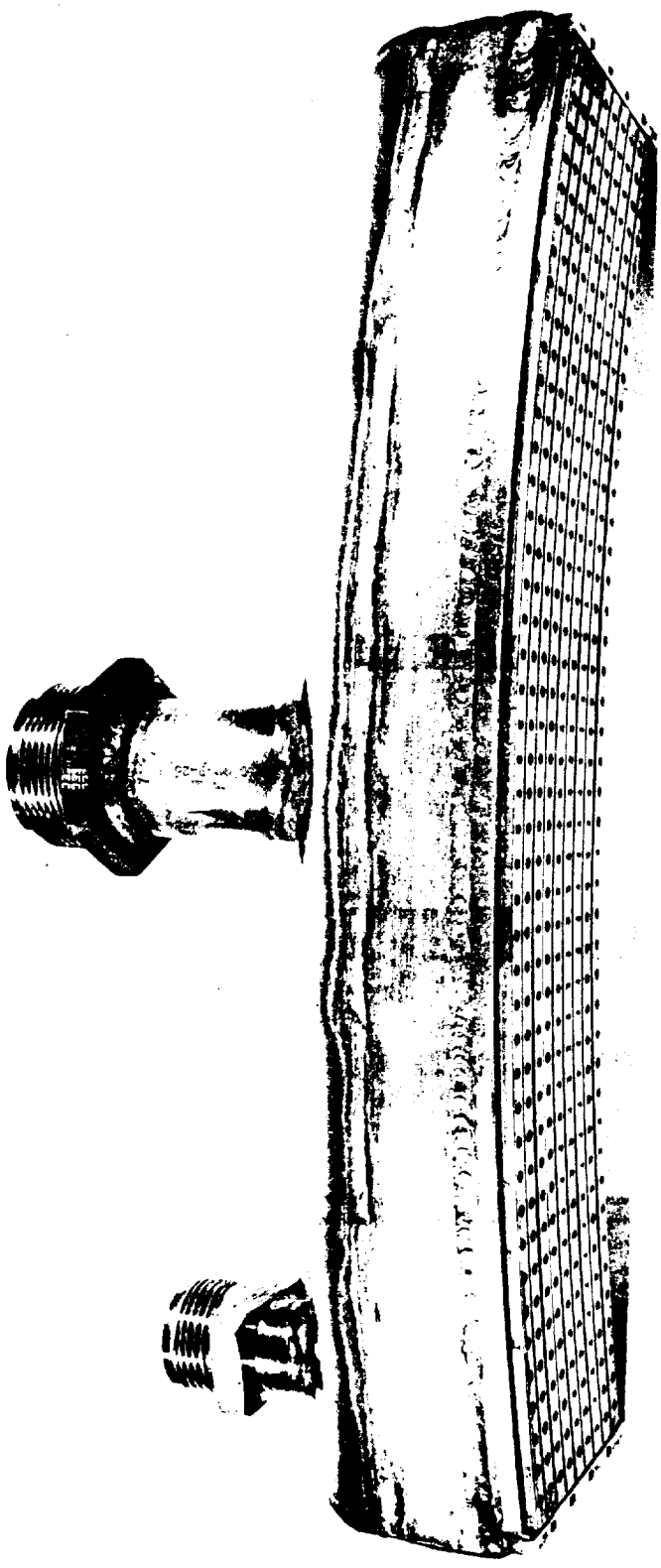

2668-1

Figure 18 Final Injector

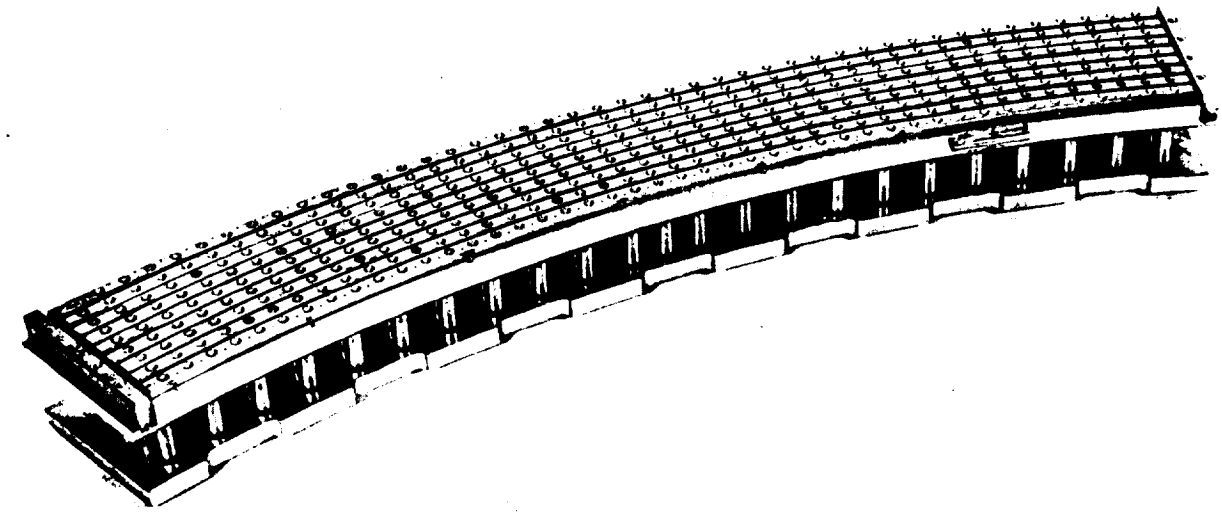

2662-1

Assembly A

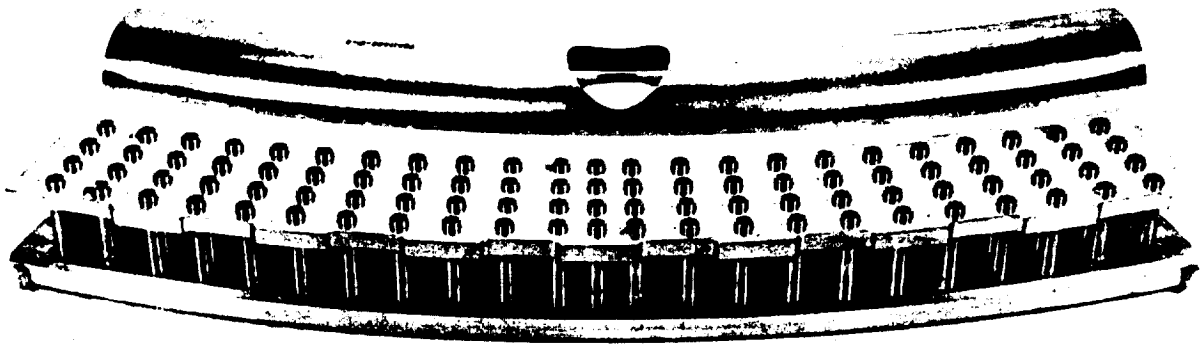

2662-2

Assembly B

Figure 19 Final Injector - Partially Assembled (Assemblies A and B)

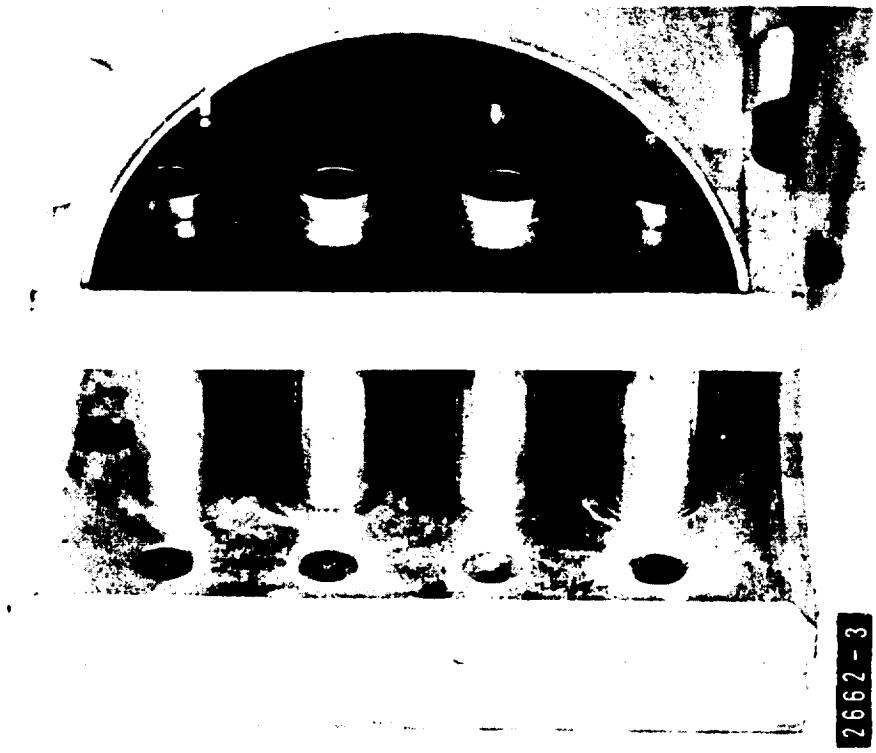

Assembly C

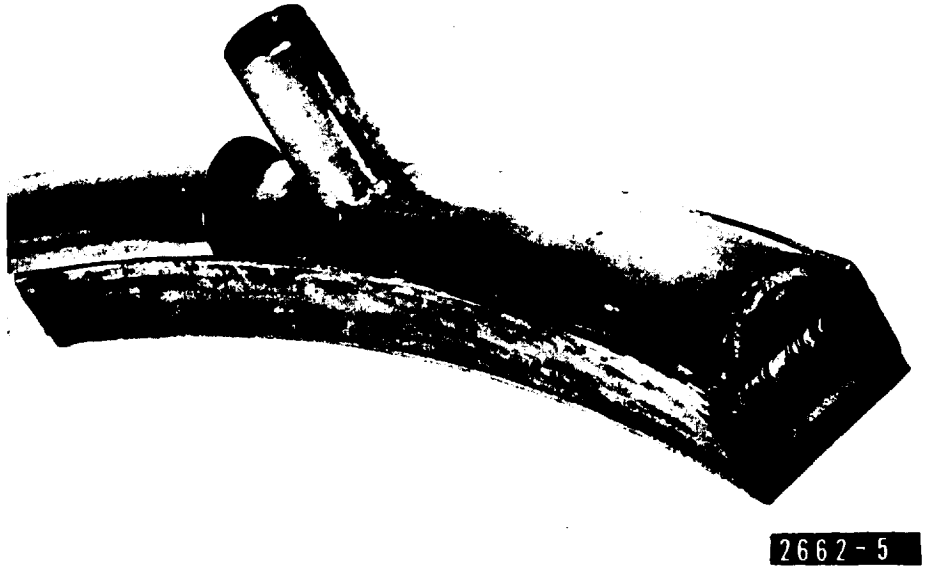

Assembly D

Figure 20 Final Injector - Partially Assembled (Assemblies C and D)

1. Task II-A. Final Injector Checkout

In total, 13 tests (Runs 51-63) were conducted with the final injector in conjunction with the heat transfer segment (Figure 12) to complete Task II-A. The results of these tests indicated that the final injector yielded: 1) reasonable heat transfer rates throughout the chamber, 2) stable operation over the required range of chamber pressures, and 3) very satisfactory performance.

Figure 21 presents a stability diagram (chamber pressure versus reactant ratio) for the final injector. It will be noted that satisfactory operation resulted between chamber pressures of approximately 200 and 320 psia and between reactant ratios of approximately 1.8 and 2.4. The required chamber pressure range for the final engine is 220 to 300 psia (under conditions of thrust vector control). It will be noted from Figure 21 that one unstable run did result at a chamber pressure of approximately 198 psia and a reactant ratio of 2.16. Actually, this particular run was stable for the first 15 seconds before going unstable, indicating that the lower stability limit was being very closely approached. A stable run near the same operating conditions (P_c = 192 psia, O/F = 2.11), which was conducted after the unstable run, confirmed this conclusion.

Figure 22 presents the measured performance of the final injector as a function of reactant ratio and indicates that the final injector yielded reasonable performance (C* ≈ 5125 ft/sec). As with the previous models of this injector, performance appeared to reach a maximum at a reactant ratio of 2.1. This injector was employed throughout the remainder of the program.

In calculating the values of C* reported in Figure 22, a corrected throat area was employed. The explanation for the use of a correction factor is as follows: Figure 23 presents a curve showing the measured thrust coefficient as a function of pressure ratio for all the tests in this

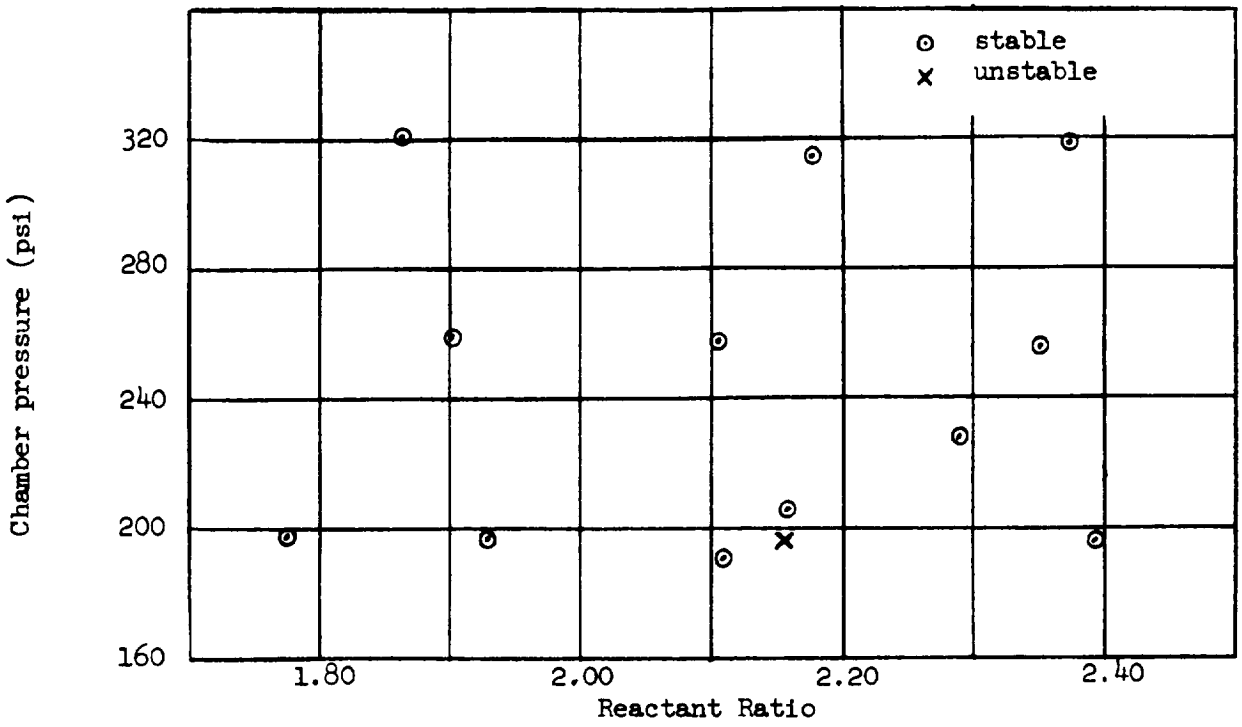

Figure 21 Stability Diagram for Final Injector

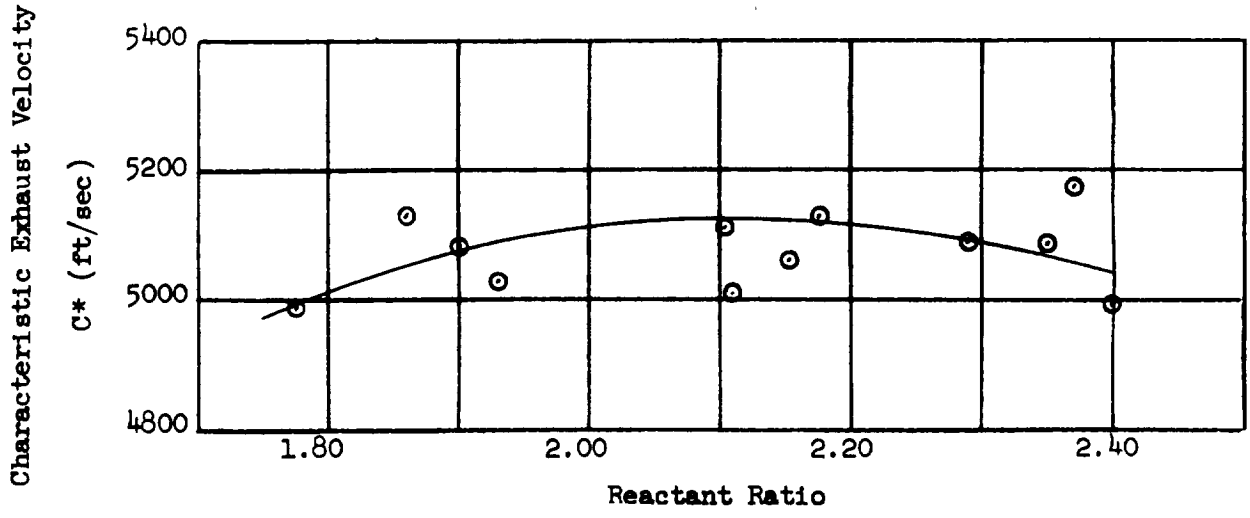

Figure 22 Characteristic Exhaust Velocity for Final Injector

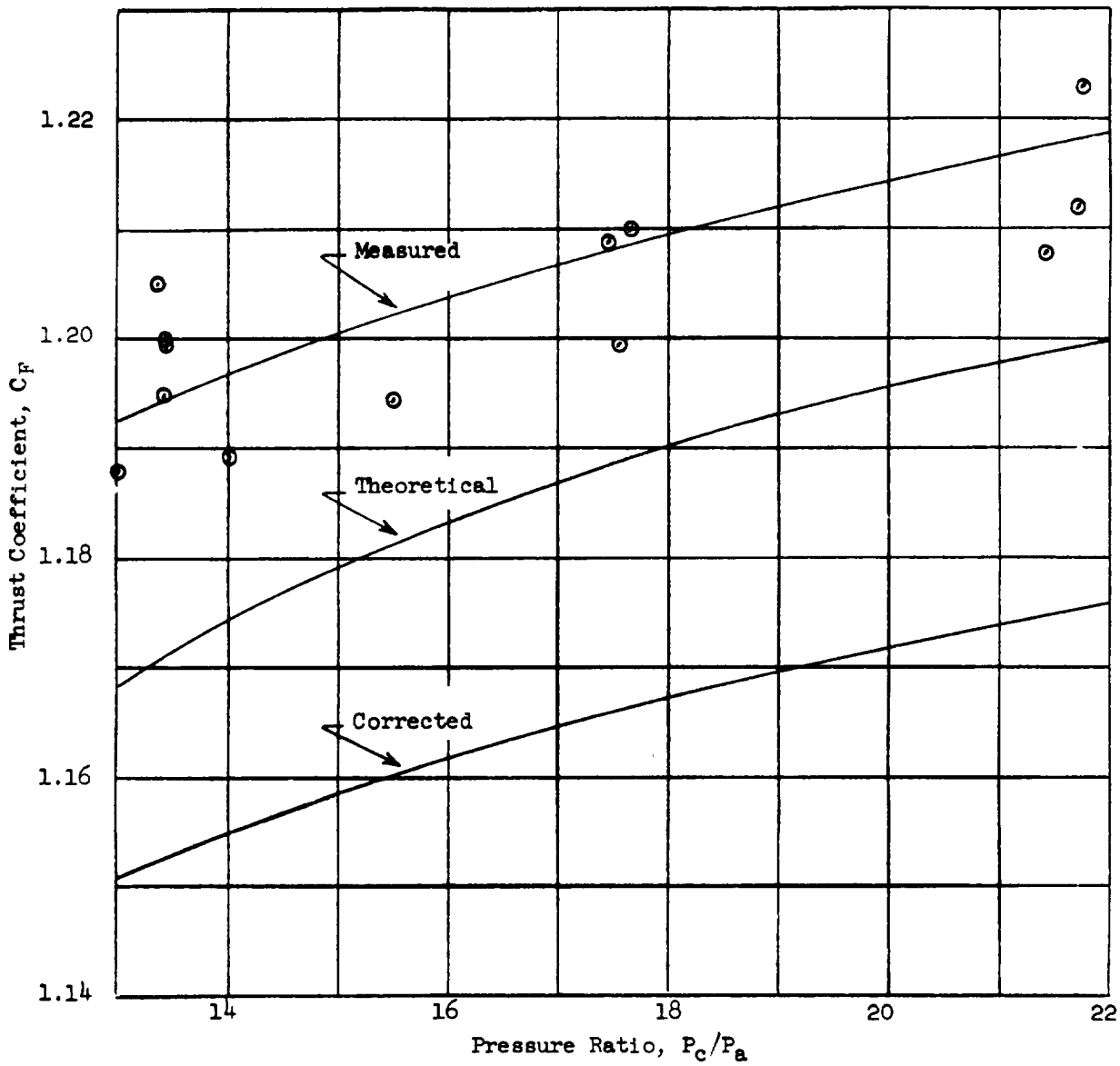

Figure 23 Thrust Coefficient as a Function of Pressure Ratio

phase of the work. Also included in this figure is the curve which gives the theoretical values of thrust coefficient.[1] The experimental thrust coefficients shown are actually higher than theoretical (by approximately 2 percent). Such results are possible only if the throat area used was incorrect. It was therefore concluded that the true throat area could not be measured satisfactorily. In order to obtain a reasonable estimate of the actual throat area, it was assumed that the thrust coefficient was equal to 98.5 percent of theoretical (1.5 percent below theoretical). On that basis the measured throat area value was increased by 3.5 percent (2.0 percent plus 1.5 percent). The lower curve of Figure 23 presents the corrected thrust coefficient based on the adjusted throat area. The measured performance of the final injector (Figure 22) was based on the adjusted throat area. Tabulated results for Task II-A are presented in Table B-III, Appendix B.

2. Task II-B. Cooled Segment Development Tests

This task was concerned with the testing of complete cooled one-eighth segments in conjunction with the final injector as illustrated earlier in Figure 17. These segments comprised the same components which were later employed in the final engine assembly.

The basic objectives of these tests conducted under this task were: 1) to establish exact start sequences to be employed when testing the complete engine, and 2) to completely prove out a final cooled segment (eight of which comprise a complete engine) under exactly the same operating conditions to which it would later be subjected in the final engine tests.

These objectives had to be accomplished under both water-cooled and regeneratively cooled conditions, since start-up information was required for both Tasks III and IV. The start sequence established under water-cooled

---

[1] The thrust coefficient is extremely low, since these tests were conducted with a chamber which terminated at the throat (area expansion ratio = 1.0)

conditions was directly applicable to the start sequence later employed in the complete uncooled engine testing (Task III), while the start sequence established under regeneratively cooled conditions was directly applicable to the complete engine testing later conducted under Task IV.

For the Task II-B series of tests, the cooled segment was enclosed in a special test fixture (Figure 24, View A). The purpose of this test fixture was twofold: 1) it provided structural support for the segment being tested (structural support of individual segments was inherent in the over-all engine design, but not for an individual segment), and 2) it confined the exhaust jet downstream of the throat by means of radial walls (segment partitions end at the throat). These radial walls are clearly visible in Figure 24, View B (looking upstream from the exit section) which shows the segment in its test fixture.

Results of the tests conducted under this task are presented below.

Runs 64 through 77 were employed to determine the start sequence (Objective 1) and resulted in the following start sequence for the case of water cooling. *

At shoot switch, electrical power was applied to open the low stage oxidizer valve, allowing oxidizer to flow into the chamber at approximately 20 percent of the nominal flow rate; at the same time the oxidizer purge valve was closed and the TEA valve supplying igniter fluid to the chamber was opened. Approximately one-half second later, a low pressure TEA - gaseous oxygen fire was established in the chamber. At 0.5 seconds after shoot switch, electrical power was supplied to close the fuel purge valve and open a methane gas valve located immediately downstream of the fuel low-stage valve. Combustion of the methane gas, TEA, and oxidizer generated a chamber pressure of approximately 1 psig. Since the methane entered the chamber through the

---

* This corresponds to the sequence that was later employed in Task III (complete uncooled engine testing) of the program.

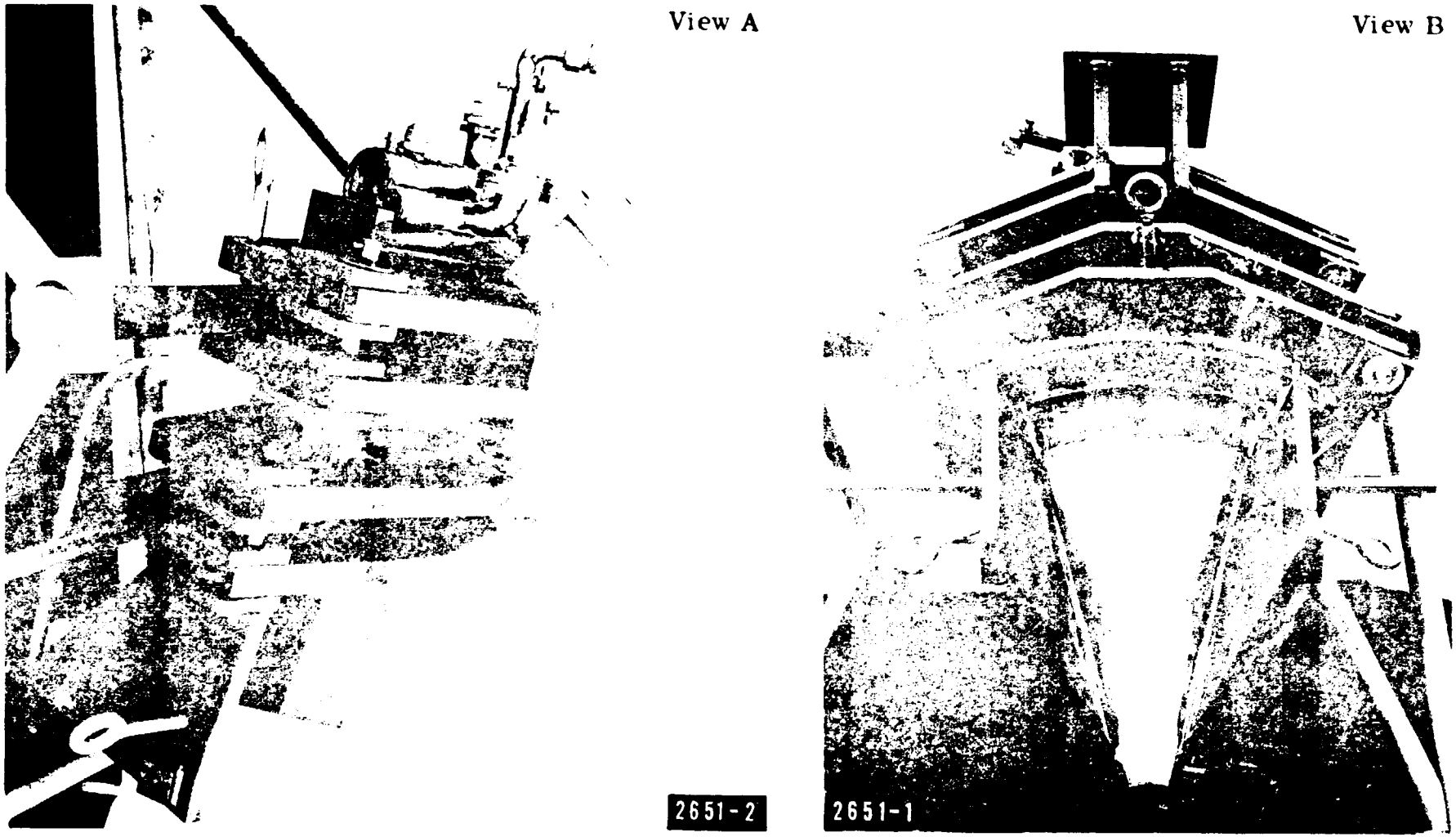

Figure 24 Cooled Segment in Test Fixture

fuel injection holes, a smooth, even-burning fire was established across the injector face prior to fuel injection. At 2.9 seconds, both the fuel low-stage valve and the methane valve feeding gas to the fuel injector opened (a second methane valve was required, since the flow of low-stage fuel terminated the initial methane flow by closing a system check valve). Approximately eight-tenths of a second later, low-stage fuel arrived at the injector, terminating methane flow to the injector through the second valve, and igniting with the low-stage oxidizer flow. At 3.9 seconds, the fuel mainstage valve opened, initiating full fuel flow to the chamber and establishing preliminary stage combustion at a reactant ratio of 0.55 and a chamber pressure of 75 psia. Also at 3.9 seconds, the electrical signal to the main oxidizer valve was applied; 0.3 seconds later the TEA valve and both methane valves were closed (the flow through these valves had been previously terminated by system check valves). If a positive indication of 40 psig chamber pressure was not received by the engine sequencer within 4.4 seconds after shoot switch, the engine shutdown sequence was initiated before the main oxidizer valve had time to open.

The start sequence employed for the case of regenerative cooling (established by Runs 86 - 92) was for all practical purposes the same as that described above. The chief difference was the initial actuation of the oxidizer side of the system with respect to the fuel side, since time had to be allowed for the coolant passages to fill with fuel. This same sequence was later employed in Task IV (Complete Cooled Engine Testing) of the program.

Tabulated results for the tests employed to establish the start sequences for water cooled and regeneratively cooled conditions are not included in this report. Since these were short-duration ignition tests, the usual performance parameters were not meaningful under the test conditions as performed.

Table B-IV, Appendix B, presents the results obtained for all of the long-duration water cooled tests (Runs 78 through 85) conducted with the cooled segment. Runs 78 through 81 and Run 85 were conducted at nominal operating conditions of chamber pressure and reactant ratio. Run 82 was conducted at low chamber pressure conditions (nominal low chamber pressure = 220 psia), and Runs 83 and 84 were conducted under high chamber pressure conditions (nominal high chamber pressure = 300 psia). The majority of the runs in this series had a duration of 20 seconds.

The only difficulty encountered in this series of tests was in Run 79 (Table B-IV, Appendix B) In this run, the divider post at one end of the cooled segment was damaged, and the segment had to be removed from the pit. Examination of the hardware showed that excessive localized heat transfer rates had occurred in that region where the divider post joins the inner tube bundle assembly. In this particular segment, the divider posts were brazed to the inner and outer tube bundle assemblies from the outside of the combustion chamber only. This resulted in small open "slots" between the tube bundle assemblies and the divider posts along the four internal corners of the combustion chamber. It appears that the small hydraulic diameter of the slots resulted in excessive heat transfer rates in those regions. A new segment was fabricated in which the aforementioned slots were filled with braze material from the inside of the combustion chamber. This latter modification resulted in satisfactory operation in all subsequent tests.

In total, eleven regeneratively cooled tests were conducted (see Table B-V Appendix B). Seven tests were of nominal 20 second duration, three were start tests (1 second duration), and one test (Run 101) resulted in an erroneous instability shutdown. Runs 93 through 96 were conducted at nominal chamber pressure. Runs 97 through 99 were conducted at 15 percent below nominal chamber pressure, and Runs 100 through 103 at 15 percent above nominal chamber pressure. The average reactant ratio for all of the long duration tests

was 2. 14. For Runs 97 through 103, a special piping arrangement was employed which maintained the fuel coolant flow (through the motor body) at nominal conditions for high and low values of chamber pressure.

The aforementioned tests simulated engine operation under thrust vector conditions. Table B-V in Appendix B summarizes the results of the regeneratively cooled tests; performance and heat transfer data are included only for the long duration tests.

In Table B-V, Q_2 and Q_3 refer to the total heat rejected to the coolant; Q_2 is the peak heat rejection rate (which occurs at the beginning of the run) and Q_3 is the steady-state heat rejection rate. Steady-state operation was generally achieved within 10 seconds after the aforementioned peak value occurred. According to Table B-V, the indicated peak heating rates are of the order of 25 percent greater than the steady-state values. At steady-state conditions the average over-all heat flux to the segment (ratio of total heat rejected to total surface area) was 0. 77 BTU/sec in^2, and the data from all runs were within ± 7 percent of this value. Calculations based on the experimental values of total heat rejected to the segment showed that the maximum coolant side wall temperature was approximately 631 degrees F at steady-state conditions.

In Run 96 a minor leak developed in the combustion chamber. Examination of the hardware indicated that this leak occurred as the result of a crack which developed between two of the cooled tubes. This allowed the combustion gases to escape by gradually burning through the thick (approximately 1/4 inch) film of epoxy resin which held the cooled segment in its test fixutre. The cooled segment was removed from the pit, the necessary repairs were made and the segment was reinstalled in the pit, after which no further difficulties were encountered.

It should be noted that such cracks between the tubes of rocket motor chambers are quite common. However, in general they cause no difficulties as long as the chamber is wire-wrapped, with a thin layer of epoxy resin

between the wire wrapping and the tube bundle. The difficulty encountered in Run 96 was therefore not considered serious insofar as the complete cooled engine (which is wire-wrapped) was concerned, and was simply peculiar to the tests that were conducted with the individual cooled segments (which were not wire-wrapped).

C. TASK III. UNCOOLED CHAMBER TESTING (COMPLETE ENGINE)

This phase of the program consisted of testing a complete uncooled chamber consisting of eight individual segments identical to those employed in the final cooled engine. The primary objectives of this task were as follows:

1. To obtain start information, with respect to the test system as well as for the complete engine, to be employed later, when testing the complete cooled chamber.

2. To check out all of the untested injectors from the standpoint of stability prior to their installation in the final cooled engine.

3. To obtain both performance and thrust vector control data with respect to the complete engine.

In addition to the above objectives these tests served to check out the test stand, including the thrust vector system, without endangering the more expensive cooled hardware.

Figure 25 presents an exploded view of the components which comprise the uncooled chamber. Figure 26 presents two views of these same components assembled prior to the installation of the eight injectors. The internal and external geometry of this chamber was identical to that employed in the final cooled chamber so that all operating conditions were exactly duplicated. Figure 27 is a photograph of the uncooled chamber with its eight injectors installed, while Figure 28 shows the complete uncooled chamber with some of its associated manifolds installed.

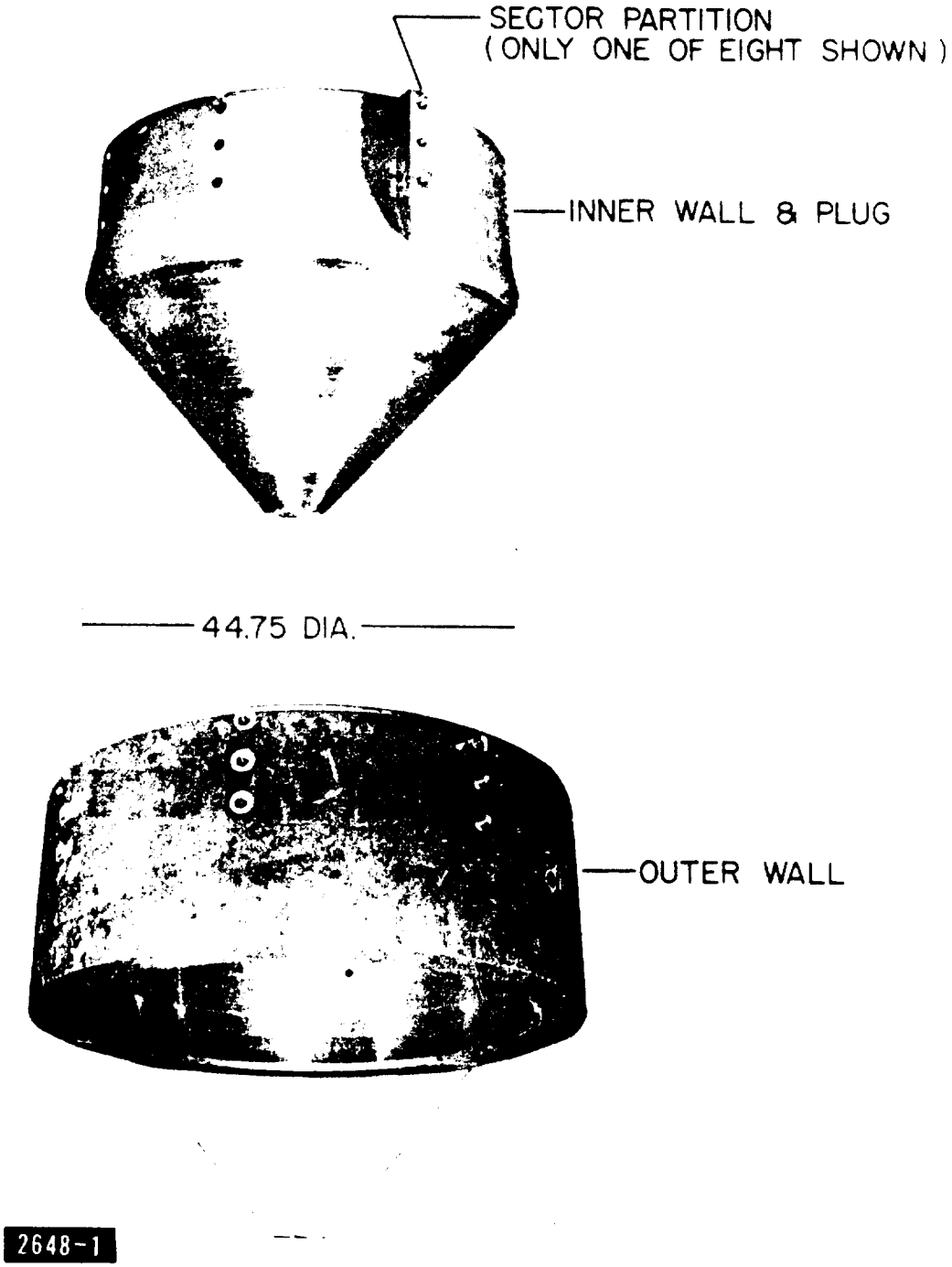

Figure 25 Exploded View of Uncooled Chamber

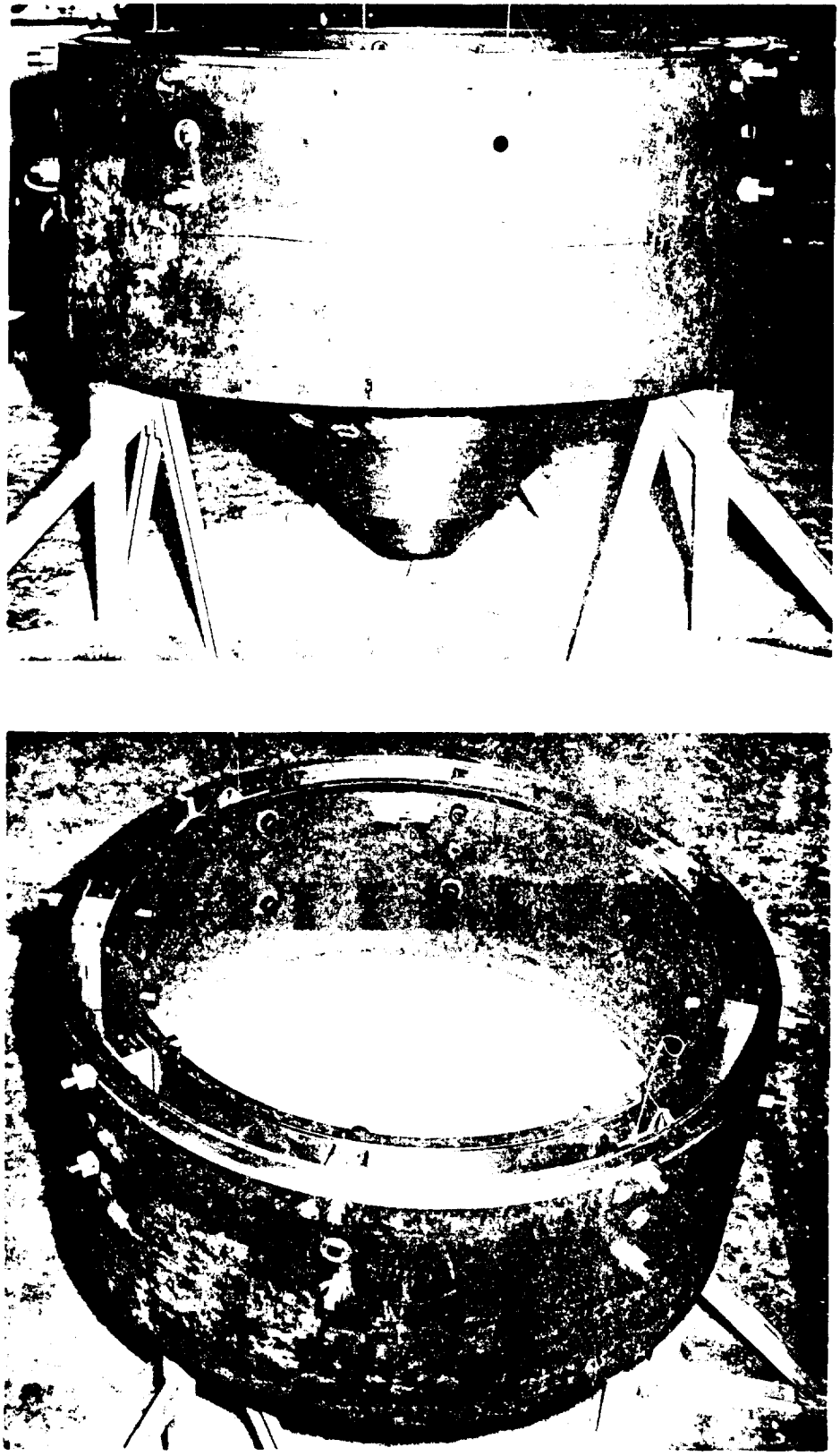

Figure 26 Uncooled Chamber Assembly

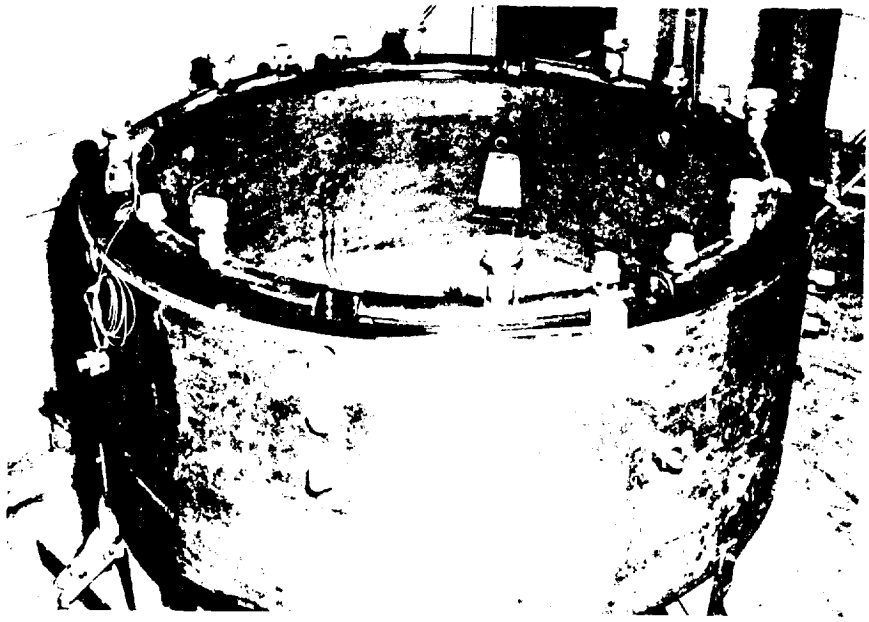

Figure 27 Uncooled Engine Assembly

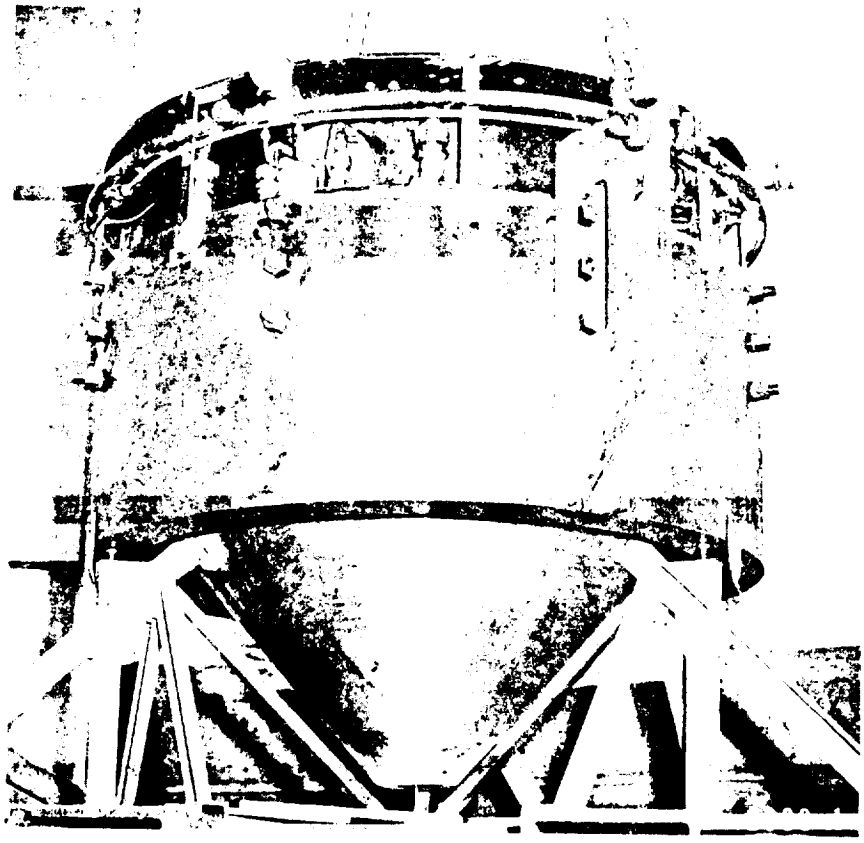

Figure 28 Uncooled Engine Assembly with Manifolds

In total, 14 tests were conducted with respect to establishing start techniques, which culminated in two short duration full thrust tests.[1] Very satisfactory operation of the complete engine resulted, with all of the individual chamber pressures being within approximately 2 psi of one another. Following the start tests a series of 17 hot tests were conducted under full stage conditions. Figure 29 is a photograph of one of these mainstage tests. A total accumulated run time of 59 seconds under full thrust conditions was achieved under this series of tests. Pertinent data for these tests is presented in Table B-VI - Appendix B.

In analyzing the data of Table B-VI only Runs 45 through 54, (which followed a recalibration of the thrust system) were considered. A statistical analysis of the primary data for these runs indicates the following average parameter values and associated variations. Percentage variations, 2σ, correspond to two standard deviations, as shown in Table II.

TABLE II

AVERAGE PARAMETER VALUES

Average chamber total pressure, psia	P_{oa}	$= 254.8 \pm 0.768\%\ 2\sigma$
Average reactant ratio	$R_{O/F}$	$= 2.087 \pm 1.373\%\ 2\sigma$
Average specific impulse, sec.	I_{sp}	$= 201.1 \pm 1.86\%\ 2\sigma$
Average thrust coefficient	C_F	$= 1.241 \pm 0.762\%\ 2\sigma$
Average characteristic exhaust velocity, ft/sec.	C^*	$= 5216 \pm 1.251\%\ 2\sigma$

Figure 30 presents a bar graph which compares the experimental plug nozzle thrust coefficients to those for a bell nozzle. The value indicated by the top of each of the bars in Figure 30 was obtained by dividing the experimentally determined values of thrust coefficient by the thrust coefficient for a bell

[1] No tabulation of test data of these runs is included in Appendix B, except for the two full thrust tests.

Figure 29 Firing of Uncooled 50,000-Pound Thrust Plug Nozzle Engine

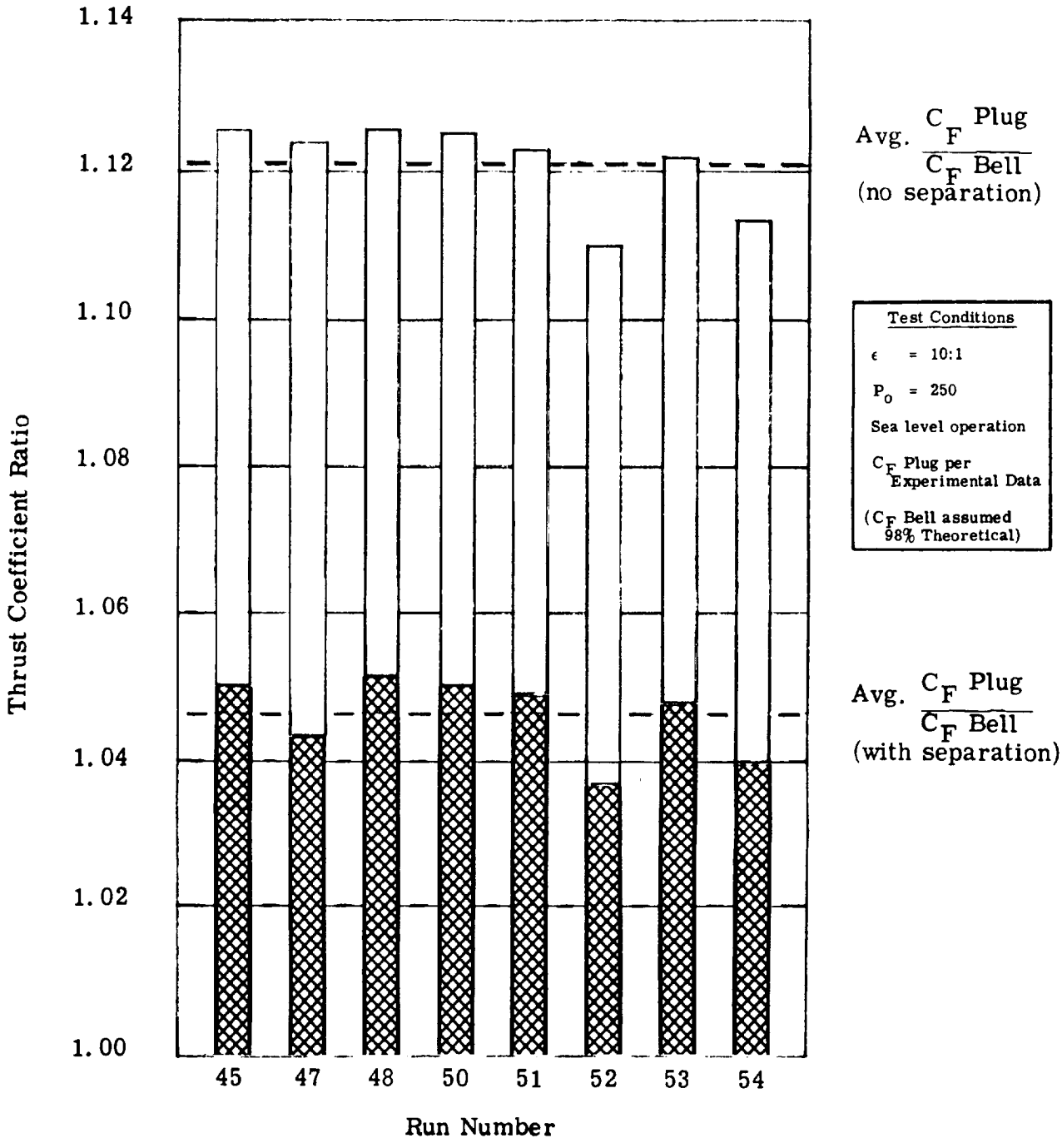

Figure 30 Comparison of Plug and Bell Nozzle Performance

nozzle having the same area ratio and operating at the same pressure ratio under nonseparated conditions (assuming the bell nozzle operates at 98 percent of theoretical thrust coefficient). Figure 30 shows that the measured thrust coefficients were approximately 12 percent greater than those which would be expected for a bell nozzle operating under nonseparated conditions. The value indicated by the top of the cross-hatched section (lower value) for each of the bars in Figure 30 was obtained by dividing the experimentally determined value of thrust coefficient by the thrust coefficient for a bell nozzle having the same area ratio and operating at the same pressure ratio under separated conditions. These results indicate that the thrust coefficients obtained were approximately 5 percent greater than those that would be expected with a bell nozzle under actual operating conditions.

It should be noted that the plug nozzle employed in these tests had a cone half angle of 42.5 degrees. According to previously obtained results (see Reference 2) even higher values of thrust coefficient would be expected if smaller values of cone half angle (nearer isentropic) were employed.

Seven tests were conducted with the uncooled 50K engine operating under vectored conditions. Thrust vector variation was obtained by means of orifices inserted in series with the propellant injector feed lines. These orifices served to increase the chamber pressure in four of the segments and reduce the chamber pressure in the remaining four segments. Experimental data were obtained at an average operating pressure ratio (P_c/P_a) of 17.3, with overpressures ($\Delta P_{ch}/P_{ca}$) at 4.6, 8.5, 12.4 and 17.3 percent. To be consistent with the standard method employed for presenting vector data the results are presented in terms of a vector angle and vector shift as referred to the engine lip. The data presented in Figure 31 were corrected for engine misalignment by subtraction of the vector angle and vector shift obtained during a reference (balanced chamber pressure) run from each of the vector data points; this reference run (Run 45) is shown at the origin in both parts of Figure 31.

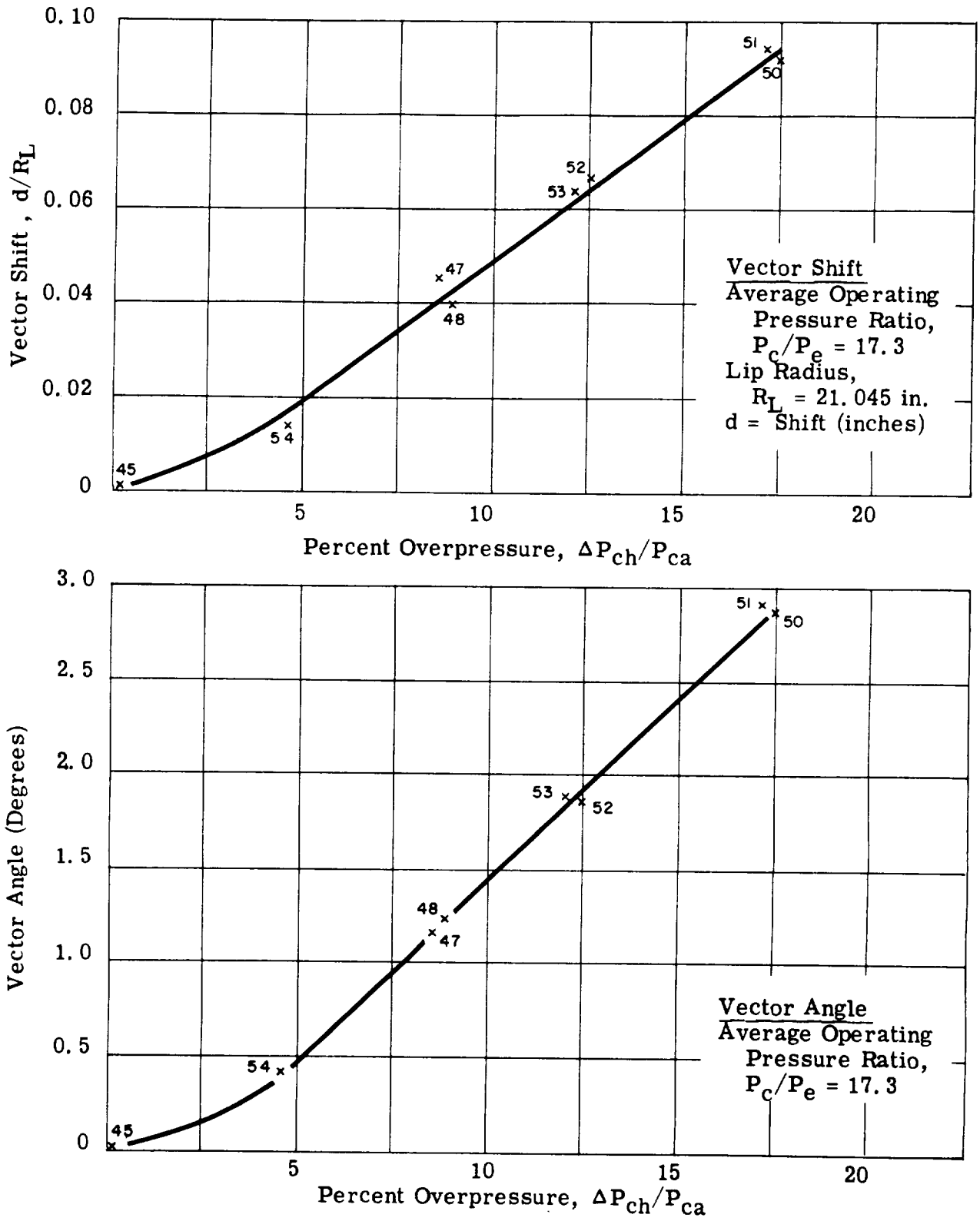

Figure 31 50K Engine - Thrust Vector Results

Figure 31 shows that nonlinearity exists in the region $0 < P_{ch}/P_{ca} < 5$ percent. The cause of this nonlinearity is suspected to be either an error in the reference run (Run 45) or a small amount of hysteresis in the thrust system, which could occur at low vector angles. In either case the reported results can be considered conservative; the assumption of linearity for the first portion of Figure 31 would increase the reported results by approximately 0.5 degrees.

As shown in previous plug nozzle investigations, the vector angle and vector shift combine to produce an effective vector angle. This effective vector angle can be shown to be a function of the distance from the engine lip to the center of gravity of the vehicle.

Figure 32 presents the effective vector angle as a function of the distance from the engine lip to the center of gravity of the vehicle. This curve was obtained by combining the results of Figure 31 for various values of the distance to the center of gravity of the vehicle at a fixed value of percent overpressure $\Delta P_{ch}/P_{ca} = 15$ percent which is considered a reasonable operating condition. To obtain a closer estimate of the effective vector angle, the distance to the center of gravity of the vehicle must be estimated. Such an estimate was made by assuming a pressurized two-stage vehicle having equal thrust-to-weight ratios ($N_{01} = N_{02}$), equal payload ratios ($\lambda_1 = \lambda_2$), and equal loading fractions ($f_1 = f_2$). The center of gravity as measured from the engine lip was thus determined, and found to be 10.1 feet, as indicated in Figure 32. The effective vector angle for this condition is seen to be 3.28 degrees at 15 percent overpressure.

During the vectored runs, engine performance (specific impulse) was also measured, and the results are presented in Figure 33. It is significant that engine performance is independent of percent overpressure over the range of experimental test data. This effect was also proven analytically and demonstrated experimentally in previous plug nozzle investigations.

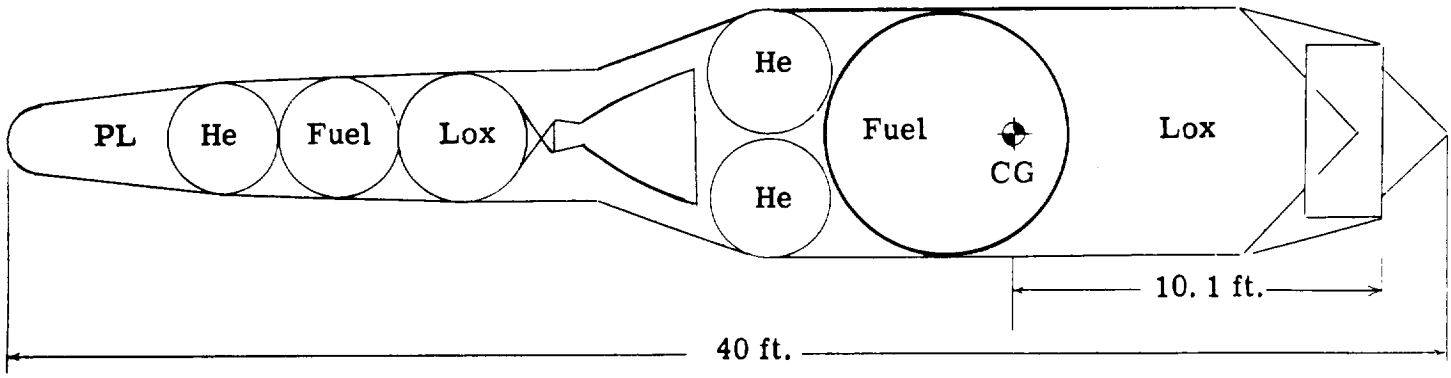

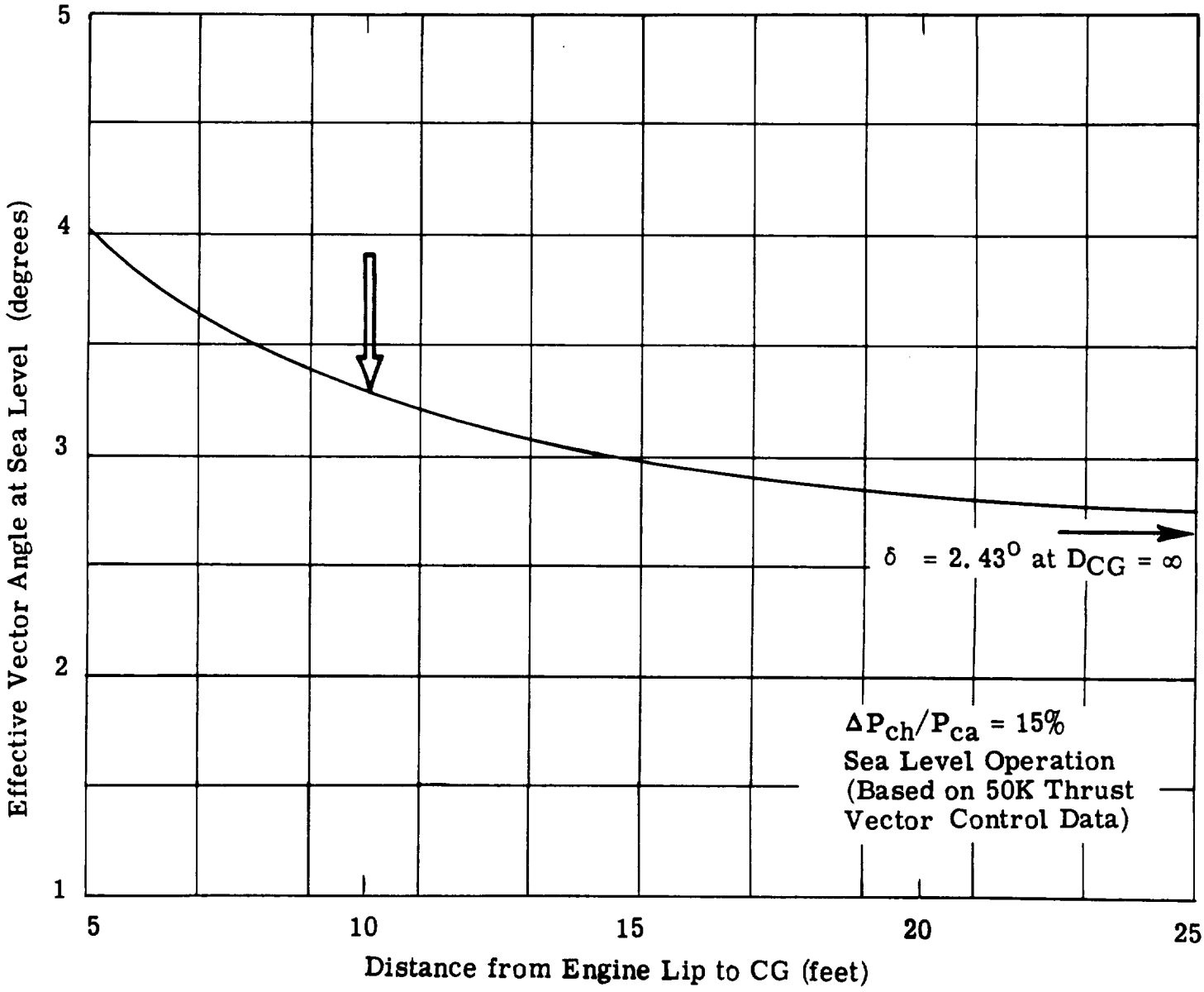

Figure 32 Variation in Effective Vector Angle

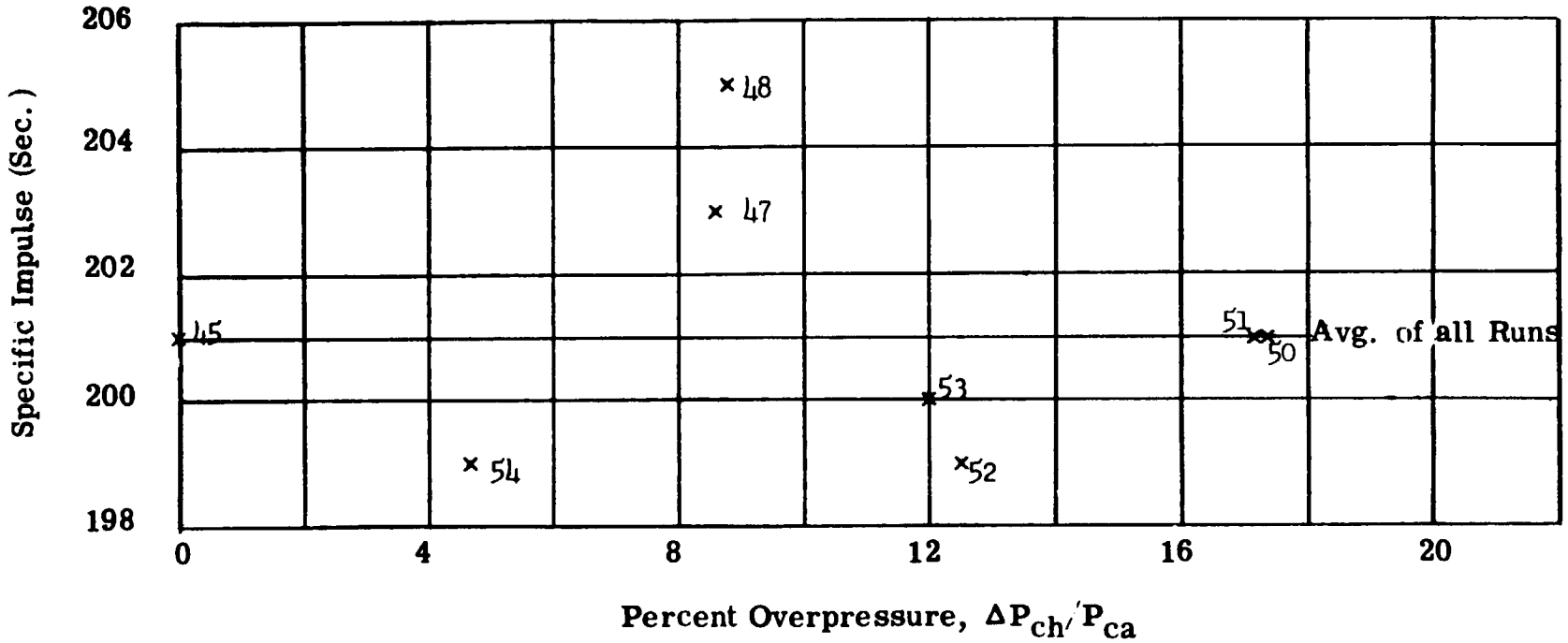

Figure 33 Variation in Performance with Percent Overpressure

D. TASK IV. COOLED CHAMBER TESTS (COMPLETE CHAMBER)

A photograph of the first complete cooled engine is presented in Figure 34. This engine is composed of eight individual segments, identical to that shown in Figure 17. Figure 34 shows the engine with the thrust mount in place, and Figure 35 is a photograph of the engine prior to wire-wrapping and installation of the thrust mount.

Extensive pressure checks and flow calibrations of each of the individual passages were conducted at all stages of the assembly operation, to assure as near perfect a chamber as possible. Any leaks that were detected or any improper flow characteristics displayed by these passages were corrected before proceeding to the next phase of the assembly operation. No difficulties were encountered in the assembly process.

A second engine, assembled later, was felt to be somewhat superior to the first engine, due to various techniques evolved during the assembly of the first engine. No tests have been conducted with the second engine.

Following engine installation (Figure 36), six tests (Runs 68 - 73) were conducted, culminating in the first main stage tests of 5.3 seconds duration at full thrust. These tests are discussed below.

Run 68 was a cold start test, conducted for the purpose of determining fuel system hydraulic and electrical delays. Runs 69 through 71 were hot starts conducted at low stage conditions (low oxidizer flow and nominal fuel flow) for the purpose of setting system interlocks and obtaining general startup information. Runs 72 and 73 were conducted under main stage conditions, and resulted in 1.2 and 5.3 seconds of operation at full thrust.

After the second preliminary stage hot start (Run 70), the engine filters on the fuel side of the system were examined and found to contain a considerable amount of foreign matter, some of which appeared to have entered the engine

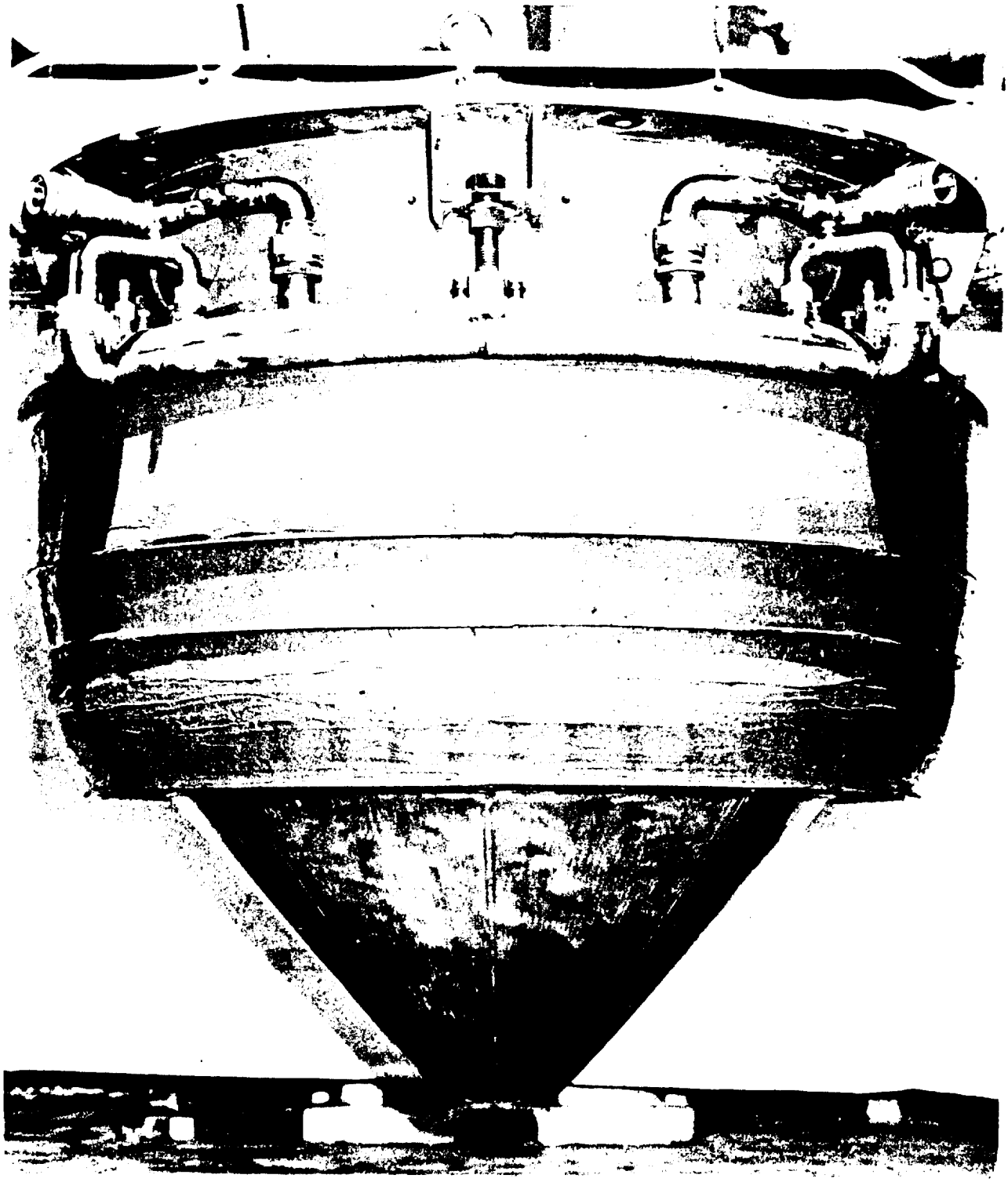

Figure 34 Complete Cooled Engine

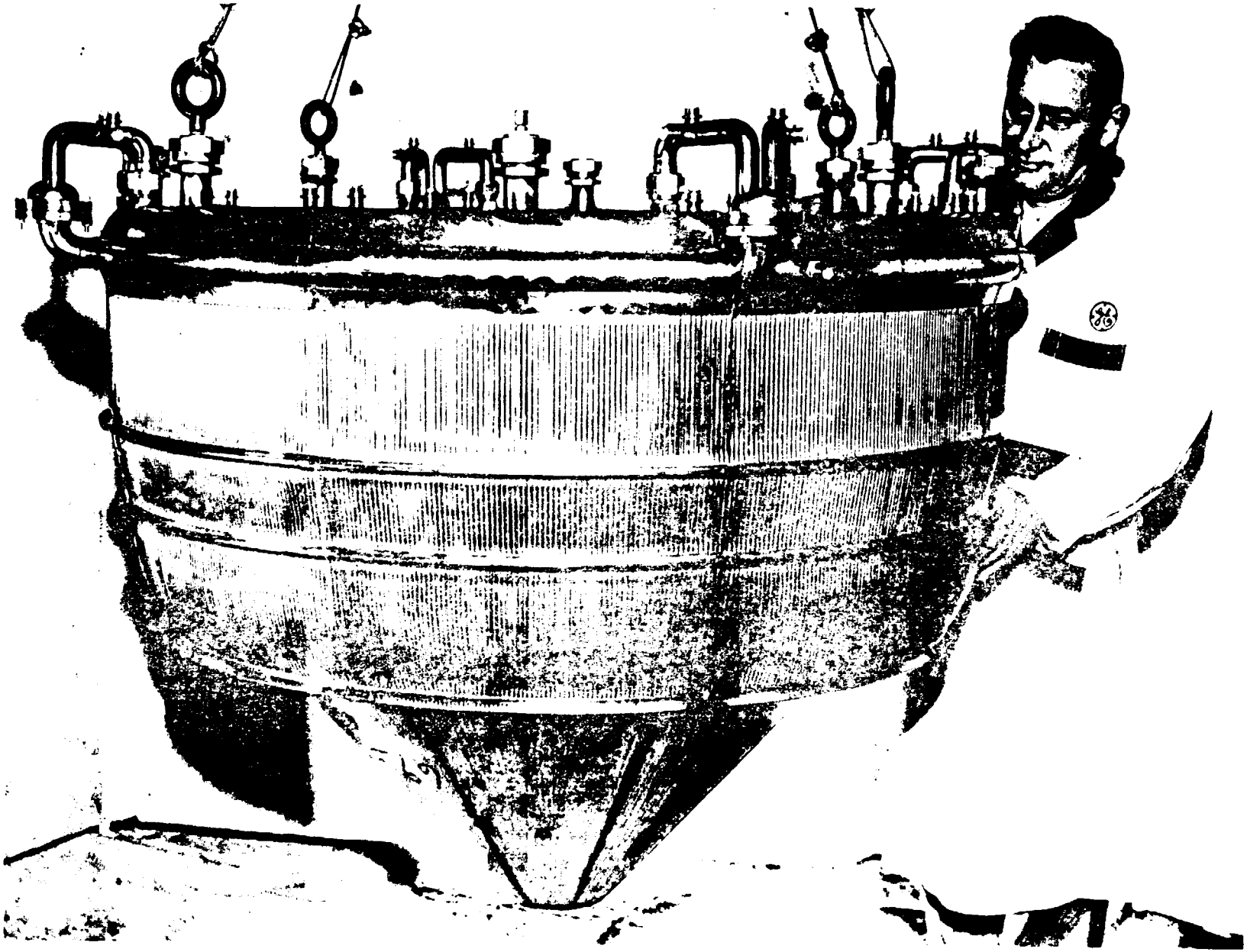

Figure 35 Cooled Engine Prior to Wire Wrapping and Thrust Mount Installation

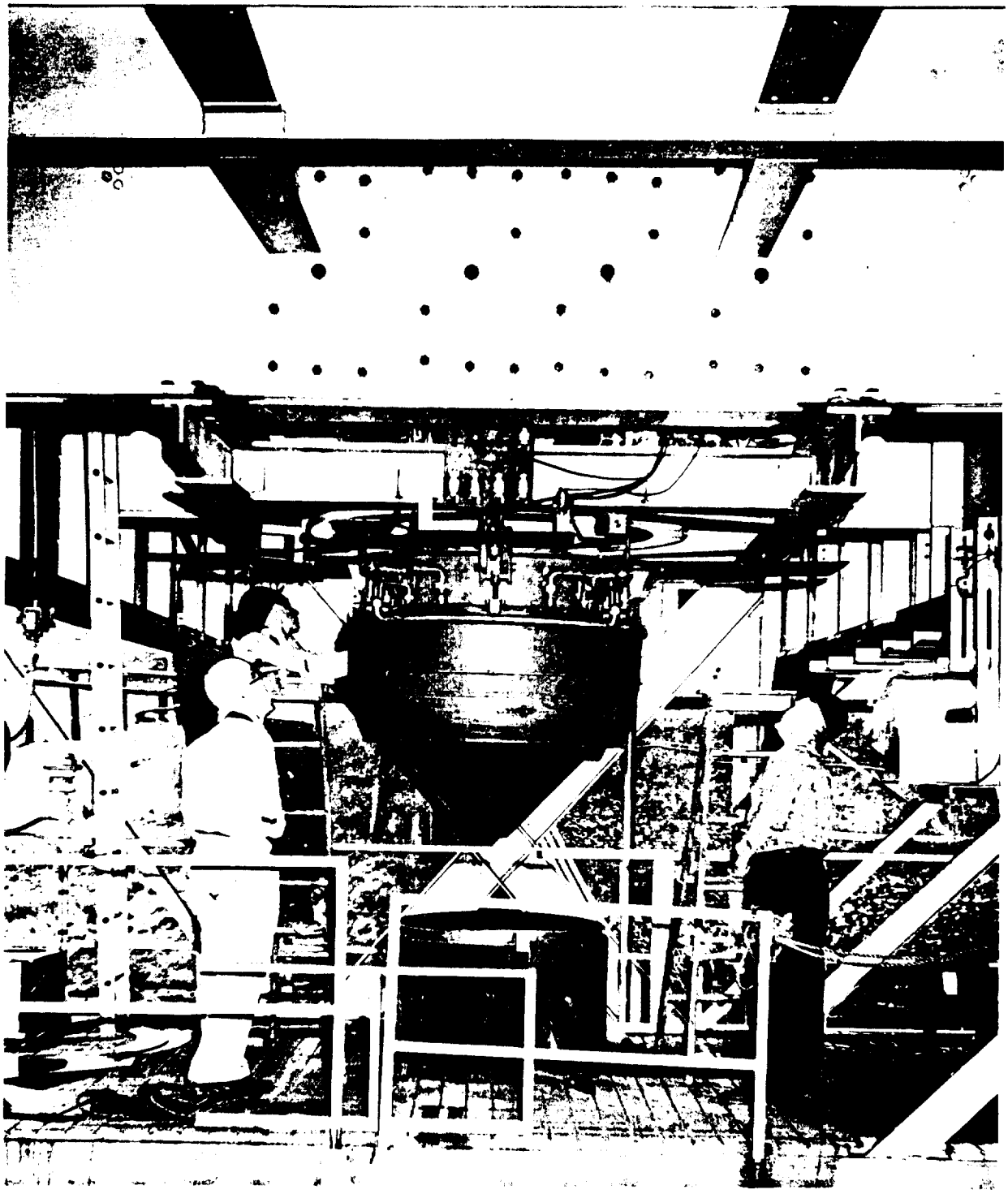

Figure 36 Cooled Engine Installed in Test Stand

coolant passages. Consequently, the fuel system was disassembled and thoroughly cleaned, and the engine coolant passages and injectors were thoroughly back-flushed to remove all such material. Examination of the system and engine after subsequent tests revealed no further difficulties, and it was concluded that all of the foreign material had been removed.

The following table presents the pertinent performance parameters obtained for Run 73 (duration 5.3 seconds at main stage); performance data was not obtained for the shorter duration runs.

TABLE III

PERFORMANCE DATA FOR RUN 73

Oxidizer flow rate, lb/sec	149.9
Fuel flow rate, lb/sec	71.0
Average chamber pressure, psia	245*
Thrust, lb	44,040
Reactant ratio	2.104
Specific impulse, sec	200
Thrust coefficient	1.247
Characteristic exhaust velocity, fps	5156
Heat flux (peak value) BTU/sec. in^2	1.1

It will be noted in the above table that the thrust was only 44,040 pounds at a chamber pressure of 245 psia. At the nominal engine chamber pressure of 250 psia, thrust is expected to be 45,000 pounds, which is 10 percent less than the design value of 50,000 pounds. This discrepancy is largely due to a reduction in throat area of 6.2 percent, incurred when the wire wrap was applied at the throat section.

---

* Average chamber pressure is average of eight cells; the standard deviation of eight cells was ±2.7 percent.

Following Run 73, some minor hardware damage was discovered. Two small cracks (approximately 2 in. x 1/16 in.) had developed in the cone section, and the wire wrap on the internal expansion section of the chamber was found to be loose. The two cracks in the cone section were repaired by welding and the wire wrap on the internal expansion section of the chamber was replaced. In addition, the cone section of the plug was flame-sprayed with aluminum oxide to provide added heat protection.

After the necessary repairs were made, a third mainstage run (Run 86) was conducted. The run duration was 5.4 seconds at main stage (approximately 11 seconds total duration); Figure 37 is a photograph of the engine operating at main stage. The following table presents the pertinent performance data obtained during this run.

TABLE IV

PERFORMANCE DATA FOR RUN 86

Oxidizer flow rate, lb/sec	150.8
Fuel flow rate, lb/sec	72.7
Average chamber pressure, psia	275
Thrust, lb	44670
Reactant ratio	2.074
Specific impulse, sec	200
Heat flux (peak value) BTU/sec in^2	1.05

As indicated in this table, the average chamber pressure was 10 percent higher than the nominal value of 250 psia; this discrepancy is attributed to additional reduction of the throat area as a result of wire wrapping.

Visual observation during the run indicated a smooth transition to main stage with apparently normal functioning of the engine for the planned 5 seconds of main stage operation. Thrust chamber inspection following the

Figure 37 Firing of Cooled 50,000-Pound Thrust Plug Nozzle Engine

run, however, revealed that three of the coolant tubes, upstream of the throat section, were split open. The location and magnitude of the leaks resulting from these splits made further testing impractical and the engine was removed from the pit. Further repair of the thrust chamber was not attempted, since fabrication of the second development chamber was complete.

Although the aforementioned splits in the coolant tubes could have been due to obstructions which blocked the coolant flow through those tubes, it appears more likely that an over-temperature condition may have occurred during the shutdown and purging transients. Since there was no evidence of burning at the points of failure, it seems highly probable that these failures must have occurred near shutdown. Otherwise some indication of burning would have been expected due to burning metal at these points of failure. With damage limited to only three tubes out of a total of 1280 tubes, no additional information regarding the tube failures was revealed by any of the recordings made during the run. Since an individual segment, identical to those employed in the complete regeneratively cooled thrust chamber, was previously operated quite satisfactorily under Task II of the program, it was concluded that the failures experienced were random in nature, and in no way attributable to the design of the thrust chamber.

Although all of the tests originally planned for this phase of the program were not completed, it is nevertheless felt that the basic objectives of this task were actually accomplished under Tasks II and III. The testing under Task II completely demonstrated the operating capabilities of an individual cooled segment identical to those used in the final engine, and the testing under Task III established the performance and thrust vector capabilities of the complete engine. It should be realized that this was the first complete regeneratively cooled engine of this type ever tested, and it is felt that, in view of this fact, the tests wer actually quite successful. It appears that the minor difficulties encountered were due to the type of shutdown technique employed and not related in any way to the engine hardware. If further testing is conducted with such an engine, a different type of shutdown procedure would be recommended.

SECTION V

CONCLUSIONS AND RECOMMENDATIONS

A. CONCLUSIONS

1. This investigation demonstrated that the plug nozzle design concept is a valid concept. It proved conclusively that by using the segmented combustor approach, a true segment of the final engine can be completely tested and developed prior to testing the complete engine. This not only reduces cost by a large factor but also saves a considerable amount of time in the development cycle.

2. Task I of the program showed that an operational injector could be developed in a very short time by this technique. Three basic injectors were initially selected, and in only three months' time one of these injectors was proven to be satisfactory from the standpoint of combustion stability, heat transfer and injector performance; all necessary modifications to this injector were also made during this same period. At a later point in the program(Tasks III and IV) eight identical injectors were operated satisfactorily in the complete engine, proving the validity of the segment approach.

3. Task III of the program further verified the segment approach. Under this task, the already developed injector was operated in a regeneratively cooled segment planned for later use in the complete engine. Again, all necessary modifications were effected at this time, thus establishing the final design for the regeneratively cooled segment employed in the complete engine.

4. Task III of the program showed that satisfactory thrust vector control could be achieved by operating half of the cells at 15 percent above nominal chamber pressure with remaining cells at 15 percent below nominal chamber pressure. Under these conditions, an effective vector angle of approximately 3.5 degrees was obtained.

5. Task III of the program also demonstrated the performance obtainable with this type of nozzle. It was found that this engine yielded thrust coefficients approximately 5 percent greater than a conventional nozzle operating under similar conditions with separation. Even larger gains in performance could be obtained by making the plug shape slightly longer (closer to isentropic).

6. Task IV of the program employed the final regneratively cooled chamber, and demonstrated that this thrust chamber was basically satisfactory. Some minor difficulties were encountered in that, following one test, two cracks developed in the cone section and after another test, two cracks developed in three of the tubes upstream of the throat. In both of these instances no burning of the metal adjacent to these cracks occurred and it was concluded that these cracks developed during the shutdown cycle. Both of the aforementioned tests had a total duration of approximately 10 seconds and resulted in approximately 5 seconds of operation under full thrust conditions. It was felt quite definitely that a change in the shutdown cycle would preclude such difficulty in future tests. No further testing was conducted with this chamber since it was concluded that all of the basic concepts involved in the plug nozzle concept had been proven. Task II showed that the final segments were completely satisfactory from every standpoint, including the heat transfer aspect. Task III proved operational capability as well as the performance and thrust vector control obtainable with this engine. It also demonstrated that there were no problems with regard to startup, running, or shutdown from the standpoint of hydraulic inter-action between the various cells. All of the chamber pressures and injection pressures increased very uniformly and had no influence upon one another.

7. The feasibility of a new type of material for use in rocket engine construction was also demonstrated by this program. The major portion of the plug was fabricated from a laminated sandwich type material which consisted of an inner and outer shell separated by ribs which were welded into place. This type of construction was shown to be satisfactory and is believed to provide an

inherently superior structure, which should result in weight saving advantages with further development.

B. RECOMMENDATIONS

1. The thrust vector control results obtained in this program were obtained under static conditions; that is, the engine was started up and shut down in a vectored condition through the use of orifices. It would definitely be advisable to conduct additional tests with the cooled engine to demonstrate thrust vector control under dynamic conditions, in which case valves would be inserted in the propellant feed lines to the injector. These valves would be capable of operating at various closing and opening rates so that system response could be investigated. Such tests would not only demonstrate thrust vector control under actual (dynamic) operating conditions but would also provide hardware checkout under rapidly changing conditions such as would be encountered in the actual application.

2. The over-all purpose of this particular program was to demonstrate that, after developing a basic cell, a group of these cells could be assembled to form a complete, integrated unit. Although the engine that was designed was considered to be semi-flyable, it was beyond the scope of the program to completely optimize the cell configuration. Studies have indicated that other cell shapes (in particular, square or semi-round combustor cells) should be investigated. Before proceeding to the design and development of a production type engine, it would be strongly recommended that a program involving the testing of other cell shapes be undertaken, using liquid oxygen and liquid hydrogen as the propellants.

3. It is strongly recommended that this concept should be limited to high thrust rocket engines (of the order of 500,000 pounds or larger). Although the 50,000 pound thrust size was quite suitable to demonstrate the objectives of this particular program, it was shown that this is too low a thrust level for the practical application of the plug nozzle engine (as was expected at the outset of

the program). The coolant passage pressure drop of this particular engine was considerably higher than it would be for a conventional engine having the same thrust. However, as higher thrust levels are approached, the coolant passage pressure drop for each type of engine becomes about equal. In addition, injector performance for this particular engine was somewhat low because of the large amount of wall area as compared to the flow area of the combustor gases; this necessitated using excessive quantities of fuel for curtain cooling, thus reducing performance below that which would be desirable. It was demonstrated under Contract NASw-40 that segments operating at a thrust level of 30,000 pounds yielded performance equivalent to that for a conventional engine.

APPENDIX A

DESIGN STUDY

APPENDIX A

DESIGN STUDY

Contract NAS5-445 specified the following parameters or design requirements applicable to the 50K Plug Nozzle engine.

TABLE A-I
DESIGN SPECIFICATIONS

Sea Level Thrust, lbs.	50,000
Propellant Feed	Pressurized
Propellants	Liquid Oxygen - RP-1
Expansion Ratio (A_e/A_t)	Between 10:1 and 20:1
Chamber Pressure (P_o total), psia	150 to 300

A. CONFIGURATION

Optimization studies for typical boost vehicles having a fairly wide range of thrust-to-take-off weight ratios indicated that a chamber pressure (total pressure at nozzle entrance) of 250 psia was close to optimum over a range of area expansion ratios from 10 to 15. An area expansion ratio of 10 was selected for design purposes.

A partial internal expansion nozzle configuration was selected, in which the propellant exhaust gases are contained by the diverging section of the nozzle during only a portion of the total gas expansion. This design would facilitate aerodynamic control of the thrust vector and also allow the segment to be mounted in a position providing axial flow of combustion gases through the combustion chamber. In addition this arrangement would simplify the fabrication of the segments.

The specific objectives of the 50K Plug Nozzle Project dictated that the design and production of an easily fabricated, reliable injector, capable of stable operation over a wide range of chamber pressures and reactant ratios was of greater significance than refinement of the design to obtain the highest possible injector performance. To insure that the injector performance would not be excessively low, a chamber characteristic length (L*) of 30 inches (approximately 50 percent larger than that normally employed with these propellants) was selected.

A conical type plug was assumed, since previous investigations (3) indicated that this configuration would yield additional thrust vector control with no significant losses in nozzle performance; this type of configuration also results in a more compact unit. The resulting plug apex angle was 84 degrees for an area expansion ratio of 10.

From the engine specifications and the selected value of characteristic length (L* = 30 inches), the total combustion chamber volume was computed to be 4080 cubic inches. The selection of a contraction ratio of 2.5 yielded a computed chamber width (outer annular radius minus inner annular radius) of 2.5 inches and a mean annular radius of 22.625 inches, with a mean annular circumference of 143.62 inches.

In keeping with the basic plug nozzle design concept, the annular combustion chamber must be divided into several individual segments. To achieve thrust vector control, the number of segments had to be divisible by four, so that one or more of the individual segments would form a complete control quadrant. However, four segments, each with a mean circumferential length of approximately 36 inches, would have been likely to promote combustion instability in the circumferential direction. (Furthermore, extensive studies on large engines had indicated that a large number of relatively small segments is desirable from the standpoint of construction.) Consequently, it was deemed

advisable to divide the annular chamber into eight individual segments, each having a mean circumferential length of 18 inches. After subtraction of the space required by the partitions between the individual segments, the mean circumferential length of the individual segments was reduced to approximately 17 inches. This circumferential segment length was of the same order of magnitude as that employed successfully under the NASw-40 contract.

The partitions dividing the annular combustion chamber into eight individual segments extended only to the throat, since previous investigations (3) had indicated that this design yielded a maximum amount of thrust vector control. In addition, the contract specified that the chamber should be capable of being converted to a skirted plug configuration, and partitions which stop at the throat make this most feasible. The results of the previous plug nozzle program (NASw-40) were used as a basis for the development of the configuration. A fairly conservative approach was employed, in an effort to accomplish all the objectives of this program at minimum cost.

B. HEAT TRANSFER ANALYSIS AND COOLANT PASSAGE DESIGN

The design of the coolant passages around the combustion chamber, nozzle, and plug dictated the selection of an axial flow approach, with flow passages in planes containing the engine axis, in preference to circumferential passages, which require more reversals of flow and hence a higher pressure drop.

A heat transfer analysis for the selected axial flow design was made in which the additional parameters of specific impulse of 214 seconds and reactant ratio of 2.2 were assumed. Inclusion of a fuel-rich curtain along the chamber walls would lower the heat flux to 31 percent of theoretical value, which is consistent with experimental results. Results of the analysis are presented in Table A-II.

TABLE A-II

HEAT TRANSFER ANALYSIS RESULTS

Station	Heat Flux (Btu/in^2-sec)	Coolant Velocity (ft/sec)	Gas Side Wall Temp. (^oF)	Liquid Side Wall Temp. (^oF)
Cone				
Apex	0.75	17.5	540	450
Center	0.78	15.1	565	495
Base	0.85	13.7	700	598
Thrust Chamber				
4 Inches Below Throat	0.89	21.1	493	422
Throat	2.12	31.3	824	654
Combustion Chamber	0.96	15.6	686	610
Combustion Chamber Separators				
Combustion Chamber	0.96	18.7	702	626
1 Inch Above Throat	1.65	35.6	783	651
Thrust Chamber Outer Lip				
Combustion Chamber	0.96	24.0	702	626
4 Inches Below Throat	1.29	44.4	617	514
Throat	2.12	47.5	824	654
End of Lip	0.89	41.1	511	440
Coolant Passage Pressure Drop (with manifolds)		95 psia		
Coolant Temperature Rise		232^oF		

It should be noted that in no case was the liquid side wall temperature allowed to exceed 675^oF; above this temperature, residue from the RP-1 begins to form on the walls. The predicted coolant temperature rise was 232^oF. The maximum coolant velocity required was 47.5 ft/sec. which would yield a predicted pressure drop (including manifolding), of 95 psi.

The cooled walls of the thrust chamber were to be fabricated from tubing tapered for velocity control and formed to the required contours. A uniform tube wall thickness of 0.020 inches was specified. Such tubular construction would

present some fabrication problems. However, previous experience in using tubes for combustion chamber walls indicated that such construction was practical under the time and cost restrictions of the development effort. The plug itself was to employ a sandwich-type, channeled, cellular construction.

The coolant flow path through each engine segment was completely isolated from that of adjacent segments. Fuel (coolant) entered at the tip of each plug segment through a separate feed line. It flowed up along the plug portion of the segment, through the tubular inner thrust chamber segment and up to a manifold at the injector end of the thrust chamber segment. From that manifold it was fed to the chamber partitions at each end of the segment where it flowed down the partition wall to the tip of the partition at the throat. There it reversed and flowed upwards through a second manifold. This latter manifold distributed the fuel (coolant) to the thrust chamber outer wall tubes which were cooled by a double pass arrangement; after leaving these tubes the fuel was collected in one common engine manifold which is wrapped about the periphery of the top of the engine. From the engine manifold, four lines distributed the fuel through four control orifices to the injector quadrants. This type of arrangement would permit independent cooling of the individual segments; tests on individual segments were therefore meaningful.

C. MATERIALS OF CONSTRUCTION

With the proposed propellants the only material restrictions were those on components which came in contact with liquid oxygen. Experience had shown that the 18-8 stainless steels were suitable for this application. Although no special material was required for contact with the RP-1 fuel, here again experience had shown that, with thin walled construction, the use of non-corrosion-resistant steels under normal atmospheric conditions could result in pin-hole leaks and other defects. Therefore it was established that corrosion-resistant steels would be used in both the segments and the engine fuel passages.

Chamber stresses would be contained by winding the high pressure section with high strength music wire. A flexible epoxy resin was specified to bind the wire to the chamber and to provide a tough, resilient protective coating over the wire.

Brazing of the tube segments would be accomplished with high temperature nickel brazing alloys. All of these materials and processes are common to the industry and would present no difficulties.

D. THRUST STRUCTURE

In keeping with the design specification that the engine be of a semi-flyable configuration, the airframe-engine interface contours were designed so that the engine could be installed over the elliptical end of a conventional propellant tank. In this configuration the tank wall could support any pressure load which might tend to collapse the segment and would pick up the thrust directly from the engine.

For development testing it is not practical to install the engine with the segments mounted around the end of the testing facility propellant tank. Therefore the rocket tank wall would be simulated by a heavy cylinder attached to the segment to take compressive loads and thrust. A flange was provided at the top of the cylinder to mate with the thrust measuring instrumentation. Adjusting pads between the flange and the segment would permit accurate installation of the thrust mount and support the engine in the test cell. Low carbon steel was specified for all parts of the thrust structure

E. THRUST VECTOR CONTROL

The thrust vector positioning method was based upon the premise that the total engine axial thrust remains constant. For a total decrease in thrust in certain quadrants there is a corresponding total increase in the thrust in other quadrants. Since cooling is rather critical for this engine design, the coolant flow rate through any segment could not be permitted to decrease with decreasing thrust in that segment.

The engine was therefore designed to maintain a nominal one-eighth total flow through each segment at all times. All of the fuel flow is collected in a common manifold after leaving the coolant passages. It is then redistributed to the quadrants as required for thrust vector control. Liquid oxygen flows directly to each of the quadrants from the main supply line.

In the development engine, thrust vector control was to be accomplished by placing orifices in the propellant feed lines just upstream of the injector. Provisions were made in the pipe lines for easy insertion and removal of such orifices.

This method of thrust vector control had been used on monopropellant developmental plug nozzle engines and had proved quite satisfactory.

APPENDIX B

TABULATED RESULTS

50K COMPONENT AND ENGINE TESTS

TABLE B-I	TASK IA. UNCOOLED INJECTOR TESTS
TABLE B-II	TASK IB. COOLED INJECTOR TESTS
TABLE B-III	TASK IIA. FINAL INJECTOR CHECKOUT
TABLE B-IV	TASK IIB. COOLED SEGMENT DEVELOPMENT. WATER COOLED TESTS
TABLE B-V	TASK IIB. COOLED SEGMENT DEVELOPMENT. REGENERATIVE COOLING TESTS
TABLE B-VI	TASK III. UNCOOLED CHAMBER TESTING. (COMPLETE ENGINE)

TABLE B-I

TASK I A UNCOOLED INJECTOR TESTS

Run No.	P_c (Psia)	Ratio O/F	C* (fps)	Duration (Sec)	Stable	Injector Type	Comments
1	--	--	--	--	--	I	Start Tests
2	--	--	--	--	--	I	
3	--	--	--	--	--	I	
4	--	--	--	--	--	I	
5	--	--	--	2	No	I	Unstable, Too Short to Evaluate Data
6	--	--	--	4	No	II	
7	--	--	--	4	No	II	
8	--	--	--	1.5	No	II	
9	304	2.40	5435	9	No	II	
10	--	--	--	0	No	II	
11	240	1.89	4235	9	Yes	II-A	
12	233	1.98	3998	7.5	No	II-A	
13	--	--	--	1	No	I-A	
14	281	2.15	5108	9	Yes	III	
15	286	2.19	5377	9	Yes	III	
16	264	2.41	5273	10	Yes	III	
17	264	2.36	5420	10	Yes	III	
18	265	2.21	5417	10	Yes	III	
19	262	1.88	5388	10	Yes	III	
20	282	1.95	5382		Yes	III	Data Evaluated at Both 5 & 10 secs.
	297	2.09	5550	10			
21	310	2.16	5519	10	Yes	III	
22	312	1.83	5439	10	Yes	III	
23	304	2.40	5435	9	Yes	III	
24	301	2.33	5449	10	Yes	III	
25	--	--	--	--	No	III	Unstable, Too Short to Evaluate Data
26	--	--	--	--	No	III	
27	200	1.90	--	--	No	III	
28	227	2.17	5368	9	Yes	III	
29	200	2.10	--	--	No	III	Unstable, Too Short to Evaluate Data
30	198	1.89	5321	9	Yes	III	
31	218	2.33	5346	9	Yes	III	
32	180	1.81	--	--	No	III	Unstable, Too Short to Evaluate Data
33	397	2.18	5178	7	Yes	III	
34	403	2.40	5437	7	Yes	III	
35	379	2.00	5446	7	Yes	III	

TABLE B-II

TASK IB. COOLED INJECTOR TESTS

Run No.	P_c (Psia)	Ratio O/F	C* (fps)	Duration (Sec)	Stable	Approx. Chamber Heat Flux (BTU/In^2-sec)	Comments
36	252	2.24	5086	6.5	Yes	--	
37	259	2.18	5171	24.5	Yes	0.55	
38	322	2.22	5181	24.5	Yes	0.77	
39	387	2.12	5267	20.5	Yes	0.73	
40	375	1.97	5162	13.5	Yes	0.55	
41	370	2.29	5030	7.5	Yes	0.64	
42	--	--	--	--	--	--	Oxygen Reg. Failure Shutdown due to Unstable Startup
43	--	--	--	--	--	--	
44	--	--	--	--	--	--	
45	260	2.23	5102	20.5	Yes	0.30	
46	241	1.77	5064	20.5	Yes	0.28	
47	220	1.81	5069	20.5	Yes	0.35	
48	--	--	--	--	--	--	Shutdown due to Unstable Startup
49	241	2.10	5094	20.5	Yes	--	
50	199	2.11	4814	10.5	No	--	Unstable due to low P_c

TABLE B-III

TASK IIA FINAL INJECTOR CHECKOUT

Run No.	P_c (Psia)	Ratio O/F	C* (fps)	Duration (Sec)	Comments
51	260	1.90	5087	30	
52	258	2.11	5117	30	
53	197	1.93	5030	30	
54	197	2.40	4999	30	
55	274	1.72	5050	30	
56	315	2.17	5134	30	
57	319	2.37	5181	30	
58	320	1.86	5132	30	
59	197	2.16	4995	15	Unstable at 15 sec.
60	206	2.15	5064	30	
61	192	2.11	5013	30	
62	228	2.29	5098	30	
63	-	-	-	7	Shutdown due to warm oxygen

TABLE B-IV

TASK IIB. COOLED SEGMENT DEVELOPMENT

WATER COOLED TESTS

Run No.	P_c (Psia)	Ratio O/F	C* (fps)	Duration (Sec)	Comments
78	247	2.16	5043	13	
79	268	2.07	5320	10	Divider Post Burnout
80	241	2.15	5029	20	
81	254	2.18	5073	20	
82	214	2.34	5071	20	
83	285	2.10	5018	11	
84	299	2.15	5147	20	
85	253	2.07	5114	25	

TABLE B-V

TASK IIB. COOLED SEGMENT DEVELOPMENT

REGENERATIVE COOLING TESTS

Run No.	Duration (Sec)	P_o (Psia)	Ratio O/F	Total Flow (lb/sec)	C* (fps)	Q_2 (BTU/sec)	Q_3 (BTU/sec)
93	1	236	1.86	27.1	-	-	-
94	20	258	2.07	29.0	5177	989	809
95	20	259	2.16	30.1	5012	900	764
96	20	256	2.16	30.0	4974	984	777
97	1	225	2.10	25.0	-	-	-
98	20	226	2.17	25.5	5158	975	755
99	20	225	2.14	25.5	5142	893	705
100	1	287	2.10	32.1	-	-	-
101	5	283	2.10	31.6	-	-	-
102	20	301	2.20	33.8	5189	916	771
103	20	312	2.05	34.7	5233	1031	786

TABLE B-VI

TASK III. UNCOOLED CHAMBER TESTING (COMPLETE ENGINE)

Run No.	Duration at Mainstage (Sec)	Ratio O/F	P_{oa} [1] (Psia)	C* (fps)	I_{sp} (Sec)	C_F	
38	1.33	2.08	242	-	-	-	No performance data reported for short runs
39	1.38	2.09	245	-	-	-	
40	1.96	2.08	260	-	-	-	
41	3.40	2.05	252	5134	193	1.21	
42	4.37	2.11	253	5141	-	-	No thrust record obtained. Thrust system recalibrated after Run 44.
43	4.37	2.09	252	5134	-	-	
44	-	-	-	-	-	-	Erroneous shutdown; mainstage time gate malfunction
45	4.40	2.10	255	5197	201	1.25	
46	4.38	2.43	283	5190	204	1.27	High chamber pressure due to oxidizer flow 15% above nominal
47	4.41	2.06	255	5246	203	1.25	
48	4.40	2.07	256	5270	205	1.25	
49	-	-	-	-	-	-	Erroneous shutdown; instability shutdown device malfunction
50	4.44	2.09	254	5184	201	1.25	
51	7.01	2.09	254	5197	201	1.24	
52	4.38	2.09	255	5214	199	1.23	
53	4.39	2.09	254	5174	200	1.24	
54	4.38	2.10	256	5193	199	1.24	

1. Chamber pressure is average of the eight segment pressures.

APPENDIX C

DETAILED DESCRIPTION
OF
COOLED 50K THRUST CHAMBER

APPENDIX C
DETAILED DESCRIPTION OF COOLED 50K THRUST CHAMBER

Although all of the hardware employed in the subject investigation has been described elsewhere in this report, it was deemed advisable to include a more detailed description of the cooled 50K Thrust Chamber. Detailed specifications of the 50K Thrust Chamber, which was regeneratively cooled, are presented in Appendix A. In general, the thrust chamber was fabricated from several components, which in turn were fabricated from Type 347 stainless steel, employing both brazing and heliarc welding techniques. This thrust chamber comprised eight identical segments, one of which is shown in Figure C-1. Figure C-1 shows that each segment consisted of five principal components; 1) the cone assembly, 2) the inner tube bundle assembly, 3) the outer tube bundle assembly, 4) two divider posts, and 5) the propellant injector. Before discussing these individual components, it will be useful to examine the coolant flow path through the segment.

Referring to Figure C-1, the coolant (fuel) first enters the coolant inlet and flows upward through the cone assembly and the inner tube bundle assembly. After leaving the inner tube bundle assembly, it is collected in the inner collection manifold which distributes it to the divider posts at either end of the combustion chamber. Each of the divider posts consists of a two-pass arrangement (see Figure C-5) such that the coolant (fuel) first flows down the hot side of the divider post and is then returned up the back side of the post, after which it is collected in the outer collection manifold. There it is redistributed and is caused to flow downward through each alternate tube in the outer tube bundle assembly. The coolant (fuel) is then collected in the return manifold which directs the coolant upward through all of the remaining tubes in the outer tube bundle assembly. Finally, it is collected in the exit manifold, from which it leaves through the coolant outlet. Details of the individual components are described below.

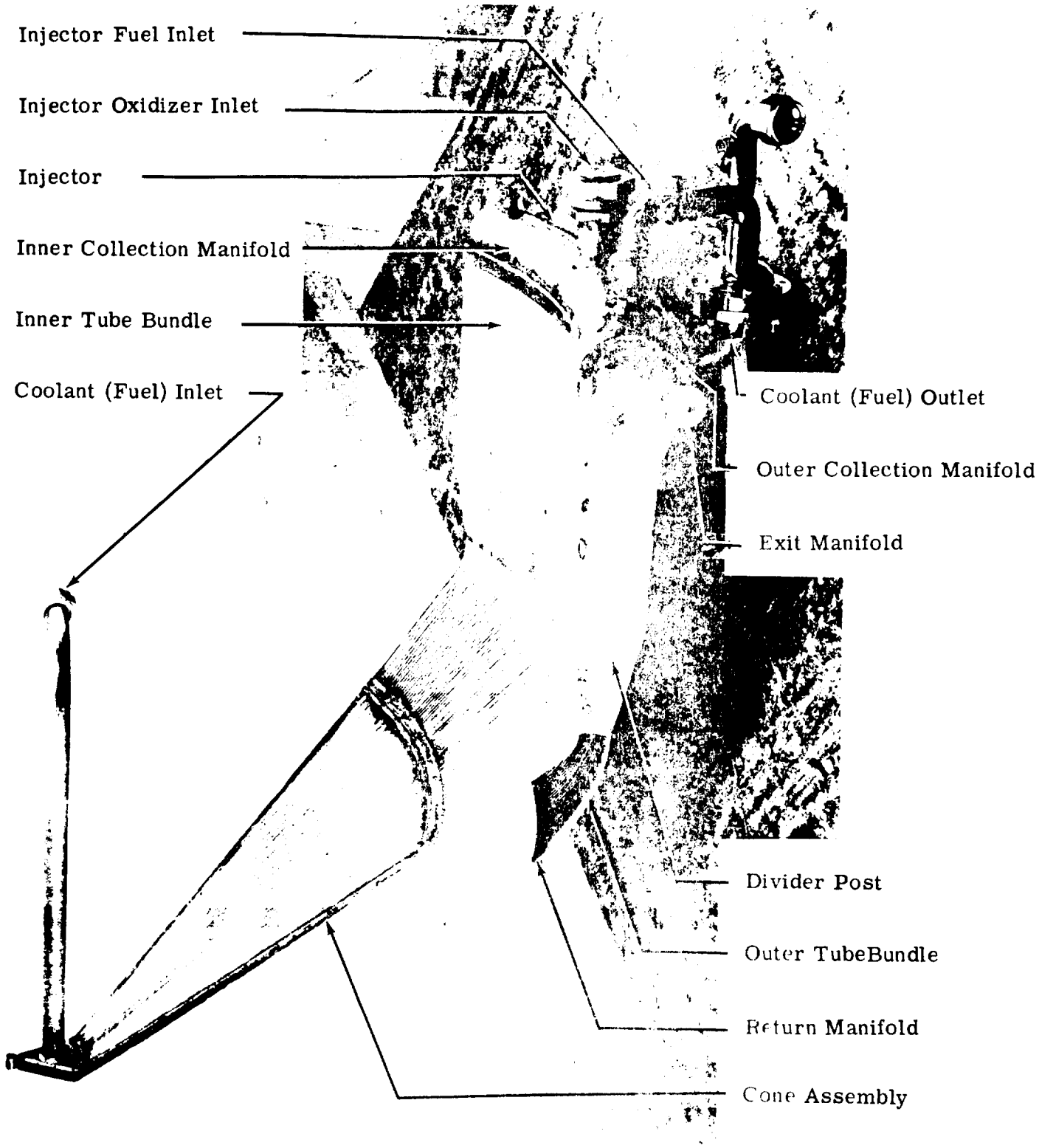

Figure C-1 Cooled Segment, with Components Listed

Figure C-2 shows a photograph of the cone segment, which is seen to be constructed of a sandwich type material. This component was fabricated by first shaping two sheets of Type 347 stainless steel to the proper contours and then continuous resistance welding the two sheets to the longitudinal supporting ribs, seen in Figure C-2. Extensive tooling was required to align the welding wheel over the 0.030 inch thick rib. The height and spacing of the ribs were adjusted so as to provide the required coolant velocity of 15 fps at all cross-sections. From the standpoint of strength, this unit was quite satisfactory. Units such as shown in Figure C-2 were tested to 1000 psi without permanent set. It should be noted that similar samples have been tested as high as 9000 psi with considerable deformation but no weld failure; this is particularly significant, since a weld failure under continuous pressure application would be progressive.

The inner and outer tube bundle assemblies are for all practical purposes identical from the standpoint of fabrication. Figure C-3 presents a photograph of the outer tube bundle assembly and shows that it consists of 80 tubes which enter a manifold ring at the upper end. These tubes are furnace-brazed to one another. The differences that do exist between the inner and outer tube bundle assemblies are only differences in the over-all assembly contour and the cross-sectional flow areas in the tubes themselves. Aside from the above noted differences, the fabrication techniques employed for both the inner and the outer tube bundle assemblies were the same.

As mentioned earlier, the basic parts which comprised these components were the tapered tubes and the manifold ring. The tubes had a wall thickness of 0.020 inches and were of welded construction. The basic design criterion was to maintain a circular tube cross-section at the injector end of the chamber. In addition, it was necessary that the proper gas profile and the required coolant velocity be maintained. This resulted in the requirement that the tubes not only have a double taper but also that they be formed so as to provide rectangular cross-sections in some regions. This was accomplished by a series of swaging

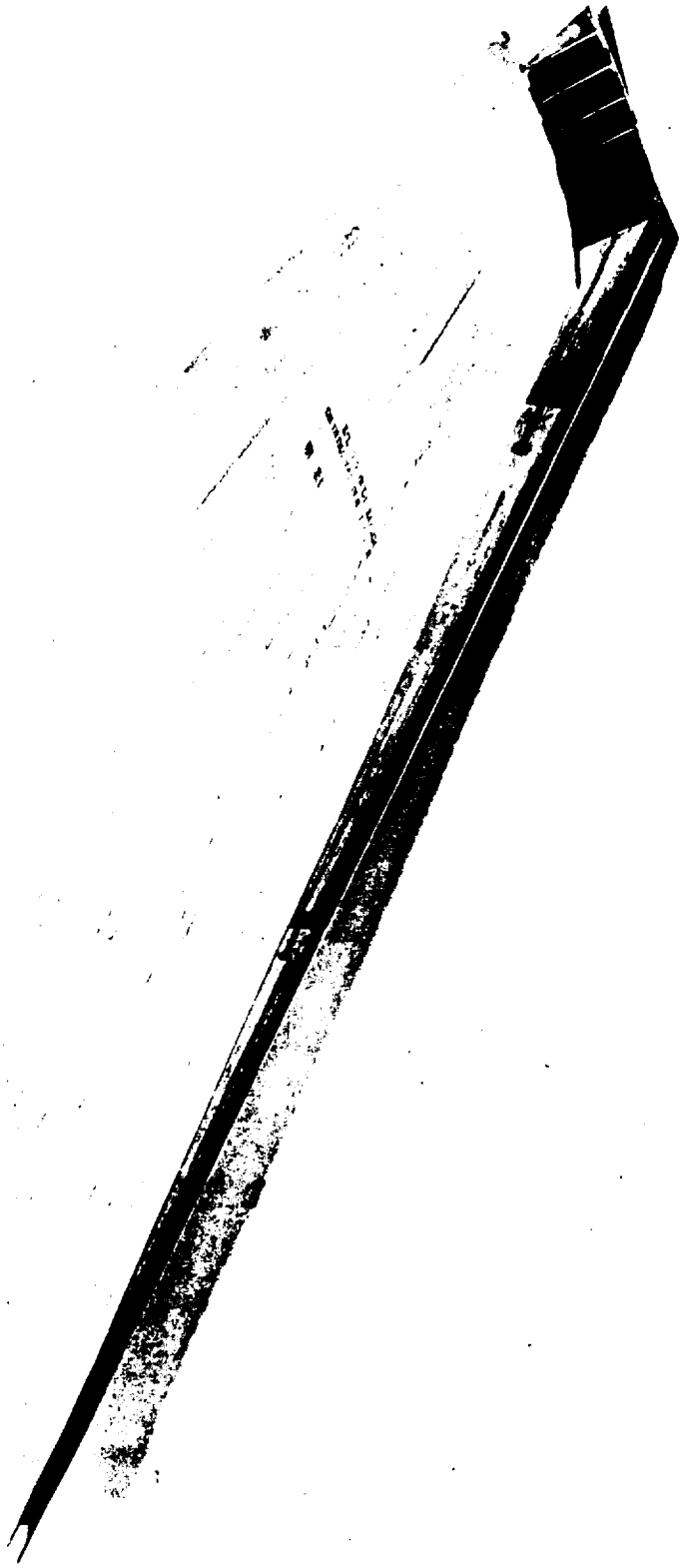

Figure C-2 Cone Segment

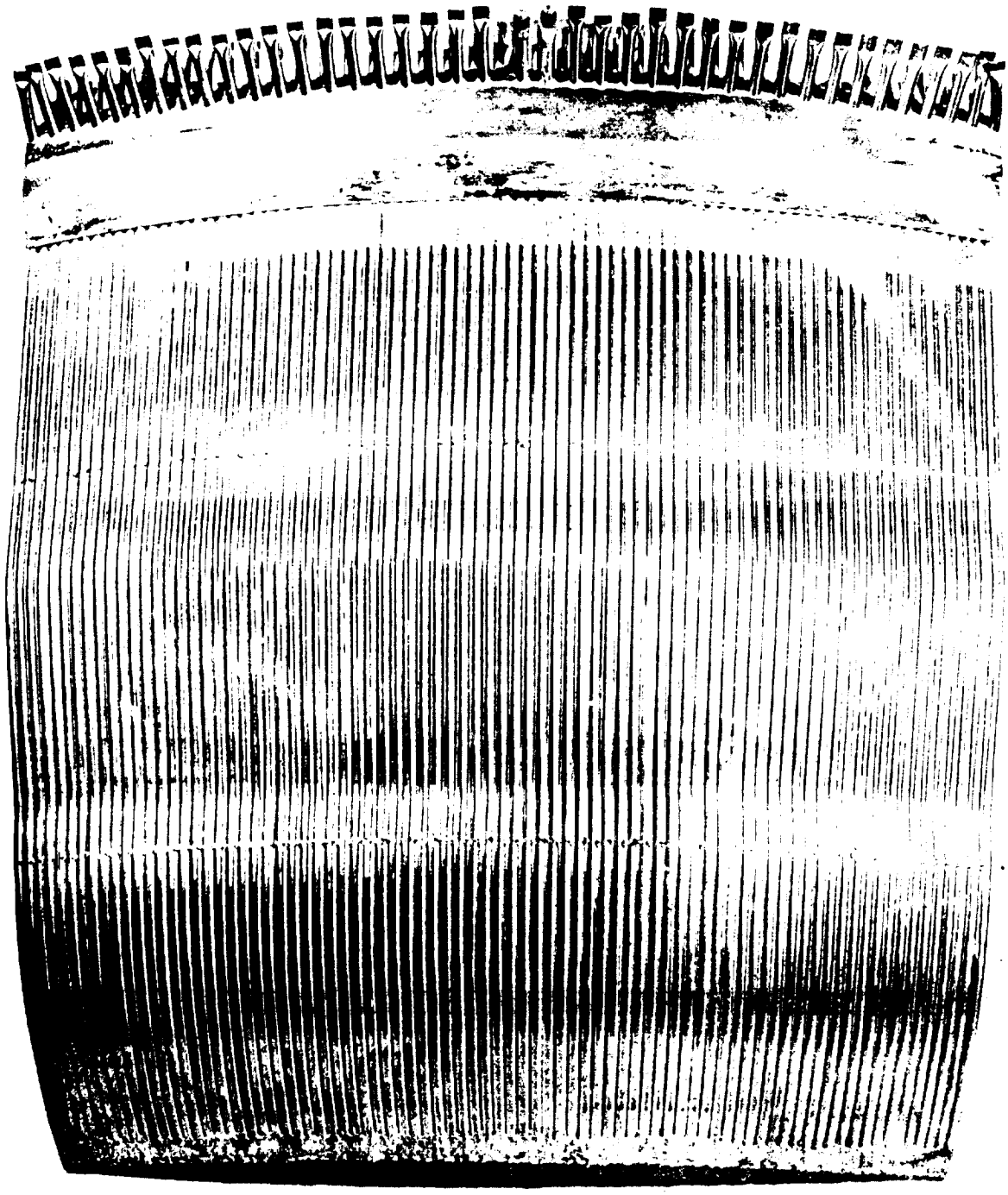

Figure C-3 Outer Tube Bundle Assembly

and forming operations. First a double taper was swaged into each tube, then the tapered tube was formed to the required cross-section, and finally it was bent to produce the proper chamber contour.

These tubes were assembled into a panel by first inserting them into the manifold ring, which had a series of drilled holes to accept the ends of the tubes. The assembly was then supported in an assembly fixture (Figure C-4) while the tubes were spot welded to the manifold ring; two additional rows of spot welds were employed to hold the tube bundle assembly together. As seen in Figure C-4, one row is located at the throat and the other midway between the throat and the ring. Finally, the downstream ends of the tubes were welded to one another. This welding performed two necessary functions. First, it held the parts together in the proper position prior to and during the brazing cycle and secondly, the end welds sealed this joint against leakage when the unit was assembled as part of the thrust chamber.

After the unit was welded, it was cleaned in an acid bath (20 percent nitric acid and 2 to 4 percent hydrofluoric acid) at 165°F prior to brazing. The braze operation was accomplished in a vacuum furnace at about 2025°F using a modified nicro-braze alloy. This operation sealed all hot gas and coolant leakage paths and bonded the component into an integral unit.

The third major component is the divider post (see Figure C-1). A photograph of the divider post is shown in Figure C-5, and it is seen that this component is also of sandwich-type construction. Three plates run the entire length of the piece. For flow control and structural reasons, ribs were brazed between the plates. In the converging section of the nozzle, the post tapers in two directions, for the following reasons. First, to conform to the contour of the converging section of the combustors; and second, to present as small a cross-sectional area as possible at the throat, to maintain the base drag at a minimum.

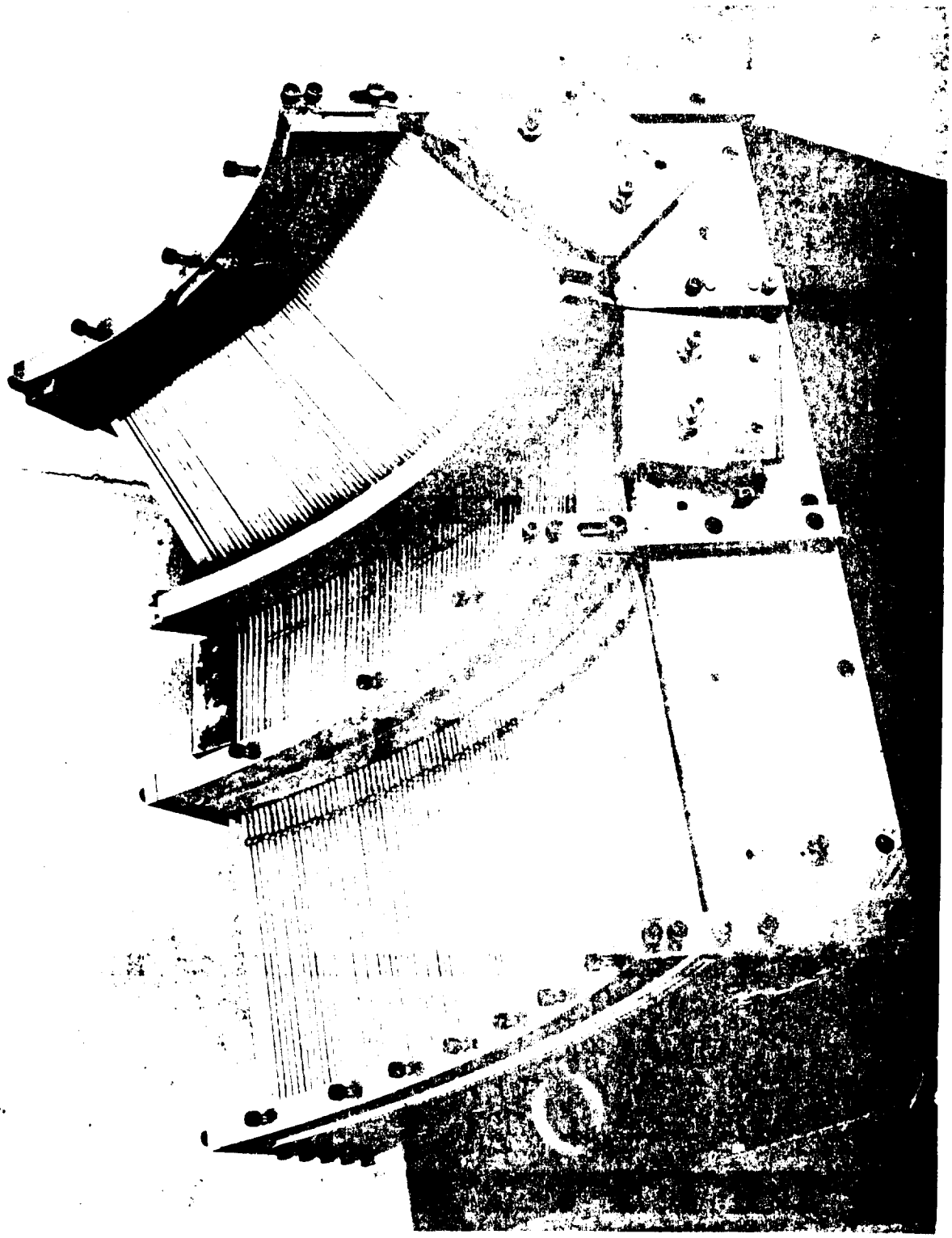

Figure C-4 Inner Tube Bundle in Assembly Fixture

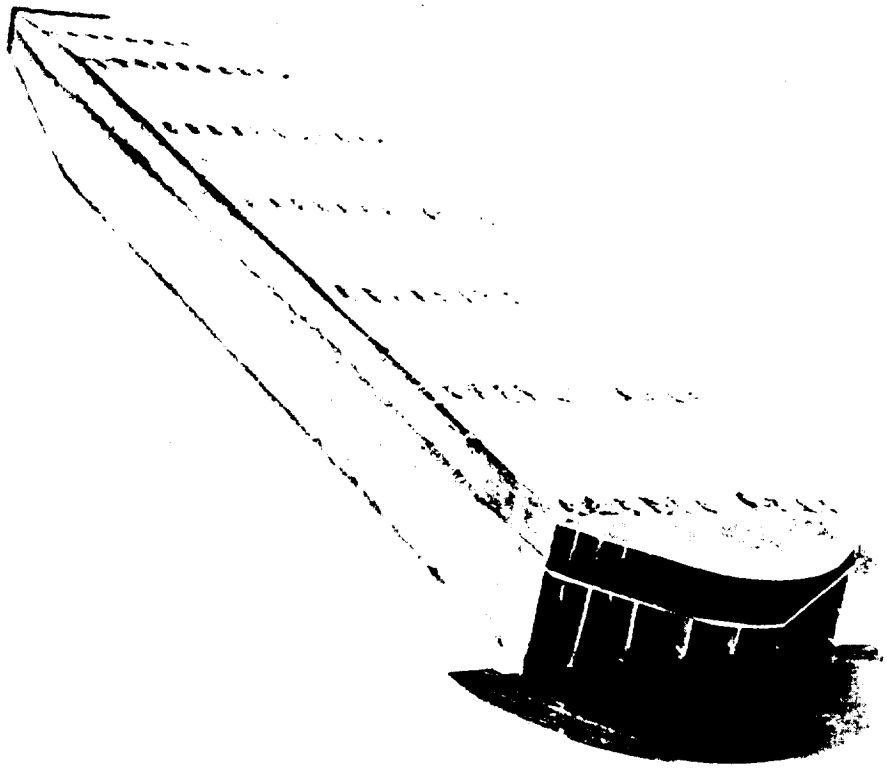

Figure C-5 Divider Post

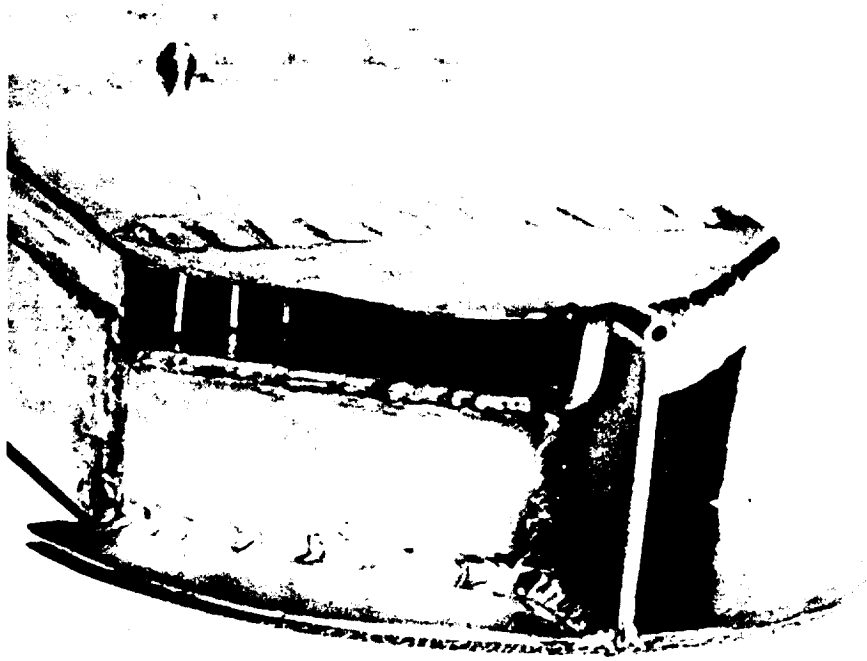

Figure C-6 Detail View of Divider Post

In earlier discussions, it was noted that the post is a modified two-pass component. The coolant enters the small openings on the hot side of the post and flows axially toward the throat. At the base of the post there is a small return manifold to turn the flow 180^{o} and direct it back up the cold side of the post. (No cooling is accomplished on this second pass.) To maintain the coolant velocity at reasonable values in the tapered section, by-pass holes were provided in the center plate to bleed off part of the main flow into the return pass.

The small tube (Figure C-6) which passes down one of the coolant passages and comes out through the wall on the hot gas side of the post allows measurement of chamber pressure and provides a means for injecting TEA (used for initiating combustion).

The only remaining component is the propellant injector. This component will not be discussed here, since it has already been thoroughly discussed in Section IV.

The assembly techniques employed in assembling both a single segment and the complete engine are well worth noting; they are described below.

The initial step in assembling a one-eighth segment consisted of brazing the divider posts to the inner and outer tube bundle assemblies, thus completing the basic combustor assembly. Next, the cone segment was welded in place to the inner tube bundle assembly. The injector was then installed and also welded in place. Finally the necessary manifolding employed to distribute the coolant was added at the injector end of the assembly (see Figure C-1).

As mentioned earlier, it was necessary to enclose the complete segment assembly in a heavy test fixture, since a single segment is not structurally self-supporting. To insure uniform support throughout, the chamber was imbedded in an epoxy resin plastic in the test fixture (see Figure C-7).

View A

View B

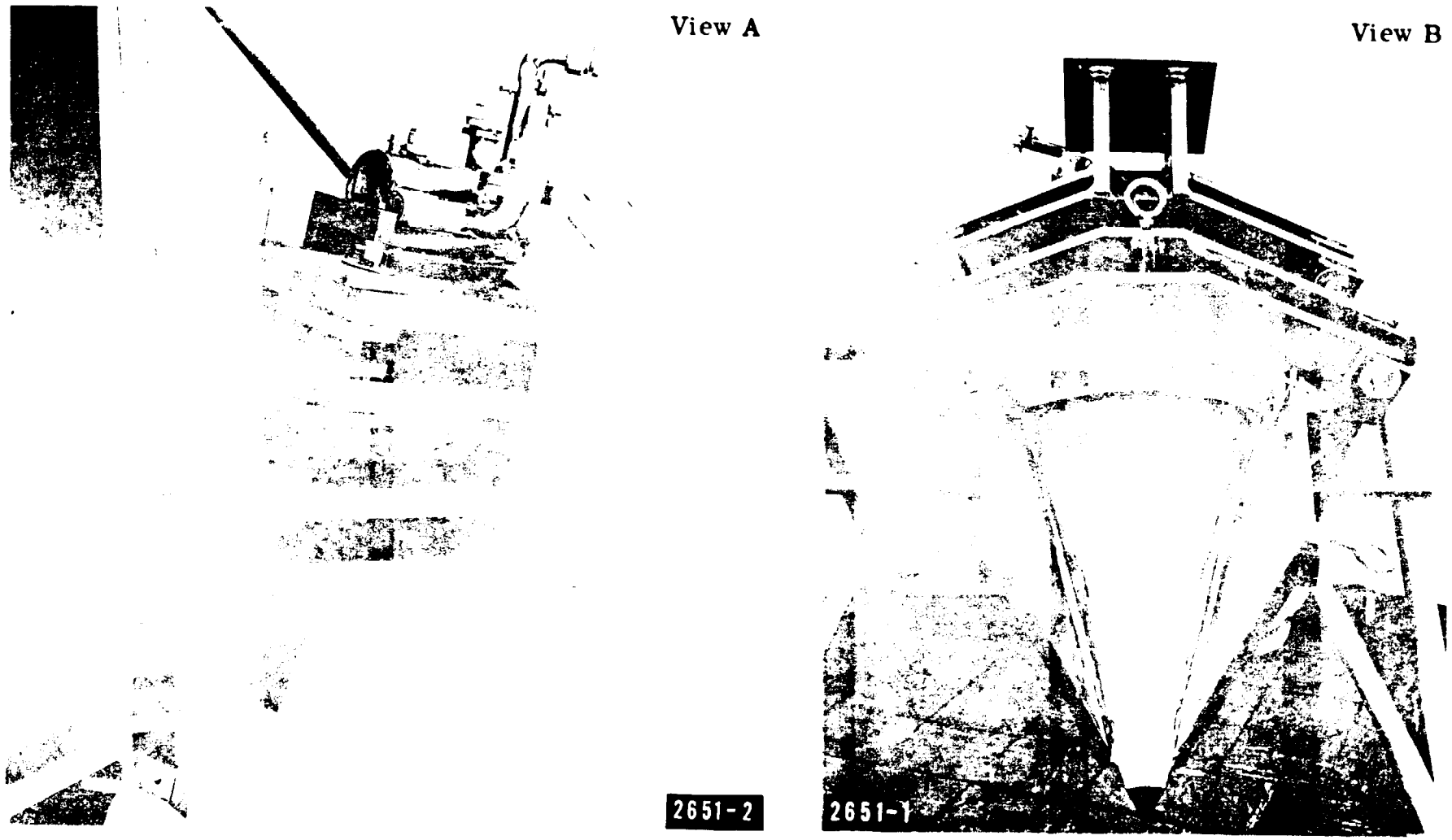

Figure C-7 Cooled Segment in Test Fixture

The technique employed to assemble the complete engine was somewhat different from that for an individual segment, since the engine was not assembled segment by segment. The first step in this assembly process was to fit and secure all inner panels in the assembly fixture (see Figure C-8, Assembly A). The next step was to braze the divider posts in position about the periphery of the inner tube bundle assembly, as illustrated in Figure C-8, Assembly B. Next, the cone segments, which had been preassembled (by welding) were welded to the base of the inner tube bundle assembly (see Figure C-9, Assembly C). Finally, the outer tube bundle assemblies were brazed to the posts to complete the basic engine assembly (see Figure C-9, Assembly D). It will be noted that "T" bar stiffener bands were added at three locations about the periphery of the outer tube bundle assembly. This was done to prevent the panels from collapsing due to pressure from the wire wrapping when the segments were operated at different combustion pressures (for purposes of obtaining thrust vector control). At this point the assembly was removed from the assembly fixture and the installation of injector and coolant manifolds was completed in the same manner as for the assembly of the individual segments. Finally, the thrust mount was installed. The thrust mount itself consisted of a flange (for attaching the engine to the thrust vector system) with a cylindrical section that extended down the interior of the inner tube bundle assembly to a location slightly beyond the throat.

The thrust mount was first accurately aligned with respect to the engine, and then bolted to four mounting "pads". These pads are located at the injector end of the chamber and are capable of transmitting the thrust developed by the engine. The gap between the flange and the inner tube bundle assembly was then filled with epoxy resin to provide uniform structural support for the complete engine.

On completing the installation of the thrust mount, the complete assembly was locked in a lathe (using the thrust mount as the attachment) and was wrapped with two layers of 1/16 inch diameter music quality steel wire. Prior to installing

Assembly A

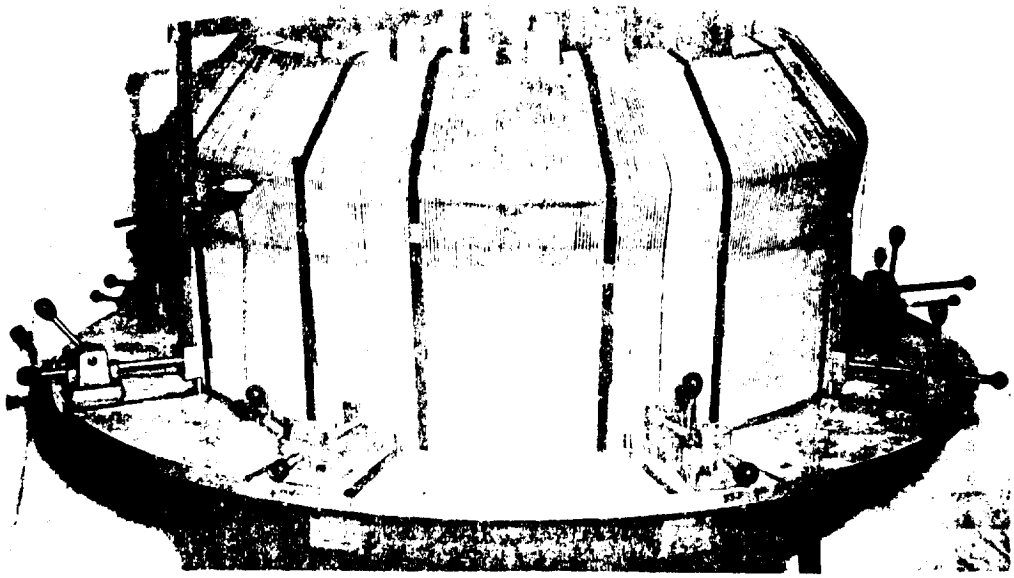

Assembly B

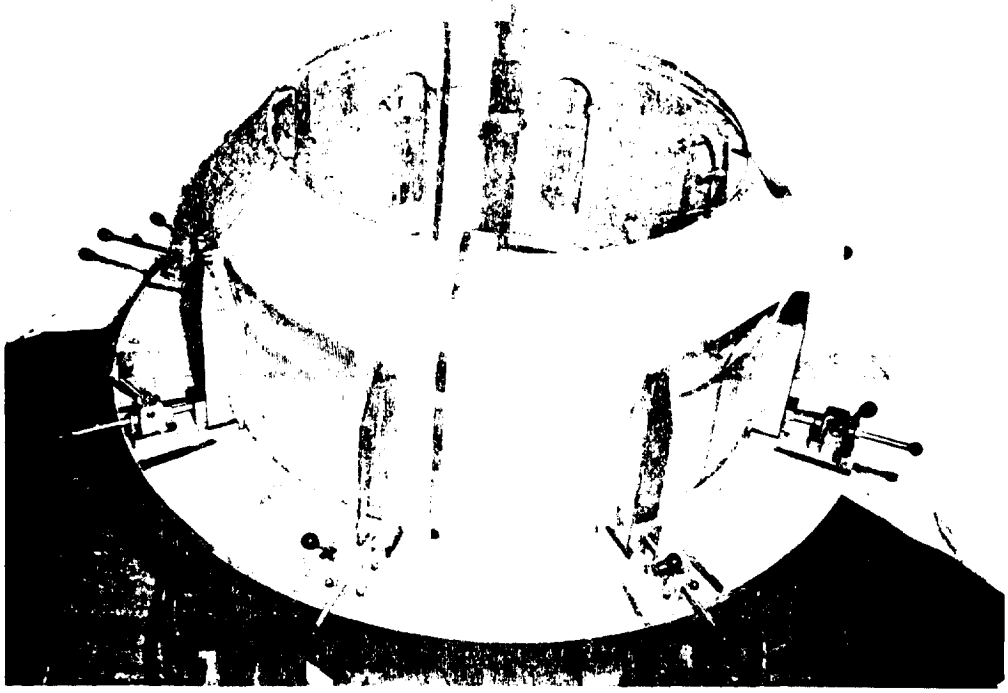

Figure C-8 Cooled Engine Assembly Technique (Assemblies A and B)

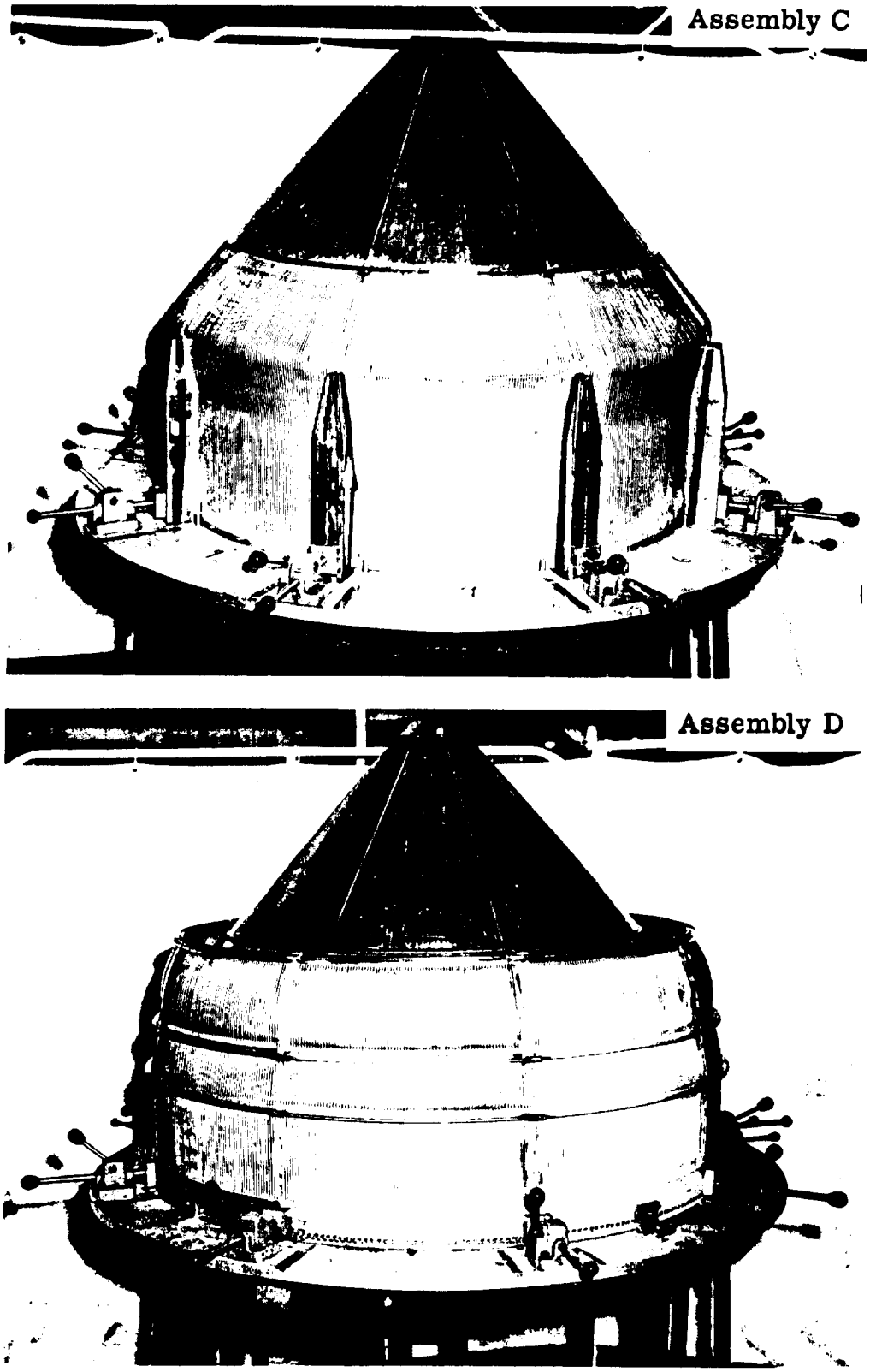

Figure C-9 Cooled Engine Assembly Technique (Assemblies C and D)

the first layer of wire wrapping, the entire outer tube bundle assembly was coated with a layer of epoxy resin. The wire wrapping was immediately applied under tension, prior to the "curing" of the epoxy. This same operation was repeated when installing the second layer of wire wrapping. Finally a thin layer of epoxy was applied to the outside of the second layer of wire wrapping, to protect the engine from oxidation and other damage. The complete engine assembly is shown in Figure C-10.

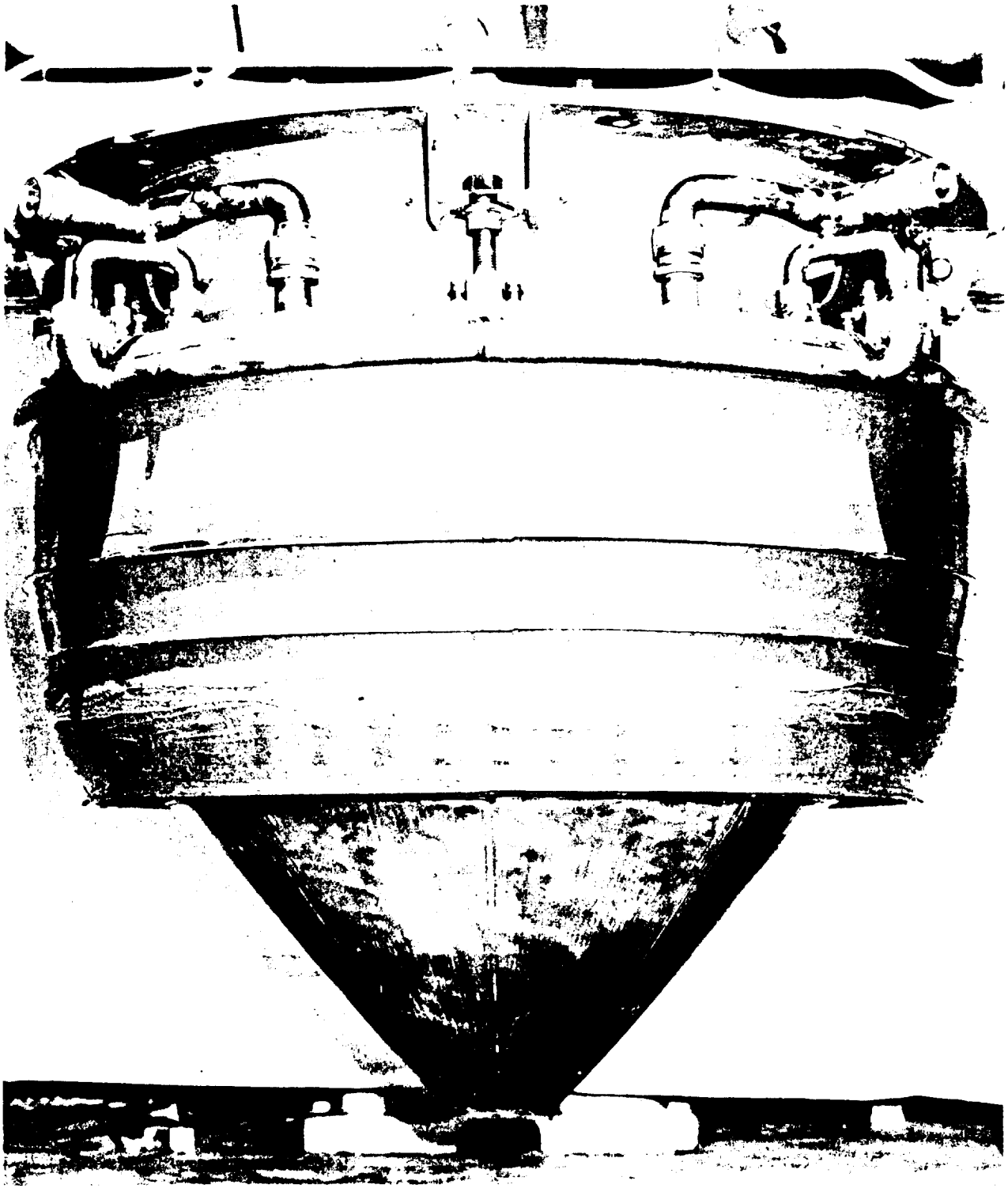

Figure C-10 Complete Cooled Engine

APPENDIX D

REFERENCES

APPENDIX D

REFERENCES

1. Plug Nozzle Program, Final Report, Tasks I and II, Contract NASw-40, General Electric Company, April 1960.

2. Plug Nozzle Program, Final Report, Task III, Contract NASw-40, General Electric Company, April 1960.

3. Plug Nozzle Program, Final Report, Supporting Task, Contract NASw-40, General Electric Company, April 1960.

FINAL REPORT DISTRIBUTION LIST

	Number of Copies
NASA Headquarters 1512 H Street, N. W. Washington 25, D. C. Attention: LPL	6 and 1 reproducible
Officer-in-charge Jet Propulsion Laboratory 4800 Oak Grove Drive Pasadena 2, California Attention: Mr. Earl E. Newlan Reports Group	2
George C. Marshall Space Flight Center Huntsville, Alabama Attention: ORDAB-DST	3
Central Intelligence Agency 2340 E Street, N. W. Washington 25, D. C. Attention: FTRDL	2
Commander Air Research and Development Command Andrews Air Force Base Washington 25, D. C.	2
Lewis Research Center 2100 Brookpark Road Cleveland 35, Ohio	3
Aerospace Corporation P.O. Box 95085 Los Angeles 45, California Attention: Mr. Warren Amster	1
Boeing Airplane Company Box 3707 Seattle 24, Washington Attention: T.M. Davidson	1

[redacted]

FINAL REPORT DISTRIBUTION LIST (CONT'D)

	Number of Copies
Convair, A Division of General Dynamics Corp. 3165 Pacific Highway San Diego 12, California Attention: Harry Steele	1
Douglas Aircraft Company, Inc. 3000 Ocean Park Boulevard Santa Monica, California Attention: T. DeGenaro	1
Grumman Aircraft Engineering Corporation Bethpage, Long Island New York Attention: T. Kelly	1
Lockheed Missiles & Space Division P.O. Box 504 Sunnyvale, California Attention: Bernard Karen	1
Republic Aviation Corporation Conklin Street Farmingdale, Long Island New York Attention: J. Jackson	1
Change-Vought P.O. Box 5907 Dallas, Texas Attention: F. Esenwein	1
The Martin Company P.O. Box 179 Denver 1, Colorado Attention: Eliot Ring	1
The Martin Company Baltimore 3, Maryland Attention: M. Stoiko	1

[redacted]

FINAL REPORT DISTRIBUTION LIST (CONT'D)

	Number of Copies
McDonnel Aircraft Corporation Lambert - St. Louis Municipal Airport P.O. Box 516 St. Louis 66, Missouri Attention: Cliff Marks	1
Temco Aircraft Corporation P.O. Box 6191 Dallas 22, Texas Attention: K. Hawkins	1